

Novel pharmacological strategies for neurological conditions involving glutamate and adenosine

Laura I. Sarasola Telleria

ADVERTIMENT. La consulta d'aquesta tesi queda condicionada a l'acceptació de les següents condicions d'ús: La difusió d'aquesta tesi per mitjà del servei TDX (www.tdx.cat) i a través del Dipòsit Digital de la UB (diposit.ub.edu) ha estat autoritzada pels titulars dels drets de propietat intel·lectual únicament per a usos privats emmarcats en activitats d'investigació i docència. No s'autoritza la seva reproducció amb finalitats de lucre ni la seva difusió i posada a disposició des d'un lloc aliè al servei TDX ni al Dipòsit Digital de la UB. No s'autoritza la presentació del seu contingut en una finestra o marc aliè a TDX o al Dipòsit Digital de la UB (framing). Aquesta reserva de drets afecta tant al resum de presentació de la tesi com als seus continguts. En la utilització o cita de parts de la tesi és obligat indicar el nom de la persona autora.

ADVERTENCIA. La consulta de esta tesis queda condicionada a la aceptación de las siguientes condiciones de uso: La difusión de esta tesis por medio del servicio TDR (**www.tdx.cat**) y a través del Repositorio Digital de la UB (**diposit.ub.edu**) ha sido autorizada por los titulares de los derechos de propiedad intelectual únicamente para usos privados enmarcados en actividades de investigación y docencia. No se autoriza su reproducción con finalidades de lucro ni su difusión y puesta a disposición desde un sitio ajeno al servicio TDR o al Repositorio Digital de la UB. No se autoriza la presentación de su contenido en una ventana o marco ajeno a TDR o al Repositorio Digital de la UB (framing). Esta reserva de derechos afecta tanto al resumen de presentación de la tesis como a sus contenidos. En la utilización o cita de partes de la tesis es obligado indicar el nombre de la persona autora.

WARNING. On having consulted this thesis you're accepting the following use conditions: Spreading this thesis by the TDX (**www.tdx.cat**) service and by the UB Digital Repository (**diposit.ub.edu**) has been authorized by the titular of the intellectual property rights only for private uses placed in investigation and teaching activities. Reproduction with lucrative aims is not authorized nor its spreading and availability from a site foreign to the TDX service or to the UB Digital Repository. Introducing its content in a window or frame foreign to the TDX service or to the UB Digital Repository is not authorized (framing). Those rights affect to the presentation summary of the thesis as well as to its contents. In the using or citation of parts of the thesis it's obliged to indicate the name of the author.



DOCTORAL PROGRAM in BIOMEDICINE

Novel pharmacological strategies for neurological conditions involving glutamate and adenosine

Doctoral thesis submitted by:

Thesis director:

Laura I. Sarasola Telleria

Francisco Ciruela Alférez

Thesis codirector:

Glòria Salort Flaquer

Department of Experimental Pathology and Therapeutics

Faculty of Medicine and Health Sciences

Bellvitge Campus-Universitat de Barcelona-March 2025

AUTHORIZATION FOR THE PRESENTATION OF THE THESIS

Dr. Francisco Ciruela Alférez, Professor at the Pharmacology Unit, Department of Experimental Pathology and Therapeutics, Faculty of Medicine and Health Sciences, University of Barcelona, L'Hospitalet de Llobregat, Spain, with Identity card: 43504115Y; and Dr. Glòria Salort Flaquer, postdoctoral researcher at Institut d'Investigació de Bellvitge (IDIBELL), with identity card: 41570083K

DECLARE THAT: The thesis memory presented by Ms. Laura I. Sarasola Telleria with title "Novel pharmacological strategies for neurological conditions involving glutamate and adenosine", has been developed under my supervision and I authorize the deposit for being defended and judged by a tribunal.

FUNDING

The studies presented in this thesis were supported by the PhD fellowship PIF Salut 2021-2024 (SLT017/20/000114) from the "Departament de Salut de la Generalitat de Catalunya". The doctoral candidate Laura I. Sarasola Telleria was also beneficiary of a research stay fellowship funded by the European Molecular Biology Organization (10966). Moreover, the doctoral candidate received the support for participating in scientific national and international conferences from the "Institut de Neurociències" (Universitat de Barcelona). The research project was funded by "Ministerio de Ciencia, Innovación y Universidades-Agencia Estatal de Investigación" **FEDER** funds/European Regional Development Fund –"a way to build Europe" grant PID2020-118511RB-I00 to Dr. Francisco Ciruela Alférez.

Thesis in classical format

This doctoral thesis consists of 3 objectives and 2 articles in preparation.

During the doctoral thesis, the doctoral candidate participated in different projects that resulted in the following publications:

Sarasola, L. I., Llinás, C., Pérez-Arévalo, A., Argerich, J., Casajuana-Martín, N., Chevigné, A., Fernández-Dueñas, V., Ferré, S., Pardo, L., & Ciruela, F. (2022). The ADORA1 mutation linked to early-onset Parkinson's disease alters adenosine A1-A2A receptor heteromer formation and function. *Biomedicine & Pharmacotherapy*, *156*, 113896–113896. https://doi.org/10.1016/j.biopha.2022.113896

Ferré, S., **Sarasola, L. I.**, Quiroz, C., & Ciruela, F. (2023). Presynaptic adenosine receptor heteromers as key modulators of glutamatergic and dopaminergic neurotransmission in the striatum. Neuropharmacology, 223, 109329. https://doi.org/10.1016/j.neuropharm.2022.109329

Sánchez-Fernández, N., Gómez-Acero, L., **Sarasola, L. I.**, Argerich, J., Chevigné, A., Jacobson, K. A., Ciruela, F., Fernández-Dueñas, V., & Aso, E. (2023). Cannabidiol negatively modulates adenosine A_{2A} receptor functioning in living cells. *Acta Neuropsychiatrica*, 1–5. https://doi.org/10.1017/neu.2023.30

TABLE OF CONTENTS

TABLE OF	CONTENTS	. 13
RESUM [DE LA TESI	. 19
	estratègies farmacològiques per a condicions neurològiques que uen el glutamat i l'adenosina	19
RESUME	N DE LA TESIS	. 23
	s estrategias farmacológicas para condiciones neurológicas que an glutamato y adenosina	23
A BBREVIA	TIONS & ACRONYMS	. 27
I. INTRO	DUCTION	. 33
1. N AN	OBODIES	. 35
1.1	Properties of nanobodies	36
1.1.1	Structural features	36
1.1.2	Low immunogenicity	38
1.1.3	High tissue and blood brain barrier penetration	38
1.1.4	Applications of nanobodies	41
1.2	Nanobodies against G protein-coupled receptors	43
2. G PF	OTEIN-COUPLED RECEPTORS	. 44
2.1	GPCR dynamics	46
2.2	GPCR-Effector Membrane Macromolecular Assemblies	50
3. NEU	ROTRANSMISSION	. 52
3.1	Dopaminergic system	52
3.1.1	Dopamine D ₂ receptor	54
3.2	Glutamatergic system	55
3.2.1	Metabotropic glutamate receptor 5	57
3.3	Adenosinergic system	58
3.3.1	Adenosine A _{2A} receptor	60
4. Psyc	CHIATRIC DISORDERS	. 60
4.1	Schizophrenia	60

	4.1.1	Definition, epidemiology and etiology 60
	4.1.2	Neurotransmission in schizophrenia
	Do	paminergic hypothesis
	Glı	utamatergic hypothesis64
	Ad	enosinergic hypothesis
	4.1.3	Pharmacology in schizophrenia67
	4.2	Bipolar disorder
	4.2.1	Definition, epidemiology and etiology71
	Ca	lcium pathophysiology72
	Fro	ontal-limbic model of BD73
	Inf	lammatory and oxidative stress73
	4.2.2	Pharmacology in bipolar disorder
11.	. НҮРОТ	HESYS & OBJECTIVES 77
Ш	I. MATE	RIAL & METHODS 81
1.	NANC	DBODY PRODUCTION AND PURIFICATION
	1.1	Nanobody production 83
	1.2	Periplasm fraction extraction
	1.3	Nanobody purification
2.	Віосі	HEMICAL CHARACTERIZATION OF NANOBODIES
	2.1	Bioinformatic predictions
	2.2	Size exclusion chromatography
3.	NANC	DBODY LABELING
	3.1	Biotinilation
	3.2	AlexaFluor 647 NHS labeling
	3.3	Radiolabeling with Tc-99m90
	3.4	Radiolabeling with ¹¹¹ In 90
	3.5	Nanobody-Drug conjugate
4.	CELLS	AND CONSTRUCTS
	4.1	Transfection93

5	. Bı	NDING ASSAYS94
	5.1	Flow cytometry in vitro94
	5.2	Flow cytometry ex vivo95
	5.3	Radiolabelled-nanobody binding assay97
	5.4	Immunocytofluorescence
	5.5	Immunohistofluorescence98
6	. In	TRACELLULAR SIGNALING99
	6.1	NanoBiT99
	6.2	cAMP assay100
	6.3	Proximity Ligation Assay101
7	. Ar	NIMALS
	7.1	Radiolabeled nanobody biodistribution102
	7.2	Catalepsy test
	7.2.1	Intranasal administration105
	7.2.2	Intracerebroventricular administration106
	7.3	Locomotion test
	7.3.1	Basal and PCP-induced locomotion
8	. М	ETANALYSIS
9	. Sт	ATISTICAL ANALYSIS
I۱	/. Res	ULTS 111
D	EVELO	PMENT AND CHARACTERIZATION OF NANOBODY-BASED DRUGS: IN VIVO
S٦	TUDIES	
	1.	Characterization of the Nb43 binding to mouse and human mGlu₅R 113
		Nb43 shows higher binding affinity to human mGlu₅R compared to mouse mGlu₅R113
		Nb43 binds to mouse mGlu₅R ex vivo115
	2.	Structural insights on the binding of Nb43 to mGlu ₅ R117
		Implication of proline 371 and histidine 350 in the binding affinity of Nb43117

3. A _{2A} R	Design and synthesis of a nanobody-based bivalent ligand for targeting 1- mGlu₅R heteromers119
	Functional characterization of the A _{2A} R-mGlu₅R heteromer in living cells
	Design and synthesis of Nb43-CGS21680 targeting $A_{2A}R$ -mGlu ₅ R heteromer
	ATION OF THE THERAPEUTIC POTENTIAL OF A NANOBODY-BASED DRUG: <i>In vivo</i>
1. syste	Behavioral effects of Nb43 and Nb43-CGS21680 at the central nervous em
	Modulation of locomotor activity by intracerebroventricular administration of Nb43 and Nb43-CGS21680
	Modulation of haloperidol-induced catalepsy by intracerebroventricular administration of Nb43 and Nb43-CGS21680
2.	Biodistribution analysis of Nb43 using SPECT/CT 129
	Comparative biodistribution of ^{99m} Tc-Nb43 following intranasal versus intravenous administration
	A longitudinal study of the biodistribution of 99mTc-Nb43 following intranasal versus intravenous administration
3.	Behavioral effects of intranasally delivered Nb43 and Nb43-CGS21680 .135
	Intranasally delivered Nb43 modulates haloperidol-induced catalepsy with long-lasting effects
	DENOSINE HYPOTHESIS IN SCHIZOPHRENIA AND BIPOLAR DISORDER: A META-
1.	Study characteristics
	Selection of double-blind, randomized controlled trials of purinergic drugs for schizophrenia and bipolar disorder
2.	Efficacy outcomes
	Purinergic drugs significantly improve total and positive, but not negative, PANSS
	Purinergic drugs significantly improve YMRS scores 144

V. Discussion	145
Novel pharmacological strategies based on nanobodies targeting	
EFFICACY OF PURINERGIC DRUGS IN SCHIZOPHRENIA AND BIPOLAR DISORDER.	155
VI. Conclusions	159
VII. SUPPLEMENTARY MATERIAL	163
VIII. REFERENCES	181
ACKNOWLEDGEMENTS	209

RESUM DE LA TESI

Noves estratègies farmacològiques per a condicions Neurològiques que impliquen el glutamat i l'adenosina

Els trastorns neuropsiquiàtrics com l'esquizofrènia i el trastorn bipolar presenten alteracions en la neurotransmissió dopaminèrgica i glutamatèrgica, cosa que ha portat al desenvolupament d'estratègies terapèutiques dirigides a aquests sistemes. Recentment, el sistema adenosinèrgic ha emergit com un regulador clau de l'activitat dopaminèrgica i glutamatèrgica, amb evidència que l'activació del receptor A_{2A} d'adenosina pot modular la transmissió dopaminèrgica i afectar els símptomes neuropsiquiàtrics. A més, la interacció entre el receptor A_{2A} i el receptor metabotròpic de glutamat tipus 5 a l'estriat representa un punt de convergència terapèutica potencial per al tractament d'aquests trastorns.

En aquest context, els nanocossos han sorgit com a eines innovadores per modular interaccions macromoleculars de membrana de manera altament específica. A diferència dels anticossos convencionals, els nanocossos són fragments d'anticossos de cadena pesada que presenten avantatges com la seva petita mida, alta estabilitat i capacitat d'accedir a regions inaccessibles de les proteïnes. En aquesta tesi, explorem el desenvolupament i la caracterització del nanocòs Nb43, dissenyat per modular el receptor de glutamat mGlu₅R, així com el seu conjugat Nb43-CGS21680, que incorpora un agonista d'A_{2A}R per potenciar-ne l'efecte.

La tesi es divideix en tres capítols. En el primer capítol, caracteritzem *in vitro* la unió i l'efecte funcional de Nb43 i Nb43-CGS21680 en sistemes cel·lulars que expressen mGlu₅R i A_{2A}R. En el segon capítol, avaluem la biodistribució,

penetració en el sistema nerviós central i activitat farmacològica d'aquests nanocossos en models murins. Finalment, en el tercer capítol, realitzem una metanàlisi de moduladors del metabolisme de l'adenosina en esquizofrènia i trastorn bipolar, per avaluar-ne l'impacte clínic i el potencial terapèutic.

Els resultats de l'estudi *in vitro* del Nb43 van mostrar que Nb43 s'uneix selectivament a m Glu_5R en un context fisiològic. D'altra banda, Nb43-CGS21680 va mostrar un perfil de doble acció, amb una modulació simultània de m Glu_5R i $A_{2A}R$. Curiosament, l'activació conjunta d'aquests receptors va resultar en una modulació més específica de l'activitat intracel·lular. Els experiments *in vitro* de PLA i NanoBiT van confirmar l'existència d'interaccions funcionals entre m Glu_5R i $A_{2A}R$, cosa que dona suport a la hipòtesi que aquests receptors formen heteròmers a la membrana neuronal.

Per avaluar la biodistribució de Nb43, vam realitzar estudis d'imatge *in vivo* després de la seva administració intravenosa i intranasal. Els resultats van indicar que Nb43 no travessa la barrera hematoencefàlica de manera significativa quan s'administra per via intravenosa. No obstant això, en l'administració intranasal es van detectar petites concentracions al bulb olfactori, suggerint una possible via d'accés al sistema nerviós central.

Els efectes conductuals de Nb43 i Nb43-CGS21680 es van avaluar després de la seva administració intracerebroventricular, cosa que va permetre analitzar l'impacte directe en el sistema nerviós central sense la limitació de la barrera hematoencefàlica. En la prova de locomoció, CGS21680 va reduir significativament l'activitat locomotora, en línia amb estudis previs que suggereixen el seu efecte anti-dopaminèrgic. De manera similar, Nb43 i Nb43-CGS21680 també van disminuir la locomoció, encara que amb menor intensitat. Aquest efecte suggereix que Nb43 i Nb43-CGS21680 podrien estar modulant la neurotransmissió dopaminèrgica a través de la seva acció sobre

mGlu₅R a l'estriat. En la prova de catalepsia induïda per haloperidol, CGS21680 va augmentar significativament la catalepsia, confirmant-ne el paper en la inhibició dopaminèrgica. De manera interessant, Nb43 també va augmentar el temps de catalepsia, cosa que indica que el seu efecte sobre mGlu₅R podria estar modulant l'activitat de la via dopaminèrgica. A diferència de CGS21680, els efectes del qual van desaparèixer a les 24-48 hores, Nb43-CGS21680 va prolongar l'efecte de catalepsia fins a 48 hores després de la seva administració, cosa que suggereix un mecanisme més sostingut de modulació de la neurotransmissió.

Addicionalment, vam realitzar experiments de catalepsia després de l'administració intranasal de Nb43 i Nb43-CGS21680. Els resultats van mostrar que Nb43 va tenir un impacte significatiu en la catalepsia induïda per haloperidol, mentre que Nb43-CGS21680 no va mostrar efectes. Això suggereix que Nb43 podria haver arribat al SNC a través del bulb olfactori, on s'expressa mGlu₅R i s'ha reportat el seu paper en la modulació de la locomoció i l'equilibri.

D'altra banda, l'estudi de metanàlisi va incloure estudis clínics que van avaluar l'impacte de moduladors del metabolisme de l'adenosina, com l'al·lopurinol, el dipiridamol, la pentoxifil·lina i la propentofil·lina, en la simptomatologia de l'esquizofrènia i el trastorn bipolar. Els resultats van indicar que l'al·lopurinol, un inhibidor de la xantina oxidasa que eleva els nivells d'adenosina, va ser el més estudiat i va mostrar efectes positius en la reducció dels símptomes positius de l'esquizofrènia i el trastorn bipolar.

El dipiridamol, un inhibidor de la recaptació d'adenosina, també va mostrar millores en els símptomes positius, encara que els estudis van ser limitats. La propentofil·lina, un derivat de les xantines amb propietats neuroprotectores i antiinflamatòries, va tenir efectes més marcats en els símptomes negatius i el deteriorament cognitiu.

Les troballes de la metaanàlisi reforcen la hipòtesi adenosinèrgica de l'esquizofrènia i el trastorn bipolar, la qual proposa que la modulació del sistema adenosinèrgic pot influir en la neurotransmissió dopaminèrgica i glutamatèrgica. En aquest sentit, els resultats suggereixen que estratègies dirigides a potenciar la senyalització adenosinèrgica podrien representar una via terapèutica prometedora.

En conjunt, aquesta tesi contribueix al coneixement sobre el paper dels nanocossos en la farmacologia dels receptors de membrana i destaca la importància del sistema adenosinèrgic en la modulació de la neurotransmissió dopaminèrgica i glutamatèrgica en trastorns neuropsiquiàtrics.

Nanocossos · Sistema adenosinèrgic · Sistema glutamatèrgic · Neurofarmacología · Metaanàlisi

RESUMEN DE LA TESIS

NUEVAS ESTRATEGIAS FARMACOLÓGICAS PARA CONDICIONES NEUROLÓGICAS QUE IMPLICAN GLUTAMATO Y ADENOSINA

Los trastornos neuropsiquiátricos como la esquizofrenia y el trastorno bipolar presentan alteraciones en la neurotransmisión dopaminérgica y glutamatérgica, lo que ha llevado al desarrollo de estrategias terapéuticas dirigidas a estos sistemas. Recientemente, el sistema adenosinérgico ha emergido como un regulador clave de la actividad dopaminérgica y glutamatérgica, con evidencia de que la activación del receptor A_{2A} de adenosina puede modular la transmisión dopaminérgica y afectar síntomas neuropsiquiátricos. Además, la interacción entre el receptor A_{2A} y el receptor metabotrópico de glutamato tipo 5 en el estriado representa un punto de convergencia terapéutica potencial para el tratamiento de estos trastornos.

En este contexto, los nanocuerpos han surgido como herramientas innovadoras para modular interacciones macromoleculares de membrana de manera altamente específica. A diferencia de los anticuerpos convencionales, los nanocuerpos son fragmentos de anticuerpos de cadena pesada que presentan ventajas como su pequeño tamaño, alta estabilidad y capacidad de acceder a regiones inaccesibles de las proteínas. En esta tesis, exploramos el desarrollo y la caracterización del nanocuerpo Nb43, diseñado para modular el receptor de glutamato mGlu₅R, así como su conjugado Nb43-CGS21680, que incorpora un agonista de A_{2A}R para potenciar su efecto.

La tesis se divide en tres capítulos. En el primer capítulo, caracterizamos *in vitro* la unión y el efecto funcional de Nb43 y Nb43-CGS21680 en sistemas celulares que expresan mGlu₅R y A₂AR. En el segundo capítulo, evaluamos la distribución,

penetración en el sistema nervioso central y actividad farmacológica de estos nanocuerpos en modelos murinos. Finalmente, en el tercer capítulo, realizamos un metaanálisis de moduladores del metabolismo de adenosina en esquizofrenia y trastorno bipolar, para evaluar su impacto clínico y su potencial terapéutico.

Los resultados del estudio *in vitro* del Nb43 mostraron que Nb43 se une selectivamente a mGlu $_5$ R en un contexto fisiológico. Por otro lado, Nb43-CGS21680 mostró un perfil de doble acción, con una modulación simultánea de mGlu $_5$ R y A $_{2A}$ R. Curiosamente, la activación conjunta de estos receptores resultó en una modulación más específica de la actividad intracelular. Los experimentos *in vitro* de PLA y NanoBiT confirmaron la existencia de interacciones funcionales entre mGlu $_5$ R y A $_{2A}$ R, lo que respalda la hipótesis de que estos receptores forman heterómeros en la membrana neuronal.

Para evaluar la biodistribución de Nb43 y Nb43-CGS21680, realizamos estudios de imagen *in vivo* tras su administración intravenosa e intranasal. Los resultados indicaron que Nb43 no atraviesa la barrera hematoencefálica de manera significativa cuando se administra per vía intravenosa. Sin embargo, en la administración intranasal, se detectaron pequeñas concentraciones en el bulbo olfatorio, sugiriendo una posible vía de acceso al sistema nervioso central.

Los efectos conductuales de Nb43 y Nb43-CGS21680 se evaluaron tras su administración intracerebroventricular, lo que permitió analizar su impacto directo en el sistema nervioso central sin la limitación de la barrera hematoencefálica. En la prueba de locomoción, CGS21680 redujo significativamente la actividad locomotora, en línea con estudios previos que sugieren su efecto anti-dopaminérgico. De manera similar, Nb43 y Nb43-CGS21680 también disminuyeron la locomoción, aunque con menor

intensidad. Este efecto sugiere que Nb43 podría estar modulando la neurotransmisión dopaminérgica a través de su acción sobre mGlu₅R en el estriado. En la prueba de catalepsia inducida por haloperidol, CGS21680 aumentó significativamente la catalepsia, confirmando su papel en la inhibición dopaminérgica. De manera interesante, Nb43 también exacerbó la catalepsia, lo que indica que su efecto sobre mGlu₅R podría estar modulando la actividad de la vía dopaminérgica. A diferencia de CGS21680, cuyos efectos desaparecieron a las 24-48 horas, Nb43-CGS21680 prolongó el efecto de catalepsia hasta 48 horas después de su administración, lo que sugiere un mecanismo más sostenido de modulación de la neurotransmisión.

Adicionalmente, realizamos experimentos de catalepsia tras la administración intranasal de Nb43 y Nb43-CGS21680. Los resultados mostraron que Nb43 tuvo un impacto significativo en la catalepsia inducida por haloperidol, mientras que Nb43-CGS21680 no mostró efectos. Esto sugiere que Nb43 pudo alcanzar el sistema nervioso central a través del bulbo olfatorio, donde se expresa mGlu₅R y se ha reportado su papel en la modulación de la locomoción y el equilibrio.

Por otro lado, el estudio de metaanálisis incluyó estudios clínicos que evaluaron el impacto de moduladores del metabolismo de adenosina, como alopurinol, dipiridamol, pentoxifilina y propentofilina, en la sintomatología de la esquizofrenia y el trastorno bipolar. Los resultados indicaron que alopurinol, un inhibidor de la xantina oxidasa que eleva los niveles de adenosina, fue el más estudiado y mostró efectos positivos en la reducción de síntomas positivos y negativos de la esquizofrenia y transtorno bipolar.

Dipiridamol, un inhibidor de la recaptación de adenosina, también mostró mejoras en síntomas positivos, aunque los estudios fueron limitados. Propentofilina, un derivado de xantinas con propiedades neuroprotectoras y

antiinflamatorias, tuvo efectos más marcados en síntomas negativos y deterioro cognitivo.

Los hallazgos del metaanálisis refuerzan la hipótesis adenosinérgica de la esquizofrenia y el trastorno bipolar, la cual propone que la modulación de sistema adenosinérgico puede influir en la neurotransmisión dopaminérgica y glutamatérgica. En este sentido, los resultados sugieren que estrategias dirigidas a potenciar la señalización adenosinérgica podrían representar una vía terapéutica prometedora.

En conjunto, esta tesis contribuye al conocimiento sobre el papel de los nanocuerpos en la farmacología de los receptores de membrana y destaca la importancia del sistema adenosinérgico en la modulación de la neurotransmisión dopaminérgica y glutamatérgica en trastornos neuropsiquiátricos.

Nanocuerpos · Sistema adenosinérgico · Sistema glutamatérgico · Neurofarmacología · Metaanálisis

ABBREVIATIONS & ACRONYMS

7TMR Seven transmembrane receptor

A

ADA Anti-drug antibody

AMT Adsorptive-mediated transcytosis

aTTP Acquired thrombotic thrombocytopenic purpura

ADBR2 β2-adrenergic receptor

AC Adenylyl cyclase AP-2 Adaptor protein

ATP Adenosine triphosphate
ADP Adenosine diphosphate
AMP Adenosine monophosphate

Ado Adenosine

ADK Adenosine kinase
ADA Adenosine deaminase
AR Adenosine receptor
ANOVA Analysis of Variance

В

BBB Blood brain barrier

BMEC Brain microvascular endothelial cell

BRET Bioluminescence resonance energy transfer BiFC Bimolecular fluorescence complementation

BD Bipolar Disorder

BDNF Brain derived neurotrophic factor

BSA Bovine serum albumin

B Biotin

C

CDR Complementarity determining region

CNS Central nervous system
CaSR Calcium sensing receptor

cAMP Cyclic adenosine monophosphate

Co-IP Co-immunoprecipitation
CSF Cerebrospinal fluid
CE Coelenterazine
CI Confidence interval

D

DAG Diacylglycerol DA Dopamine

DR Dopamine receptor

DMS-V Diagnostics and Statistical Manual of Mental Disorders

DAT Dopamine transporter

DB Double blind

DTPA Diethylene triamine pentacetic acid DAPI 4',6-diamidino-2-phenylindole

Ε

ECD Extracellular domain

ENT Equilibrative nucleoside transporter

EPS Extrapyramidal symptoms

F

F(ab) Antigen binding fragment

FR Framework region

FDA Food and drug administration FGA First generation antipsychotics

G

GPCR G protein-coupled receptor

GABA y-amino butyric acid

GRK G protein-coupled receptor kinase

GEMMA G protein-coupled receptor-effector membrane

macromolecular assembly

GS Glutamine synthetase

GWAS Genome-wide association studies

GDP Guanosine diphosphate
GTP Guanosine triphosphate

Н

HCAbs Heavy chain only antibodies
HEK Human embryonic kidney

HTRF Homogeneous time-resolved fluorescence

I

IP3 Inositol 1,4,5-triphosphate
 iGluR Ionotropic glutamate receptor
 IPTG Isopropyl-β-D-1-galactopiranoside

IMAC Immobilized metal affinity chromatography

IB Immunoblotting

iTLC Instant thin layer chromatography

Icv Intracerebroventricular IHF Immunohistofluorescence

IA Injected activity i.p. Intraperitoneal

J

Κ

L

L-DOPA Levodopa

LTP Long term potentiation LTD Long term depression

LB Luria Broth

LgBiT Large binary technology

M

mGluR Metabotropic glutamate receptor

MBq Megabecquerel

Ν

Nb Nanobody

NVU Neurovascular unit

Nb-DC Nanobody-drug conjugate Ni-NTA Nickel-nitriloacetic acid

NanoBiT Nanoluciferase binary technology

NHS Succidimyl

0

P

PET Positron emission tomography

PLC Phospholipase C

PIP phosphatidylinositol 4,5-biphosphate

PKC Protein kinase C

PLA Proximity ligation assay

PAG phosphate-activated glutaminase
PANSS Positive and Negative Syndrome Scale

PCP Phencyclidine
PEI Polyethilamine
PVA Polyvinyl alcohol
PFA Paraformaldehyde
PCP Phencyclidine

PRISMA Preferred Reporting Items for Systematic Reviews and

Meta-Analyses

Q

R

RMT Receptor-mediated transcytosis

RBC Red blood cell

RLU Relative luminescence unit RCT Randomized control trial

RoB Risk of Bias

S

scFv Single chain variable fragments

SNAT sodium-coupled neutral amino-acid transporter

SGA Second generation antipsychotic

Strep Streptavidin

SmBiT Small binary technology
SMD Standardized mean difference
SEM Standard error of the mean

T

TS1R1 Taste receptor 1 TM Transmembrane

TH Tyrosine hydroxylase

TGA Third generation antipsychotic

TR-FRET Time-resolved fluorescence energy transfer

U

UV Ultraviolet

V

VHH Variable domain of heavy chain
VMAT2 Vesicular monoamine transporter 2
VGCC Voltage gated calcium channel

W

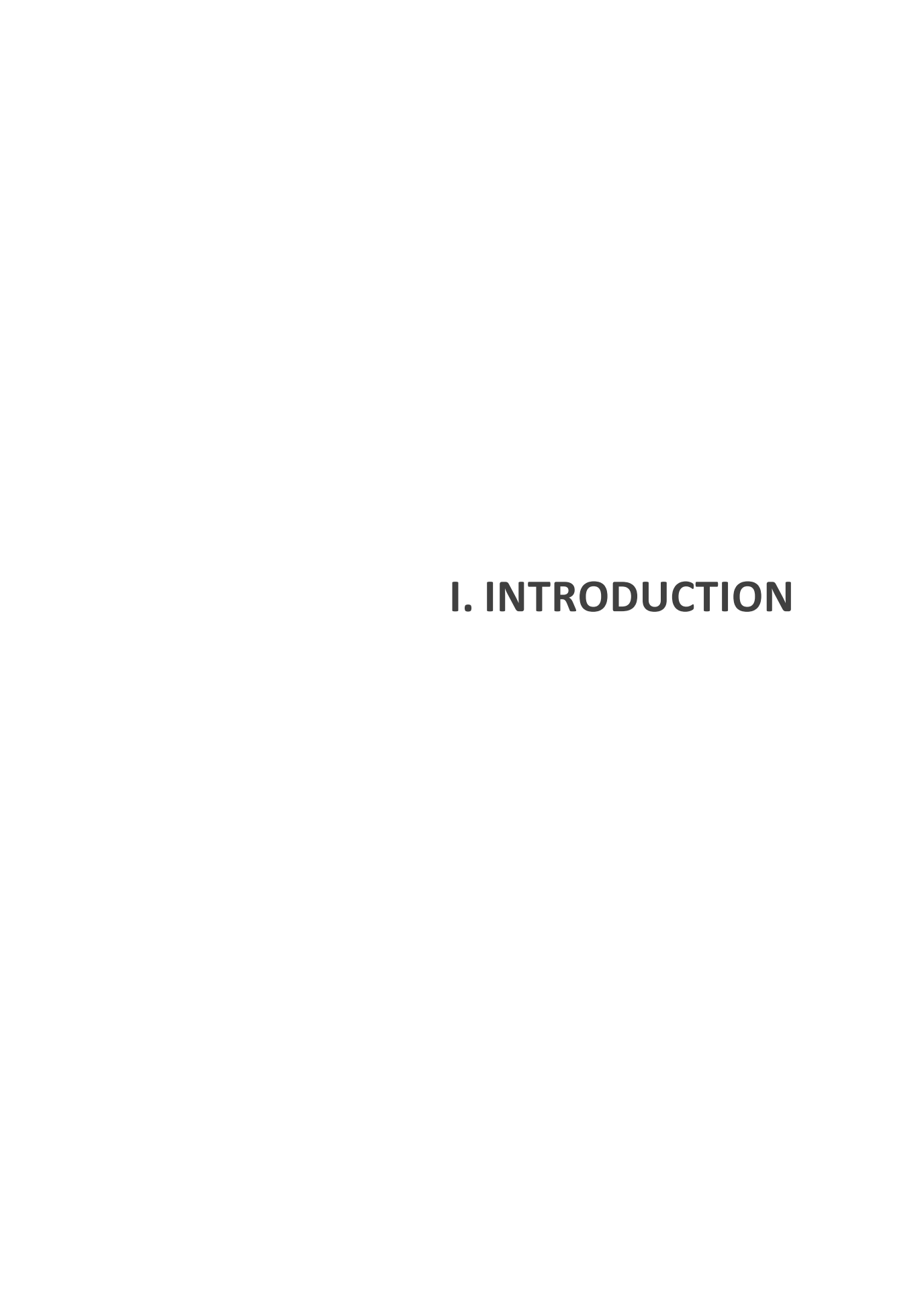
WB Western Blot WoS Web of Science

X

Y

YMRS Young mania rating scale

Ζ



This thesis explores novel therapeutic strategies based on nanobody-based immunotherapies for targeting G protein-coupled receptors (GPCRs) and GPCR heteromers. Given the critical role of these receptors in neurological and psychiatric disorders, special attention is given to their involvement in schizophrenia and bipolar disorder. The introduction will provide an overview of these conditions, the relevance of GPCRs and their heteromers in their pathophysiology, and the potential of nanobody-based approaches.

1. NANOBODIES

Antibody engineering has been extensively used to circumvent limitations of conventional monoclonal antibodies used in therapy, such as immunogenicity, delivery efficiency and production cost. In this context, engineering of smaller fragments of antibodies, such as antigen binding domains (antigen binding fragment (F(ab)) or single chain variable fragments (scFv)), (see Figure 1) significantly improves these limitations [1]. Conventional antibodies consist of heavy and light chains (Figure 1), and their variable domains must be attached to maintain full binding capacity. Consequently, modifications to the variable domains result in reduced affinity compared to the parent antibody and are more susceptible to proteolysis. Interestingly, unlike conventional antibodies, a proportion of antibodies from camelids and cartilaginous fish are devoid of the light-chain and are heavy-chain only antibodies (HCAbs) [2,3]. Therefore, in the case of these antibodies the recognition of the antigen occurs by the virtue of one single variable domain, also known as the variable domain of heavy chain (VHH) (Figure 1) [4,5]. VHHs have been engineered to bear full antigen-binding capacity within a single domain and have been named Nanobody®, a name registered by Ablynx, a Sanofi company working specifically in these proteins [3,4].

Nanobodies (Nbs) offer a wide variety of opportunities in biotechnology, molecular biology, and antibody-based therapy. While conventional antibodies have been extensively studied, nanobody-based technology has not been fully exploited yet [3]. Hereinafter, the properties and advantages of nanobodies are presented.

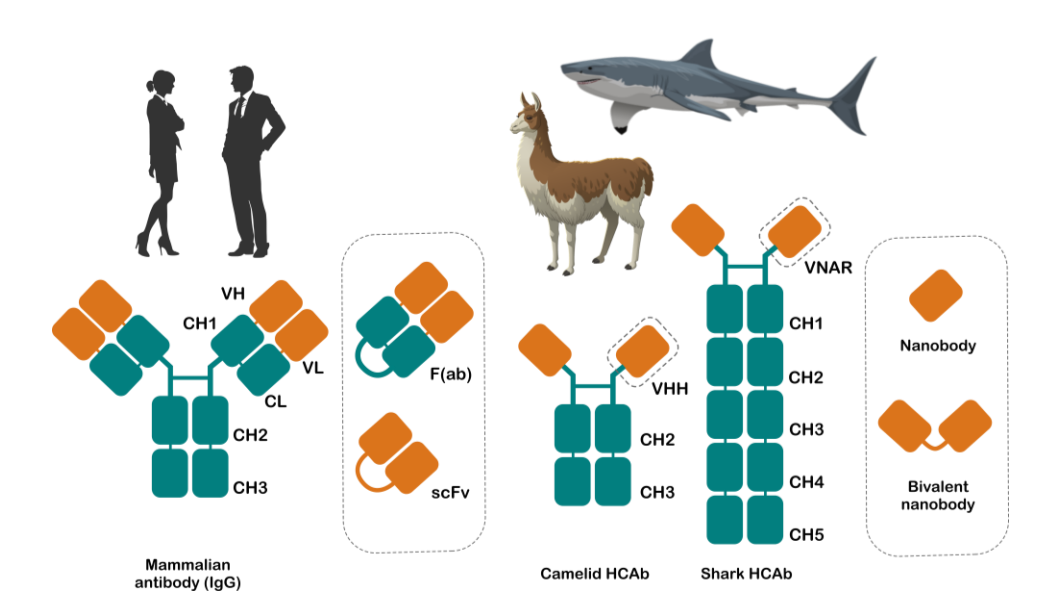


Figure 1. Comparation of mammalian and camelid or cartilaginous fish antibody structure. Mammalian antibodies consist of heavy (H) and light (L chains), whereas camelid and shark antibodies are HCAbs. Moreover, the number of constant (C, blue) and variable (V, orange) regions differ between mammals, camelids and sharks. Engineered antibodies derived from mammalian antibodies are known as F(ab) or scFv; engineered antibodies derived from camelid and shark antibodies are known as nanobodies. Figure created specifically for this thesis using Inkscape software.

1.1 Properties of nanobodies

1.1.1 Structural features

Nanobodies usually adopt typical immunoglobulin fold, which consists of nine β -strands forming two β -sheets connected by loops and by a conserved disulfide bond between cysteines (**Figure 2**) [1,6–8]. This typical

immunoglobulin β -barrel structure is comparable to other mammal's variable domains and indeed, the amino acidic sequence responsible for the immunoglobulin fold is well conserved; only a few amino acids at the framework region 2 (FR2) are distinct and have been shown to increase the solubility of the nanobodies [8–10].

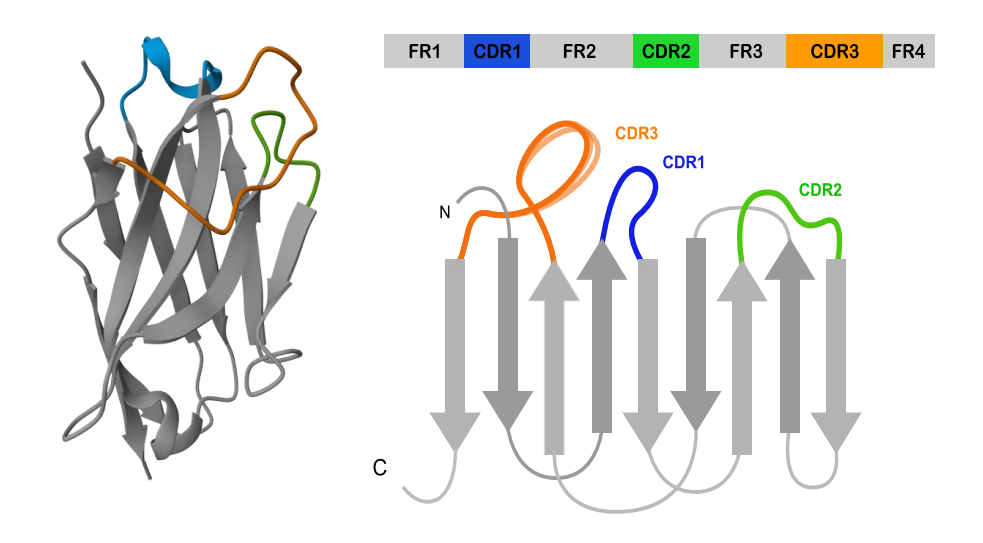


Figure 2. Primary and tertiary structure of a nanobody. In the left, structure of FP specific nanobody hFPNb1 (PDB ID:6RU3). CDR1, 2 and 3 are labeled in blue, green and orange, respectively. Grey arrows indicate β -strands. In the right, schematic representation of nanobody FR1-4 and CDR1-3. The flexibility of CDR3 is represented as several orange lines. Figure created specifically for this thesis using Inkscape software.

The antigen binding region, also known as the paratope, resides in a single domain, resulting in a significantly smaller binding surface compared to the variable domains (V_H) of conventional antibodies (**Figure 1**). The complementarity determining regions (CDRs) drive the extensive variability observed in nanobody libraries [1,8], thereby governing the majority of the antigen binding capability. Notably, nanobodies exhibit an expanded CDR3, typically consisting of an average of 16 amino acids, in contrast to the 9-12 amino acids typically found in conventional V_H domains (**Figure 2**) [1,7,10]. The

enlarged CDR3 is believed to increase the binding surface area and adopt a convex conformation, facilitating access to antigenic cavities or clefts, including receptor-binding pockets and enzyme active sites [11]. Remarkably, nanobodies exhibit a wider array of structural segment combinations for antigen binding and are capable of adopting non-canonical structures within their antigen binding loops [1,7,9,10]. Overall, these attributes are considered to offset the lack of the light chain variable domain (V_L).

1.1.2 Low immunogenicity

Immunogenicity refers to the ability of a substance, such as a therapeutic antibody, to induce an immune response in the body. When antibodies are introduced into an organism, the immune response can lead to the production of anti-drug antibodies (ADAs), which can neutralize the therapeutic effects of the antibody or cause adverse reactions [12]. In this context, nanobodies are thought to have low immunogenicity, due to their high sequence homology to human V_L (86-94%) [3,10]. Moreover, their small size (125 amino acids) might imply fewer epitopes and their high solubility avoids the formation of immunogenic aggregates [3]. Indeed, these attributes promote fast blood clearance and thus reduce exposure time to activate the immune system. In a Phase I clinical study of therapeutic nanobodies, after nanobody administration no ADAs were detected [13,14]. Overall, there is substantial evidence indicating that nanobodies exhibit low immunogenicity in humans, making them particularly suitable for therapeutic applications.

1.1.3 High tissue and blood brain barrier penetration

The effective delivery of therapeutic proteins, particularly antibodies, is constrained by their biodistribution and ability to penetrate tissues. To reach their intended targets, therapeutic proteins depend on processes such as blood extravasation and passive diffusion into tissues. The rate of passive diffusion in

tissues is inversely correlated with the molecular size of the molecule. Therefore, nanobodies, with their small size compared to conventional antibodies, are anticipated to possess superior tissue penetration capabilities [3]. Moreover, in this context, nanobodies are considered to have potential for traversing the blood-brain barrier (BBB) and reaching the central nervous system (CNS) [15,16].

The BBB is a highly selective barrier protecting the CNS by restricting the passage of substances between blood circulation and brain parenchyma. The BBB is composed of various cell types intricately connected within specialized structures known as neurovascular units (NVU). These units comprise brain microvascular endothelial cells (BMECs), pericytes, astrocytes, microglia, neurons, and extracellular matrix components (Figure 3). The tight association between these cells allows the intimate regulation of the cerebral blood flow [16]. BMECs form adherent and tight junctions, which restrict the passive diffusion to small (<400 Da) and lipophilic molecules. On the other hand, BMECs express active transport mechanisms to regulate the passage of essential molecules, while blocking the passage of harmfull molecules [15,17]. Interestingly, specific neuroactive peptides, regulatory proteins, and hormones can cross the BBB through endocytic mechanisms in a process called transcytosis, which relies on the vesicular transport. There are two main types of vesicular transport; one is based on the receptor-mediated transcytosis (RMT) and the other on adsorptive-mediated transcytosis (AMT) [17].

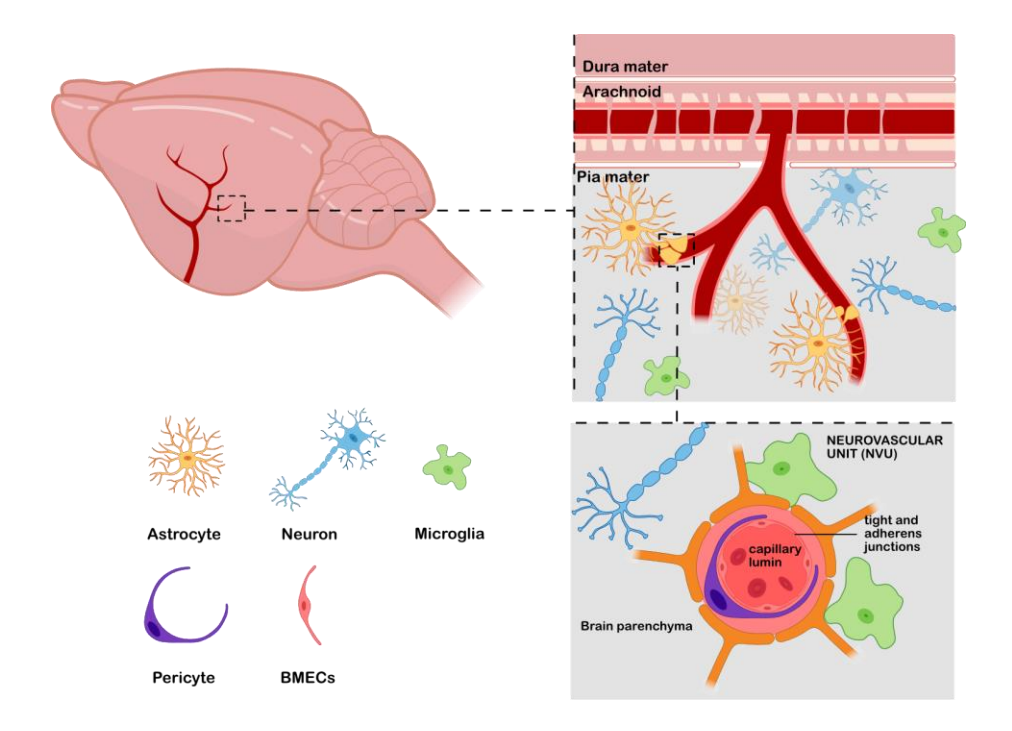


Figure 3. Representation of the BBB. Close-up view of brain capillaries and neurovascular units (NVU) forming the BBB. The NVU serves as the fundamental anatomical and functional structure of the BBB. BMECs form the vessel walls and are enveloped by pericytes and the basal lamina matrix. Surrounding the vasculature, neurons, microglia, and astrocytic endfeet create a dynamic microenvironment that regulates and communicates with the vascular components of the NVU, maintaining barrier integrity and selective permeability. Figure created specifically for this thesis using Inkscape software.

Nanobodies traversing the BBB are known to exploit the physiological mechanisms outlined previously, namely RMT and AMT. Among the pioneering nanobodies facilitating BBB passage through RMT are FC5 and FC44, which respectively target the α (2,3)-sialoglycoprotein receptor and a 36 kDa protein (still under investigation) [18]. These nanobodies are believed to engage their targets and promote clathrin-mediated endocytosis. Furthermore, a nanobody directed against the transferrin receptor has been employed to transport biologically active neurotensin into the brain through RMT [19]. While a limited number of nanobodies has been documented to traverse the BBB via AMT,

these nanobodies typically possess a higher isoelectric point or are modified with positively charged chains to enhance their penetration [16].

1.1.4 Applications of nanobodies

In the three decades since the initial discovery of nanobodies, there has been remarkable progress in their development and diverse applications. These include pivotal roles in structural biology, biosensors, probes for molecular imaging and diagnostics and innovations in therapeutics.

Structural biology. In structural studies, such as X-ray crystallography, protein conformational stability is a key factor. Due to their compact and rigid structure, nanobodies are considered potential chaperones for crystallography. Moreover, nanobodies are thought to recognize conformational epitopes, and usually trap intrinsically unstable conformations. In this context, nanobodies have a large track as crystallography chaperones and several nanobodies have been developed as active-state chaperones for enzymes and membrane proteins [20,21].

Biosensors. Nanobody-based biosensors have emerged as powerful tools for detecting biomolecules with high specificity and sensitivity. Their small size, high stability, and strong antigen-binding affinity make them ideal candidates for biosensing applications. Nanobody biosensors have been successfully integrated into diverse platforms, mainly based on optical, fluorescence and electrochemical techniques. These biosensors enable real-time monitoring of biomarkers [22], pathogens [23], and protein dynamics [24], offering advantages such as rapid detection, low background noise, and improved signal-to-noise ratios.

Molecular imaging. In the field of medicine, molecular imaging serves as a powerful tool for visualizing cellular and molecular processes within the body for diagnostic and therapeutic purposes. Utilizing advanced imaging

techniques, such as positron emission tomography (PET), enables the non-invasive detection, characterization, and monitoring of diseases at the molecular level. Antibodies, commonly employed in cancer molecular imaging, are now being complemented by nanobodies; due to their compact size, tissue-penetrating capabilities, and shorter half-life, nanobodies have potential for more precise imaging studies, with reduced signal-to-noise ratio and fewer adverse effects [3,25].

Therapeutic nanobodies. Nanobody-based therapeutics are revolutionizing medicine, particularly in the treatment of immune-related disorders, cancer, and infectious diseases. Their ability to neutralize disease-associated proteins and modulate signaling pathways has led to the development of several clinically approved treatments. One prominent example is caplacizumab, the first FDA-approved nanobody therapy, which targets von Willebrand factor to treat acquired thrombotic thrombocytopenic purpura (aTTP) by preventing excessive platelet aggregation [26]. Beyond hematology, nanobody-based immunotherapies are being explored to block immune checkpoints such as PD-L1, enhancing antitumor immune responses [27]. In infectious diseases, nanobodies have shown potent antiviral effects against SARS-CoV-2 by directly inhibiting viral entry mechanisms [28].

Nanobody-drug conjugate (Nb-DC). In cancer therapy, the conjugation of cytotoxic drugs to monoclonal antibodies has emerged as a widely utilized strategy to enhance the drugs' selectivity towards specific cells while mitigating serious adverse effects. These biopharmaceuticals typically comprise a monoclonal antibody coupled with a cytotoxic drug via a linker [29]. As linker optimization and the efficacy of antibody-drugs advance, and conjugates continue to evolve, nanobodies have garnered attention for their potential in "cargo delivery". Several Nb-DC have already demonstrated promising results

in preclinical models for cancer therapy, underscoring their potential as a targeted therapeutic approach [3].

1.2 Nanobodies against G protein-coupled receptors

Antibodies have emerged as promising tools in pharmacotherapy due to their high affinity and strong modulatory effects. However, their development faces significant challenges when targeting membrane proteins with limited surface accessibility, such as GPCRs (introduced in the next chapter). In this context, the exploration of antibodies for GPCR-targeted pharmacotherapy appears promising, given their potential as high affinity binders and strong modulators of these proteins. However, challenges arise due to the low expression of GPCRs [30] and their limited exposure on the cell surface, as they are embedded within the plasma membrane [31]. Consequently, generating antibodies against GPCRs proves to be challenging. As anticipated, nanobodies offer several advantages over conventional antibodies. Their structural properties enable the recognition of cryptic or embedded epitopes, close to the membrane. Moreover, their capability to bind conformational epitopes makes them well-suited for targeting conformationally unstable GPCRs [32].

GPCR-targeted nanobodies can be classified as intracellular or extracellular, depending on which domain of the GPCR they bind. Intracellular nanobodies have been extensively studied for the stabilization of different conformations and have been named confobodies [33]. In structural studies, the selection of nanobodies promoting the ligand-bound/active state of the receptor has shed light on the activation mechanism of GPCRs and the structure-based drug design [31]. Interestingly, the preference of nanobodies to bind specific conformations determines their ability to allosterically modulate the receptor. An intracellular nanobody against the β 2-adrenergic receptor (ADRB2), Nb80, binds to the ligand-bound conformation of the receptor and promotes this state by mimicking the $G_{\alpha s}$ -protein binding; indeed, Nb80 increases the binding

affinity of the ligand, therefore promoting positive allosterism [34]. On the other hand, nanobodies may stabilize the inactive conformation and thus are considered antagonists or inverse agonists [31].

Extracellular nanobodies are known to be scarce, probably due to the high sequence similarity and low immunogenicity of the extracellular domain which reduces the immune response in heterologous animals [35]. Most of these are reported to target peptidergic receptors, such as chemokine receptors (CXCR4 [36], ACKR3/CXCR7 [37], CXCR2 [38]); other extracellular nanobodies have been reported to bind selectively metabotropic glutamate receptors (mGluR2 [39] and mGlu₅R [40]). Interestingly, these latter nanobodies are positive allosteric modulators and promote intracellular signaling of these receptors, rendering huge therapeutic potential.

2. G PROTEIN-COUPLED RECEPTORS

GPCRs, also known as seven-transmembrane receptors (7TMRs), are a class of cell surface receptors that respond to a variety of external signals. These receptors are characterized by their ability to activate G proteins upon ligand binding, leading to a cascade of intracellular signaling events. They are involved in various physiological processes, including sensory perception, immune response and neurotransmission. Thus, it is not surprising that a large proportion of modern drugs target GPCRs [41]. In fact, approximately 34% of the US Food and Drug Administration (FDA)-approved drugs are targeted to GPCRs [42].

The diversity of GPCRs is immense, constituting the largest family of membrane proteins, with over 800 members in humans. This variety contributes to their ability to interact with a wide variety of ligands or external stimuli [43]. However, GPCRs share some structural and functional characteristics, allowing their classification and understanding of their role in different physiological

processes. These receptors are classified into five different families in humans [44,45]:

- Class A (Rhodopsin-like) is the largest GPCR family, comprising receptors for various ligands such as hormones, neurotransmitters and sensory signals. Their diversity is attributed to differences within the transmembrane regions. Aminergic receptors, such as dopamine receptors, or nucleotide receptors, such as the adenosine receptors, are class A receptors.
- Class B (Secretin-like) family is relatively small and binds hormones and peptide-hormones at its extracellular domain. Secretin subfamily members are characteristic of large extracellular domains (ECDs) and for instance, these receptors bind to vasoactive intestinal peptide, parathyroid peptide hormone, growth hormone-releasing hormone, calcitonin gene-related peptide, glucagon, and glucagon-like peptides, respectively.
- Class C contains 22 receptors, which are further divided into 5 subfamilies including 1 calcium-sensing receptor (CaSR), 2 gamma-aminobutyric acid (GABA) type B receptors (GABA_{B1} and GABA_{B2}), 3 taste 1 receptors (TS1R1-3), 8 metabotropic glutamate receptors (mGluR1-8), and 8 orphan GPCRs.
- Class F receptors are divided into Frizzled, which bind Wnt glycoproteins, and Taste2, which exhibit considerable sequence diversity and are responsible for the perception of taste.
- Adhesion GPCRs have rich functional domains in the N-termini and have important roles in specific receptor-ligand interactions.

Despite the diversity of GPCRs across different classes, they share several common structural and functional characteristics that define them as a distinct receptor family. All GPCRs are characterized by a core structure that consists of

seven transmembrane helices [41]. These helices span the cell membrane, forming the receptor's framework. The extracellular portions are primarily involved in ligand binding, although some ligands may also interact with transmembrane regions. On the other hand, intracellular loops and domains interact with intracellular signaling proteins. This seven-transmembrane configuration is the hallmark of GPCRs across all classes, despite variations in the specific sequences and binding sites [46].

2.1 GPCR dynamics

The first GPCR to be discovered was the β -adrenergic receptor, which binds to adrenaline and related molecules [47]. This discovery was pivotal and set the stage for understanding the structure and dynamics of this large family of receptors. The identification and characterization of the β -adrenergic receptor were significantly advanced through the work of Robert Lefkowitz who led to the discovery of the active structure of GPCRs and highlighted the dynamic nature of GPCRs, showing that these receptors can adopt multiple conformations [48]. In fact, the ability of GPCRs to change conformations allows them to transmit a signal through the cell membrane. The binding of extracellular ligands, such as chemokines, hormones or neurotransmitters, favors the conformational change from an 'inactive' state to an 'active' state. Active GPCRs favor the binding of G proteins, arrestins and other signaling proteins at the intracellular surface, which generate a signaling cascade (**Figure 4**) [46].

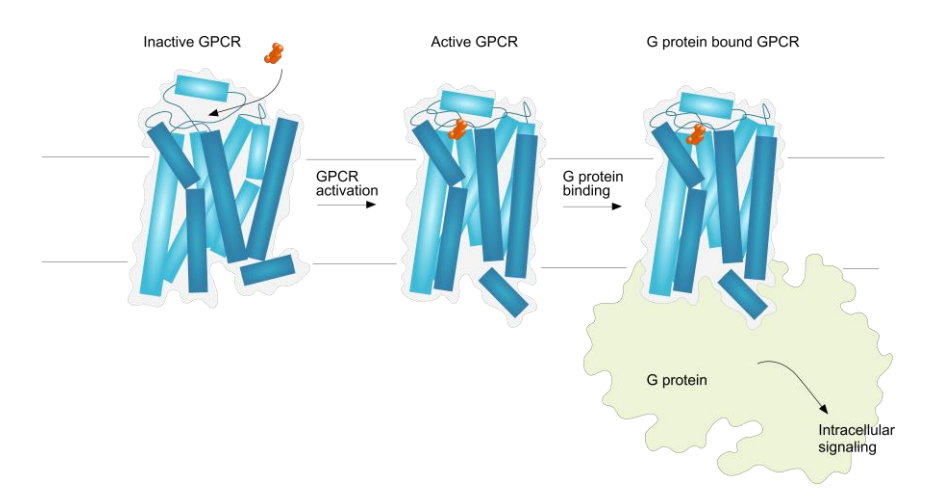


Figure 4. Representation of GPCR ligand binding, activation and G protein coupling. An orthosteric ligand (orange small molecule) binds the inactive GPCR. The ligand-bound GPCR undergoes a conformational change to its active form, which allows the coupling of the G proteins. Figure created specifically for this thesis using Inkscape software.

G proteins, which are integral components in this signaling process, play a crucial role in transmitting the signal received by GPCRs to various intracellular targets. G proteins are heterotrimeric, meaning they are composed of three subunits: $G\alpha$, $G\beta$ and $G\gamma$. Interestingly, G proteins are named after their ability to bind guanine nucleotides, which regulate their activity [49,50]. Indeed, upon ligand binding, the active GPCRs promote the exchange of guanosine diphosphate (GDP) to guanosine triphosphate (GTP) at the G protein nucleotide binding site, which leads to the dissociation of the trimer $G\alpha\beta\gamma$ into $G\alpha$ and $G\beta\gamma$. Both, $G\alpha$ and $G\beta\gamma$ subunits signal to various cellular pathways [51].

 $G\alpha$ subunits are divided into four distinct families, which activate distinct signaling pathways: $G_{s/olf}$, $G_{i/o}$, $G_{q/11}$ and $G_{12/13}$ [51]. $G_{s/olf}$ proteins directly interact with and stimulate the activity of adenylyl cyclases (AC), which increase the concentration of cyclic adenosine monophosphate (cAMP), an intracellular secondary messenger. cAMP molecules bind to protein kinase A (PKA), which in turn modulates various cellular functions. On the other hand, the inhibitory

 $G_{i/o}$ protein reduces cAMP intracellular levels and thus reduces PKA activity [52]. $G_{q/11}$ protein interacts with phospholipase C (PLC) and promotes the lysis of the membrane bound phosphatidylinositol 4,5-biphosphate (PIP₂) to diacylglycerol (DAG) and inositol 1,4,5-triphosphate (IP₃), two important second messengers [53]. DAG remains in the membrane and activates protein kinase C (PKC), whereas IP₃ stimulates the release of Ca²⁺ to the cytosol from intracellular organelles [54]. Finally, $G_{12/13}$ proteins interact with Rho guanine nucleotide exchange factors, which are implicated in the modulation of cytoskeleton dynamics [50]. Although the role of G $\beta\gamma$ was thought to be passive at first, later studies showed that it interacts with several effectors and modulates intracellular signaling. For instance, $G\beta\gamma$ subunits have been shown to directly interact and modulate membrane ion channels [55]. Moreover, $G\beta\gamma$ has been shown to interact with phospholipases and GPCR kinases (GRKs) (Figure 5) [50].

GRKs are serine threonine kinases, which are responsible for the phosphorylation of the third intracellular loop or C-terminal of the active GPCRs. This phosphorylation is known to induce the desensitization of the receptor [56]. Specifically, GPCR phosphorylation is known to promote the recruitment of β -arrestins, which displaces coupled G proteins. Moreover β -arrestins promote the internalization and trafficking of the GPCR to intracellular compartments by the recruitment of certain endocytic proteins such as clathrin and its adaptor protein (AP-2). However, β -arrestins are not only scaffolding proteins, and are known to initiate signaling cascades; for instance, GPCR phosphorylation and β -arrestin coupling can activate the tyrosine kinase c-Src signaling and ERK activation [57].

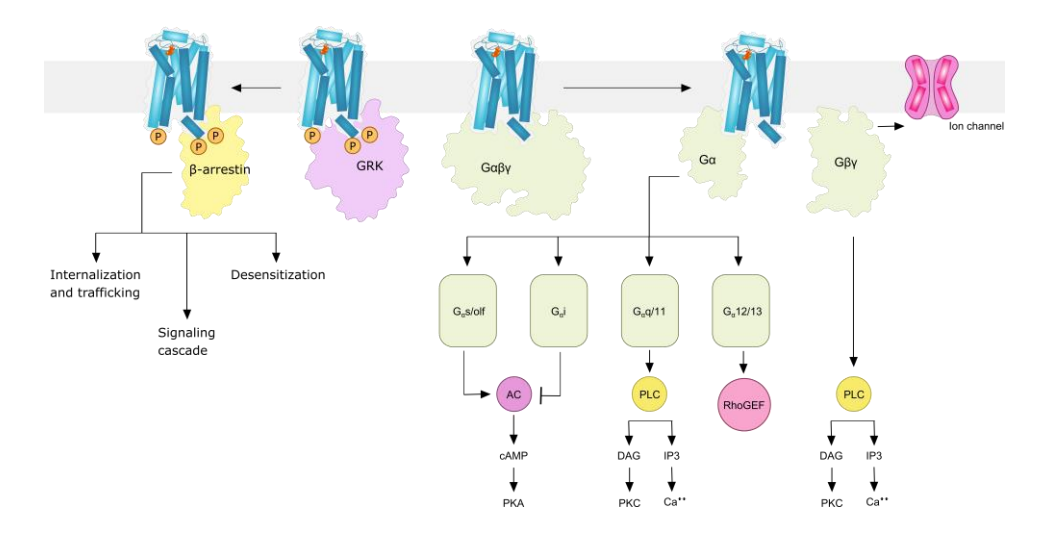


Figure 5. GPCR activation and signaling cascade. The coupling of the G protein to the active GPCR promotes the exchange of GDP to GTP, which allows the dissociation of $G\alpha$ and $G\gamma\beta$ subunits. The G protein subunits activate downstream enzymes and ion channels, modulating the levels of intracellular second messengers. The GPCR can be desensitized by phosphorylation (P), internalized, and promote alternative signaling responses. Figure created specifically for this thesis using Inkscape software.

It is worth noting that each GPCR is selective for certain G proteins and can signal differently depending on the cell type they are expressed or the cellular context, which confers them high versatility for the modulation of diverse physiological processes. Different isoforms of G proteins, GRKs and β -arrestins are expressed in a cell type-specific manner and therefore confer distinct GPCR signaling properties [56].

On the other hand, it is important to mention that some GPCR ligands can induce biased signaling, which refers to the ability to selectively activate specific signaling pathways through the same receptor. Understanding biased signaling has important implications for pharmacology, as it allows researchers to target specific signaling cascades, leading to more precise and effective therapies [58].

2.2 GPCR-Effector Membrane Macromolecular Assemblies

The concept of GPCR-Effector Membrane Macromolecular Assemblies (GEMMAs) was established by S. Ferré et al. (2022) and is defined as a preassembled signaling complex composed of a particular combination of GPCRs, G proteins, effectors and other associated transmembrane proteins localized to the plasma membrane. This model suggests that rather than a collision model, GPCR signaling is mediated by subtle conformational changes and adaptation upon ligand interactions, allowing more efficient interactions between specific signaling components [59]. In this context, it is important to underline that GPCRs usually form oligomers by interacting with identical receptors (homomers) or distinct receptors (heteromers). Moreover, these receptor oligomers are known to functionally interact and allosterically modulate the activity of the interacting receptors [60]. Currently, there is evidence of the formation of oligomers for many GPCRs, based on biochemical, biophysical and pharmacological studies (Table 1) [61-63]. Thus, in the last years oligomers have gained increasing recognition and relevance for drug targeting and design [64].

Table 1. Biochemical, biophysical and pharmacological studies of relevant heterodimers. Co-IP: co-immunoprecipitation, PLA: Proximity Ligation Assay, BRET: Bioluminescence Resonance Energy Transfer, TM: transmembrane, BiFC: Bimolecular Fluorescence Complementation, WB: Western Blot. Adapted from [24]

LIETEROMER		FUNCTIONAL INTERACTION							
HETEROMER	PHYSICAL INTERACTION	Ligand binding GPCR conform		GPCR signaling	GPCR trafficking				
D ₂ R-A _{2A} R	co-IP, PLA, BRET, TM pept.	Radioligand		cAMP assay, NanoBiT	Fluorescence imaging				
D_1R-D_2R	co-IP, PLA, BiFC, FRET, TM pept.		cpFP biosensor	cAMP, Ca++ assays, WB, promotor assay					
$A_{1A}R-D_1R$	co-IP			cAMP assay	Fluorescence imaging				
5HT2A-D₂R	co-IP, FRET, BRET	Radioligand		Ca++ assay, WB, Promoter assay					
$A_1R-A_{2A}R$	co-IP, BiFC, FRET, TM pept			cAMP assay, NanoBiT					
A _{2A} R-CB1	co-IP, BiFC, FRET, TM pept			cAMP assay, Promoter assay					
5HT2A-CB1	co-IP, BiFC, FRET, TM pept			cAMP assay, WB					
CB1-CB2	PLA, BRET			WB					
$A_{2A}R$ - $mGlu_5R$	co-IP, FRET, BiFC,			Ca++ assay, WB					
δOR-κOR		Radioligand		cAMP assay, WB	Flow cytometry				

3. NEUROTRANSMISSION

Neurotransmitters are essential chemical messengers that facilitate communication between neurons, modulating a wide range of physiological and cognitive functions. Different neurotransmitter systems, such as the dopaminergic, serotoninergic, endocannabinoid or adenosinergic, regulate distinct processes in the brain and body, such as reward, motor function, cognition or appetite. Typically, each neurotransmitter system is defined by the neurotransmitter it releases and includes the following elements: the neurotransmitter, receptors, presynaptic and postsynaptic neurons that form a synapse, transporters, enzymes and glial cells.

3.1 Dopaminergic system

Dopamine was first synthesized in 1910 and was initially considered a precursor to the catecholamines epinephrine and norepinephrine [65]. It was later in 1950 when Arvid Carlsson recognized dopamine as an independent neurotransmitter [66]. Research on the dopamine metabolism soon led to the association between dopamine and Parkinson's disease. Other disorders, such as schizophrenia and addiction, have been also associated with dopamine metabolism or signaling, emphasizing the importance of the dopaminergic system for optimal neurological and physiological function [65].

Dopamine is synthesized by dopaminergic neurons, which are a diverse group of neuronal cells. These neurons are located in several brain regions, including the diencephalon, mesencephalon, and telencephalon (specifically, the olfactory bulb and the retina). The most prominent concentration of dopaminergic neurons is found in the ventral part of the mesencephalon, housing approximately 70% of the brain's dopaminergic neurons [67,68]. These neurons play a crucial role in regulating various physiological functions such as movement, reward, and learning. The mesencephalic dopaminergic neurons in

particular, are involved in controlling three main neural circuits: the nigrostriatal, mesolimbic, and mesocortical pathways (Figure 6). Each of these pathways are essential for distinct aspects of brain function, including motor control, motivational processes, and cognitive functions [68].

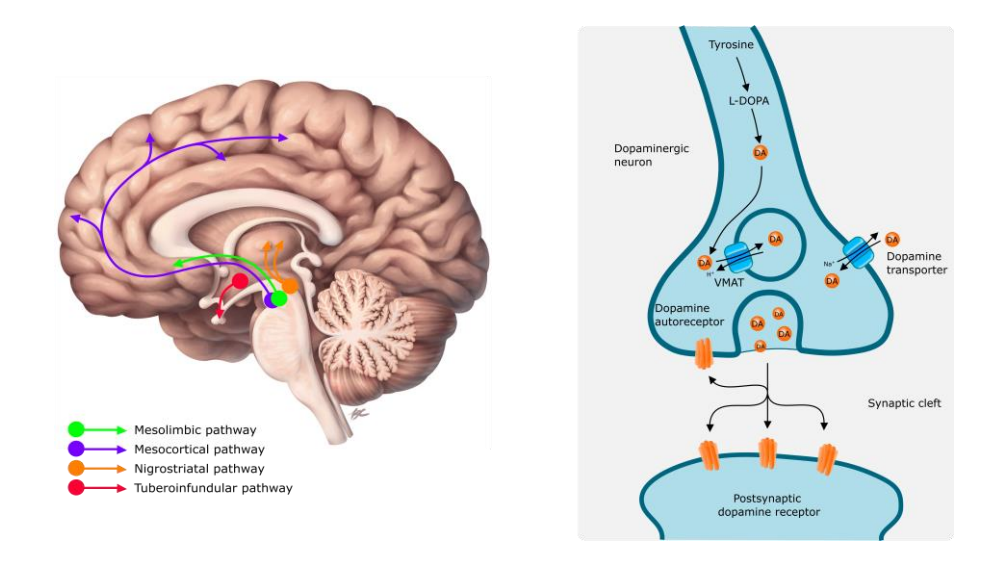


Figure 6. Dopaminergic neurotransmission and metabolism. On the left, sagittal view of a human brain and representation of the dopaminergic projections. On the right, representation of a dopaminergic synapse, showing a presynaptic and a postsynaptic neuron. Dopamine (DA) is synthesized in presynaptic neurons and stored in presynaptic vesicles. Upon stimulation, presynaptic vesicles release DA to the synaptic cleft where they bind dopamine postsynaptic or auto-receptors. Figure created specifically for this thesis using Inkscape software.

Dopaminergic neurons are characterized by the expression of enzymes of the dopamine synthesis and metabolism. Dopamine is synthesized by the tyrosine hydroxylase (TH) enzyme, which catalyzes the addition of a hydroxyl group to the amino acid tyrosine to convert it to levodopa (L-DOPA), which is then decarboxylated to convert it to dopamine. Once synthesized, the vesicular monoamine transporter 2 (VMAT2) accumulates the dopamine into vesicles to be released to the synaptic cleft (**Figure 6**) [69]. Synaptic dopamine binds and signals through dopamine receptors, that are divided into five different subtypes: D_1 - D_5 receptors. These receptors are subclassified into two groups:

(i) D_1R -like receptors (D_1R and D_5R) predominantly signal through $G_{s/olf}$ and consequently produce an intracellular cAMP increase; (ii) D_2R -like receptors (D_2R , D_3R , and D_4R) couple to $G_{i/o}$ proteins and consequently reduce the accumulation of cAMP inside the cell. Therefore, dopamine is either excitatory or inhibitory depending on which subtype of receptors is present on the cell membrane and how these neurons respond intracellularly [68]. Among the various dopamine receptor subtypes, we will focus on the D_2R due to its implication in schizophrenia and psychotic disorders.

3.1.1 Dopamine D₂ receptor

 D_2Rs are widely expressed throughout the CNS with high densities in the dorsal striatum and nucleus accumbens [70]. These brain regions are integral to motor function, motivation and reward pathways. However, D_2Rs are also expressed in the periphery, including the pituitary gland, and various organs such as the kidneys and the gastrointestinal tract [70]. Within the CNS, D_2Rs are found pre- and postsynaptically. Presynaptic receptors act as autoreceptors, inhibiting dopamine release and modulating synaptic transmission. Postsynaptic receptors are primarily involved in mediating the receptor's inhibitory effects on neural activity and excitability. This dual localization highlights the receptor's role in fine tuning dopaminergic signaling [71,72].

The implication of D_2R on motor control and voluntary movement has been well established by studying its role in Parkinson's Disease, where the loss of dopaminergic neurons in substantia nigra leads to motor dysfunction. On the other hand, its involvement of D_2R dysregulation on mood, cognitive processes and motivation control has been associated with schizophrenia, where dysregulation of D_2R activity in specific brain regions contributes to psychotic symptoms and cognitive decline [73].

3.2 Glutamatergic system

Glutamate is a ubiquitous amino acid in mammals and a key molecule in metabolism, energetics and signaling. It is abundant in the blood, but it does not cross the BBB, and thus it is synthesized in the brain from glucose.

Glutamate was first identified as a neurotransmitter by T. Hayashi who observed a rapid yet potent depolarizing effect on cortical neurons [74]. Later studies confirmed that glutamate meets all the criteria to be identified as a neurotransmitter: (i) it is accumulated in presynaptic synaptosomes; (ii) it is released upon physiological stimulation; (iii) it produces a physiological response with the naturally occurring receptors, which can be counteracted by antagonists; (iv) its response can be rapidly terminated by physiological mechanisms [75].

Besides neurotransmission, glutamate plays a key role in energy metabolism and the biogenesis of proteins. In fact, glutamate synthesis is an intricate metabolic process orchestrated by neurons and astrocytes, the so-called glutamate-glutamine cycle (Figure 7). Transporters in neuronal and astrocytic membranes are responsible for the maintenance of low glutamate levels at the synaptic cleft, in order to avoid excitotoxicity and ensure subsequent excitatory events [76]. Nevertheless, astrocytes are thought to be responsible for the synaptic uptake and recycling of glutamate, whereas a minor fraction is recovered by neurons. Mainly astrocytes express the glutamine synthetase (GS) enzyme, which converts glutamate into glutamine [77]. Synthesized glutamine can be transported from astrocytes to neurons by diverse glutamine transporter isoforms (sodium-coupled neutral amino-acid transporters (SNATs)) [78]. In neurons, glutamine can be converted back to glutamate by the phosphate-activated glutaminase (PAG) [79]. Although the glutamate-glutamine cycle is the main source of neuronal glutamate

replenishment, glutamate can derive from different metabolic pathways, and it is finely intertwined with the cytosolic energy metabolism [76].

Glutamate can bind two distinct types of receptors, ionotropic glutamate receptors (iGluR) and metabotropic glutamate receptors (mGluRs). The ionotropic receptors are divided into NMDA receptors (NMDARs) and AMPA/kainate receptors, which are both cation-specific ion channels. On the other hand, mGluRs are type C GPCRs and thus signal transduction is mediated by G proteins [80]. These receptors are differentially expressed throughout the CNS and mediate distinct responses upon ligand binding [80,81].

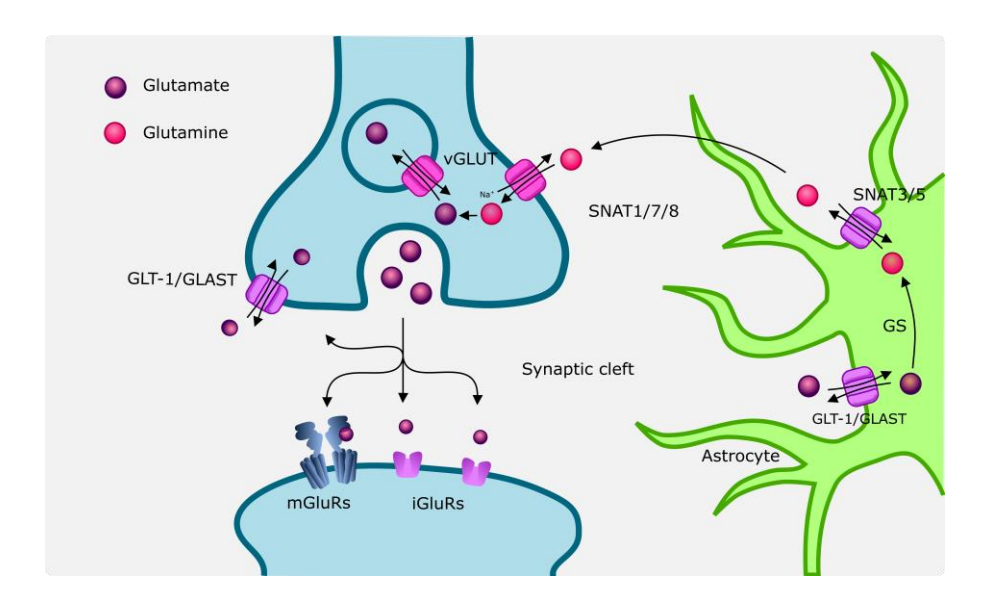


Figure 7. Glutamate-glutamine cycle. GLT1/GLAST transporters in astrocytes clear Glu from the synaptic cleft. Astrocytes then convert Glu into Gln through glutamine synthetase (GS). Gln is released from astrocytes through sodium-coupled neutral amino acid transporter (SNAT)3 and SNAT5 and taken up by neurons through SNAT1/7/8, where it is converted back to Glu by phosphate-activated glutaminase (PAG). This regenerated Glu is packaged into synaptic vesicles by vesicular glutamate transporters (VGLUTs) and released into synaptic cleft for subsequent excitatory neurotransmission. Figure created specifically for this thesis using Inkscape software.

There are 8 subtypes of mGluRs, which are subclassified into three distinct groups, based on their sequence homology and pharmacological properties: group I comprises mGlu₁R and mGlu₅R, group II comprises mGluR₂ and mGluR₃ and, group III comprises mGlu₄R, mGlu₆R, mGlu₇R and mGlu₈R. mGluRs are characterized by a large N-terminal domain, known as the Venus flytrap domain; this domain is responsible for the binding of glutamate and mediates large conformational changes in the activation process, which promote the dimerization of the receptors and signal transduction [82].

3.2.1 Metabotropic glutamate receptor 5

mGlu $_5$ R is widely expressed in both the developing and adult brain, with its highest levels observed in the hippocampus, dorsal and ventral striatum, cerebral cortex and amygdala [83]. These brain regions are crucial for cognition, emotion processing, and motor control, aligning with the receptor's role in synaptic plasticity and learning. In neurons, mGlu $_5$ R is predominantly located postsynaptically, where it modulates excitatory synaptic transmission and interacts with other neurotransmitter systems [83,84].

At the physiological level, $mGlu_5R$ plays a key role in synaptic plasticity, influencing both long-term potentiation (LTP) and long-term depression (LTD). In the hippocampus, $mGlu_5R$ -mediated signaling supports the induction of LTP, a process critical for memory storage [85]. In contrast, its role in LTD, especially within the striatum and other basal ganglia structures, is crucial for motor learning and behavioral adaptations [86]. Positive allosteric modulators of $mGlu_5R$ have shown high therapeutic potential for CNS diseases and there is an increasing interest in the development of potent, selective positive allosteric modulators [87].

3.3 Adenosinergic system

Adenosine is a purine nucleoside, ubiquitous in general metabolism, and is commonly known as the building block of the molecule adenosine triphosphate (ATP). Unlike classic neurotransmitters, adenosine (Ado) is not released from vesicles to the synaptic cleft but rather results from the intracellular metabolism of the cells; for this reason, adenosine is considered a neuromodulator [88,89].

At the synaptic cleft, adenosine can result from the hydrolysis of ATP, which is usually co-released with other neurotransmitters such as glutamate, noradrenaline, GABA, dopamine and acetylcholine. Extracellular membrane enzymes CD39 and CD73 convert synaptic ATP to adenosine diphosphate (ADP)/ adenosine monophosphate (AMP) and AMP to adenosine, respectively. Indeed, this adenosine source is considered the *rapid* extracellular conversion [90]. However, extracellular adenosine levels are continuously balanced, and never fall to zero, thanks to the membrane equilibrative nucleoside transporters 1 and 2 (ENT1 and ENT2), which allow adenosine to cross the membrane bidirectionally. Additionally, it is noteworthy that not only neurons but also non-neuronal cells such as glial cells, contribute to the metabolism of adenosine (Figure 8) [88].

Moreover, adenosine can be phosphorylated by the adenosine kinase (ADK) and converted to AMP, or deaminated into inosine by intracellular or extracellular adenosine deaminase (ADA).

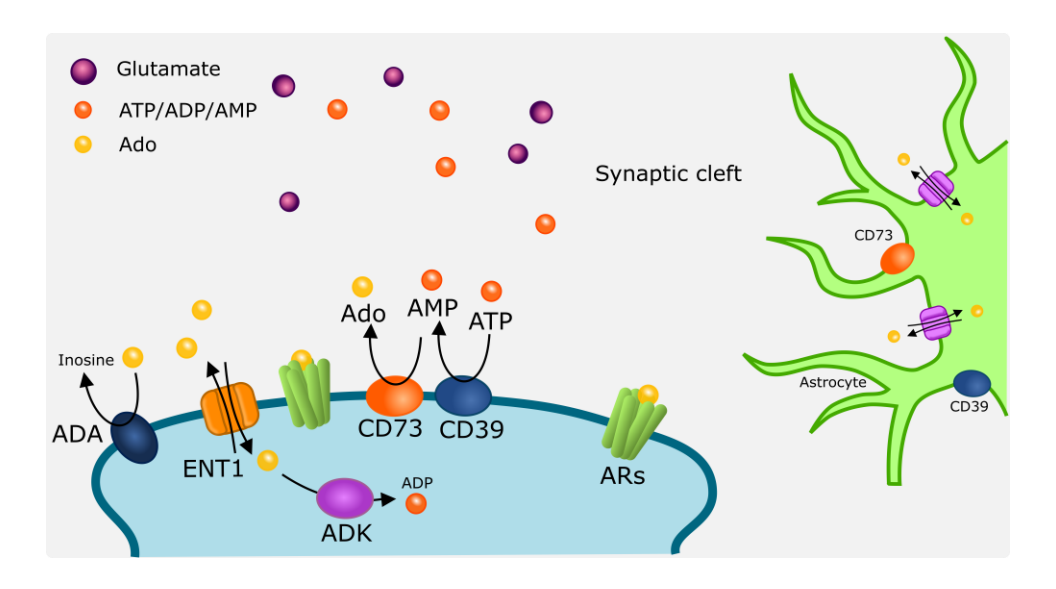


Figure 8. Schematic representation of adenosine synthesis and metabolism in the CNS. Adenosine and ATP/ADP/AMP can be co-released by neurons or equilibrated by membrane transporters (ENT1/2). Adenosine can be metabolized by membrane ectonucleotidases CD39 and CD73, and adenosine is converted to inosine by adenosine deaminase (ADA). Glial cells also participate in the adenosine metabolism. Figure created specifically for this thesis using Inkscape software.

Adenosine exerts a paracrine function at the cellular signaling and serves as a homeostatic factor. As a neuromodulator in the brain, it has an important role controlling neuronal excitability. Extracellular adenosine exerts its effects through adenosine receptors (ARs), a well-conserved family of class A GPCRs. Adenosine receptors are subdivided into four distinct subtypes (A_1R , $A_{2A}R$, $A_{2B}R$, and A_3R) which have particular physiological and pharmacological properties and are differentially expressed throughout all the organism [91]. A_1R and $A_{2A}R$ are widely expressed in the CNS, while all ARs are expressed in the periphery, mainly in the vasculature and immune system. ARs play distinct roles in regulating various physiological processes, such as neuronal excitability, neuroprotection, modulation of the immune response, and vascular tone [90].

3.3.1 Adenosine A_{2A} receptor

As mentioned above, $A_{2A}R$ is a GPCR expressed vastly across the organism; high levels of the receptor can be found at the brain's striatum, immune cells, thymus, leukocytes and platelets, and intermediate levels can be found in the heart, lungs, and blood vessels [90]. As a G_s -coupled receptor, it stimulates the production of cAMP and activates PKA; indeed, $A_{2A}R$ is known to modulate neuronal excitability, neurotransmitter release and synaptic plasticity.

It is worth noting that $A_{2A}R$ colocalizes with D_2R in certain brain regions and form heteromeric complexes which have been strongly associated with motor control. Indeed, $A_{2A}Rs$ have been shown to negatively modulate the activity of D_2Rs , either by allosteric mechanisms or intracellular signaling pathways. In fact, $A_{2A}R$ antagonists are used to increase the D_2R activity in the dorsal striatum, which has implications for Parkinson's disease [92]. Additionally, $A_{2A}R$ influences working memory and reward in the hippocampus and ventral striatum, respectively [93].

4. PSYCHIATRIC DISORDERS

4.1 Schizophrenia

4.1.1 Definition, epidemiology and etiology

Schizophrenia is a severe mental disorder characterized by a spectrum of symptoms, including positive symptoms, like delusions and hallucinations, negative symptoms, such as anhedonia and social withdrawal, and cognitive deficits, like impaired working memory and cognitive flexibility [94]. Affecting roughly 1% of the global population, schizophrenia stands among the top 10 causes of disability worldwide. Typically, schizophrenia manifests during late adolescence and early adulthood, specifically in the second and third decades

of life. Importantly, schizophrenia does not initially present psychotic symptoms; instead, it often begins with a decline in social and cognitive functioning, known as the psychosis prodrome [95]. Consequently, schizophrenia is associated with significant personal and societal costs, as well as substantial morbidity and mortality [96].

Schizophrenia is a complex disorder affected by multiple factors, both genetic and environmental. The heritability of this disease was described with familial and twin studies, and it has been shown that genetics contribute up to 60-80% of the disease etiology [95,97]. Genome-wide association studies have revealed common and rare alleles associated with schizophrenia; interestingly, loci linked to schizophrenia converge into genes implicated in functions such as neurodevelopmental processes, glutamatergic and dopaminergic synaptic activity, inflammation, or synaptic plasticity [95,96,98]. Although schizophrenia has a well-established genetic component, it is widely recognized that the risk for developing the disorder in the general population arises from complex gene-environment interactions and epigenetic mechanisms shaped by environmental factors. Epidemiological studies have identified several risk factors, including obstetric complications, trauma, social adversities, social isolation, migration, and substance abuse, such as cannabis and other drugs [99].

In the absence of reliable biological markers and given the complexity of mental disorders, diagnosis relies on a clinical evaluation of the patient's symptoms and behavior. Commonly, psychiatrists diagnose schizophrenia based on the Diagnostics and Statistical Manual of Mental Disorders (DSM-V, 2013) or the International Statistical Classification of Disease and Related Health problems (ICD-11, 2019). The main criteria are based predominantly on the positive symptomatology as shown in **Table 2**.

Table 2. Diagnostic criteria extracted from DMS-V

- Diagnostic criteria for schizophrenia
 - A. *Characteristic symptoms*: Two (or more) of the following, each present for a significant portion of time during a 1-month period (or less if successfully treated):
 - (1) Delusions
 - (2) Hallucinations
 - (3) Disorganized speech (e.g. frequent derailment or incoherence)
 - (4) Grossly disorganized or catatonic behavior
 - (5) Negative symptoms, i.e., affective flattening, alogia, or avolition

In the study of schizophrenia psychopharmacology, symptom severity is measured using The Positive and Negative Syndrome Scale (PANSS). This scale evaluates five distinct factors within the symptomatology of schizophrenia: positive, negative, excitation, anxiety/depression and disorganization (cognitive) factors [100].

4.1.2 Neurotransmission in schizophrenia

Neurotransmitter abnormalities have a significant role in schizophrenia pathophysiology. The dopamine hypothesis of psychosis has become a classic and one of the most enduring ideas in schizophrenia. However, increasing evidence implies multiple neurotransmitter systems, such as serotonin, glutamate, adenosine and cholinergic networks as well as dopamine networks in its pathophysiology and treatment. In this chapter, the dopaminergic hypothesis, glutamatergic hypothesis and adenosinergic hypothesis will be introduced [101].

Dopaminergic hypothesis

The dysfunction of the dopaminergic system has long been considered the most widely accepted hypothesis regarding the pathophysiology of schizophrenia. This hypothesis gained support from the observation that first-generation antipsychotics exerted their effects by blocking dopamine D_2 receptors (covered in the following section). Molecular imaging studies provided additional evidence by demonstrating high D_2/D_3 receptor occupancy by various antipsychotics, providing clinical validation for the dopamine hypothesis in antipsychotic drug action [102]. Additionally, different antipsychotics have been shown to have variable occupancy rates, which correlate with their receptor affinity [103]. Moreover, it has been reported that drugs that promote dopamine release, such as amphetamines, exacerbate psychosis in patients with schizophrenia and can induce schizophrenia-like symptoms in healthy individuals if given repeatedly or at high doses [104].

In schizophrenia, the strongest evidence on dopaminergic system dysfunction is reported on the presynaptic dopamine activity [105]. Several different approaches of PET studies have been conducted, providing insight into the dopamine synthesis and release capacity in schizophrenia patients; all studies have consistently demonstrated an increase in presynaptic dopamine in the striatum [106]. Interestingly, the site of action of antipsychotics, along with animal models, suggest that the limbic striatal locus is the primary locus of dopamine dysfunction in the striatum [107]. Thus, the mesolimbic hypothesis of schizophrenia has been widely accepted as the main explanation for the positive psychotic symptoms. Indeed, the positive psychotic symptoms, such as hallucinations and delusions, could be explained by an aberrant salience, mediated by a dysregulated dopamine transmission [108]. However, the whole schizophrenic symptomatology (i.e. negative and cognitive symptoms) cannot be fully explained by the mesolimbic hypothesis.

Interestingly, subcortical hyperdopaminergia has been proposed as secondary to cortical hypodopaminergia, potentially explaining the cognitive and negative symptoms of schizophrenia. However, a common factor may underlie both processes without clarifying which is primary. While cortical dysfunction remains a possibility, studies in mice overexpressing striatal D2 receptors suggest that striatal dopaminergic dysfunction alone could drive deficits in motivation and cognition [109], indicating its role in both psychosis and negative symptoms [110].

Due to the strong implication of the dopaminergic system in schizophrenia, many aspects of dopamine metabolism and neurotransmission have been studied. Changes in dopamine receptor density and dopamine transporter levels have not been observed. Although there is little evidence of D₂R density increase in schizophrenia patients, this has been linked to antipsychotic treatment rather than a hallmark of schizophrenia pathophysiology [105]. On the other hand, post-mortem studies show inconsistent results on the expression of dopamine transporter (DAT), tyrosine hydroxylase and VMAT [110].

Experimental evidence supports that the implication of dopamine in schizophrenia is strong. Nonetheless, dopamine alterations do not explain the full spectrum of the clinical symptomatology and they fail to explain the mechanisms underlying resistance to antipsychotic treatment. Therefore, alterations in other neurotransmitter systems have been hypothesized to be involved in the pathophysiology of schizophrenia.

Glutamatergic hypothesis

The initial link between glutamate and schizophrenia emerged from reports where catatonic schizophrenia patients were treated with glutamic acid [111]. Subsequent studies investigated abnormalities in the glutamatergic

system, and reduced glutamate levels were observed in the cerebrospinal fluid (CSF) of schizophrenia patients, although this finding was not consistently replicated [110]. Despite this, evidence supporting the involvement of the glutamatergic system in schizophrenia has grown. The glutamate hypothesis of schizophrenia was first proposed in 1991, based on observations that NMDAR antagonists such as phencyclidine (PCP) and ketamine can mimic positive, negative, and cognitive symptoms in healthy individuals and exacerbate these symptoms in schizophrenia patients [112]. Thus, the evidence on NMDAR hypofunction led to more extensive exploration, considering the glutamatergic system a major hallmark of schizophrenia pathophysiology [113]. Although many glutamate receptors have been implicated, the prevailing hypothesis is for the primary involvement of NMDA receptor dysfunction. Thereafter, NMDAR blockade in rodents was proposed as a pharmacological animal model of the disease. Although this model primarily intends to assess specific endophenotypes, NMDAR blocking has been shown to effectively mimic schizophrenia-like symptoms, such as positive symptoms, negative symptoms, and cognitive deficits in rodents [114–116].

Moreover, several studies have identified genetic mutations and single nucleotide variations (SNVs) in glutamatergic genes. Specifically, variations in NMDAR subunit genes (*GRIN2A*, *GRIN2B*) [117], NMDAR postsynaptic complex genes (*CACNA1C*) [118], or metabotropic group I receptor genes (*GRM5*, *GRM7*) [117] have been associated with the disease. Consequently, genetic mouse models, such as Grin1 mutants and group I metabotropic receptor knockouts, have been extensively studied, each model displaying distinct phenotypic outcomes [115].

Models involving the administration of NMDAR antagonists have suggested that NMDAR hypofunction could account for the negative symptoms and cognitive deficits in schizophrenia. It is proposed that NMDAR antagonists

act preferentially on fast-spiking GABA interneurons within the limbic circuit, which results in a decreased GABAergic inhibition of glutamatergic pyramidal cells [113]. The disinhibition of these pyramidal cells could result in elevated and uncoordinated firing across the corticolimbic circuit, which has been shown to have consequences on neurodevelopment and changes in cognition [119].

Adenosinergic hypothesis

The first evidence on the implications of adenosine on the pathophysiology of schizophrenia was the observation that the adenosine levels were significantly lower in peripheral blood and CSF samples of schizophrenic patients [120]. Although these results were not consistent, it set a precedent for the adenosinergic hypothesis of schizophrenia. Later studies suggested a possible disturbance of intracellular energy formation in schizophrenic patients, addressing ATP metabolism in peripheral blood cells [121,122].

Moreover, clinical studies in the early 70s showed that inhibitors of the adenosine reuptake, such as dipyridamole, improved schizophrenia symptomatology [123]. Further pharmacological studies demonstrated that adenosine agonists could exert antipsychotic effects; specifically, Ferré et al. (1997) reported that adenosine A_{2A} receptor agonists could counteract the psychotomimetic effects of dopamine receptor agonists in animal models [124].

This evidence led to the adenosinergic hypothesis of schizophrenia, which postulates a hypoadenosinergic state of the brain in schizophrenic patients. This was supported by the observed alterations on the expression or activity of different adenosine-metabolizing enzymes [125]. In 2006, Lara et al. first proposed that adenosine imbalance could contribute to the pathogenesis of schizophrenia [126].

Accordingly, in the last two decades purinergic drugs have been used in clinical trials as antipsychotic adjuvants. Specifically, nucleoside transporter inhibitors, such as allopurinol or dipyridamole, have shown efficacy in reducing general symptomatology in schizophrenic patients [127].

Overall, it has been suggested that strengthening of the adenosinergic signaling could be a promising therapeutic approach for the treatment of positive and negative symptoms of schizophrenia [128].

4.1.3 Pharmacology in schizophrenia

The gold standard of schizophrenia therapy is the use of antipsychotics, which are broadly divided into two groups: typical (first generation) and atypical (second and third generation) antipsychotics. These drugs primarily target dopaminergic and serotonergic neurotransmission, which are thought to be dysregulated in schizophrenia (**Table 3**) [129].

First generation antipsychotics (FGAs), also known as typical antipsychotics, include drugs such as haloperidol, chlorpromazine and fluphenazine. These medications primarily function blocking dopamine D₂Rs in the mesolimbic pathway, which reduced the positive symptoms of schizophrenia, such as hallucinations, delusions and disorganized thinking [130].

However, FGAs are associated with significant side effects due to their non-selective blockade of dopamine neurotransmission in other brain regions. For instance, blocking D_2R in the nigrostriatal pathway leads to the development of extrapyramidal symptoms (EPS), including tremors, rigidity and dyskinesia [131]. Additionally, their effects in the tuberoinfundibular pathway can cause hyperprolactinemia, which is characterized by high levels of prolactin in the blood. These adverse effects limit the long-term use of FGAs in many patients [130].

Second generation antipsychotics (SGAs), also known as atypical antipsychotics, were developed to reduce the side effects of FGAs while providing a broader efficacy. SGAs besides targeting D₂Rs also target serotonin 5-HT2A receptors. This dual action improves the treatment of both positive and negative symptoms of schizophrenia, such as social withdrawal, apathy, and cognitive dysfunction. By blocking 5-HT2A receptors, atypical antipsychotics reduce the dopamine blockade in the nigrostriatal pathway, which mitigates the risk of EPS. Additionally, the serotonergic activity helps modulate mood and cognition, offering benefits in the management of negative and cognitive symptoms that are less responsive to FGAs [132].

However, SGAs have their own side effects. They are commonly associated with metabolic syndrome, including weight gain, dyslipidemia and an increased risk of developing diabetes. Among the SGAs, clozapine is particularly effective in treating treatment-resistant schizophrenia, but its use is limited by the risk of agranulocytosis, a serious reduction in white blood cells [132].

Third generation antipsychotics (TGAs), such as aripiprazole, reflect a shift towards dopamine partial agonism. Aripiprazole acts as a partial agonist of D_2Rs , allowing a more nuanced modulation of dopaminergic activity. This approach helps maintain dopamine balance without the full antagonism of FGAs or SGAs, potentially reducing the side effects [133,134].

In addition to dopamine and serotonin receptors, new pharmacological targets are under investigation for the treatment of schizophrenia. Indeed, it is known that the dopamine hypothesis of schizophrenia does not fully explain the symptomatology and high variability in treatment response. Instead, recent research suggests that glutamatergic, GABAergic and cholinergic systems also

play significant roles in schizophrenia, leading to the exploration of novel therapeutic targets beyond dopamine.

Modulation of the glutamatergic transmission has been suggested to improve cognitive and negative symptoms. Glycine transporter inhibitors, such as bitopertin and sarcoserine, have been approved to be used in combination with standard antipsychotics to ameliorate negative symptoms of schizophrenia [129]. On the other hand, mGlu₅R agonists have been shown to ameliorate a broad range of positive, negative and cognitive symptoms in both dopaminergic and glutamatergic animal models [135].

Table 3. Receptor binding profile of typical and atypical antipsychotics. FGAs, first generation antipsychotics; SGAs, second generation antipsychotics; TGAs, third generation antipsychotics. Table adapted from [136,137]

FGAs	D ₁	D ₂	D ₃	D ₄	5-HT _{1A}	5-HT _{1B}	5-HT _{2A}	5-HT _{2B}	5-HT _{2C}	5-HT ₆	5-HT ₇	M ₁	M ₃	α ₁	a _{2A}	a _{2B}	a _{2C}
Chlorpromazine	++	+++	+++	+++			+++	+++	++	+++	+++	++	++	+++	+	++	++
Fluphenazine	++	+++	+	+			++	+	+			+		++			
Haloperidol	+	+++	+++	+++		+	+				+			++	+	+	+
SGAs																	
Clozapine	+	+	+	++	+	+	++	+++	++	++	++	+++	++	+++	++	++	++
Olanzapine	++	++	++	++		+	+++	++	++	+++	++	++	++	++	+	++	++
Quetiapine	+	+	+		++		++		+	+	++	+	+	++	+	+	++
Risperidone	+	+++	+++	+++	+	++	++++	++	++		+++			+++	++	++	+++
Paliperidone	+	+++	+++	+++	+	++	+++		++	+	+++			+++	+++	+++	+++
TGAs																	
Aripiprazole		+++	+++	+	+++	+	++	++++	++	+	++			++	++	++	++

4.2 Bipolar disorder

4.2.1 Definition, epidemiology and etiology

Bipolar disorder is a severe mood disorder marked by recurring episodes of depression that alternate with episodes of hypomania and/or mania, typically separated by intervals of relatively stable mood and functioning. This diagnosis is heterogeneous, likely encompassing a spectrum of cyclical mood disorders that vary in their clinical presentation, underlying causes, and mechanisms of development [138]. According to the DSM-V, two distinct bipolar disorders can be identified, namely Bipolar I Disorder (BD-I) and Bipolar II Disorder (BD-II). The definition given by the DSM-V are the following:

"Bipolar I Disorder is characterized by one or more Manic or Mixed Episodes, usually accompanied by Major Depressive Episodes.

Bipolar II Disorder is characterized by one or more Major Depressive Episodes accompanied by at least one Hypomanic Episode."

The distinction between these two disorders has been historically emphasized, particularly in the diagnostic system based on the DSM-IV. However, studies suggest these conditions may not be as clearly separate as once thought. Instead, it is proposed that mood disorders exist along a continuum rather than discrete, distinct categories [138].

BD affects around 1-4% of the population and it is one of the lead causes of disability due to its high morbidity. Indeed, up to 20% of the cases end up in suicide, causing high social and occupational impact [138,139]. Similarly to schizophrenia, BD is usually associated to a premorbid stage with neurocognitive deficits before the illness onset; in this stage, attention, verbal learning and memory and executive function are affected. Interestingly these deficits are more evident in acute episodes of the illness [140].

The risk of developing BD is significantly elevated in children of affected parents, with estimates suggesting they have about a tenfold increased risk compared to general population. Twin studies further support the strong genetic component of BD, with heritability estimates ranging between 0.7 and 0.8. Despite this substantial genetic influence, there is no evidence to suggest that BD follows a Mendelian pattern of inheritance (i.e., caused by a single gene with a large effect). Instead, similar to other psychiatric conditions, BD appears to be influenced by multiple genetic loci, each contributing a small effect to the overall risk [139].

The pathophysiology of BD is still under research, but several neurotransmitter systems have been under study. Specifically, dysregulation in serotonin, dopamine and norepinephrine systems is thought to play a central role in the mood fluctuations. It has been suggested that hyperactivity in the dopaminergic system may contribute to manic episodes, while deficits in serotonin and norepinephrine activity may underlie depressive episodes [141].

Calcium pathophysiology

Calcium dysregulation has been a longstanding hypothesis in BD, supported by genome-wide association studies (GWAS) identifying *CACNA1C* (coding for voltage-gated calcium channels, VGCCs) and *ANK3* (involved in cytoskeletal regulation) as risk loci. Findings suggest increased intracellular calcium signaling, which appears to be trait-related, persisting independently of mood episodes. Interestingly, lithium, a first-line treatment for BD, has been shown to modulate calcium signaling, providing potential insight into its therapeutic effects [139].

Given the role of calcium in BD, VGCC antagonists have been evaluated for potential efficacy in BD treatment. This drugs target calcium dysregulation and have shown promise in preclinical studies. Furthermore, certain

antiepileptic drugs, such as pregabalin, which act in VGCC $\alpha 2\delta$, have also been tested for BD [142]. Additionally, lamotrigine, another anticonvulsant that may block calcium channels, is an effective treatment for BD [143]. These observations support the importance of calcium channel modulation in the disease management.

Frontal-limbic model of BD

In the last few decades, research has focused on understanding the neural circuitry involved in the disorder, with the frontal-limbic model emerging as a prominent theoretical framework. This model proposes that dysfunction within the subcortical-prefrontal network underlies the symptomatology of BD. Specifically, it has been proposed that a relative loss of the regulation from the prefrontal to the subcortical and limbic regions may underlie the symptoms of BD [144]. On the other hand, it has been proposed that hyperactivity in the amygdala during manic states contributes to the emotional instability and mood changes [144,145].

Inflammatory and oxidative stress

Recent research strongly suggests the involvement of inflammatory cytokines, corticosteroids, neurotrophins and oxidative stress, among others, in a more comprehensive model of BD [146]. There is increasing evidence suggesting that proinflammatory processes are involved in the pathophysiology of BD. Indeed, it has been shown that BD episodes are associated to the activation of pro-inflammatory pathways leading to the increase of pro-inflammatory cytokines and acute-phase protein levels [146]. Moreover, epidemiologic studies have identified elevated rates of inflammatory medical comorbidities in BD subjects, such as coronary artery disease, lupus and rheumatoid arthritis [147]. On the other hand, it is not yet clear the cause-effect relationship between BD and inflammation, and the most recent hypotheses suggest that it is bidirectional, meaning that rather than one

condition (i.e. inflammation or BD) increasing the risk of development of the other condition (i.e. BD or inflammation), both conditions reinforce the development of each other bidirectionally [148].

4.2.2 Pharmacology in bipolar disorder

Treatment of BD must consider the patient condition phase or episode; in fact, each phase (i.e. euthymia, mania, hypomania or depression) require different therapeutic management. In the acute management of the disease, mood stabilizers and antipsychotics are the foundation for treatment (**Table 4**) [141].

Mood stabilizers balance mood swings and prevent future manic or depressive episodes and therefore are usually prescribed as long-term treatments. Lithium is the oldest mood stabilizer used in the clinic and is still one of the most effective treatments in BD. However, the mechanism of action of lithium is still not fully clear. Rather than one single target, lithium is thought to affect many signaling pathways, either directly or indirectly [149]. Research has revealed that at physiological concentrations, lithium interacts directly with two proteins, the IMPase phosphomonoesterase and the GSK3 [149–151]. At the physiological level, lithium has been shown to modulate the neurotransmitter release (increased norepinephrine release) and other neurotransmitter activity (serotonin and dopamine, specifically). Moreover, lithium increases brain-derived neurotrophic factor (BDNF) levels and reduces oxidative stress, promoting neuroprotective effects and neurogenesis [149].

On the other hand, although not as effective as lithium, some anticonvulsants (i.e. valproate, lamotrigine, and carbamazepine) have shown efficacy as mood stabilizers. The mechanisms of these anticonvulsants are mainly related to the modulation of different neurotransmitter systems (GABAergic, glutamatergic, dopaminergic and serotoninergic). Interestingly,

they do not share the mechanism of action, and their impact on metabolism and the synaptic action strongly differ [152].

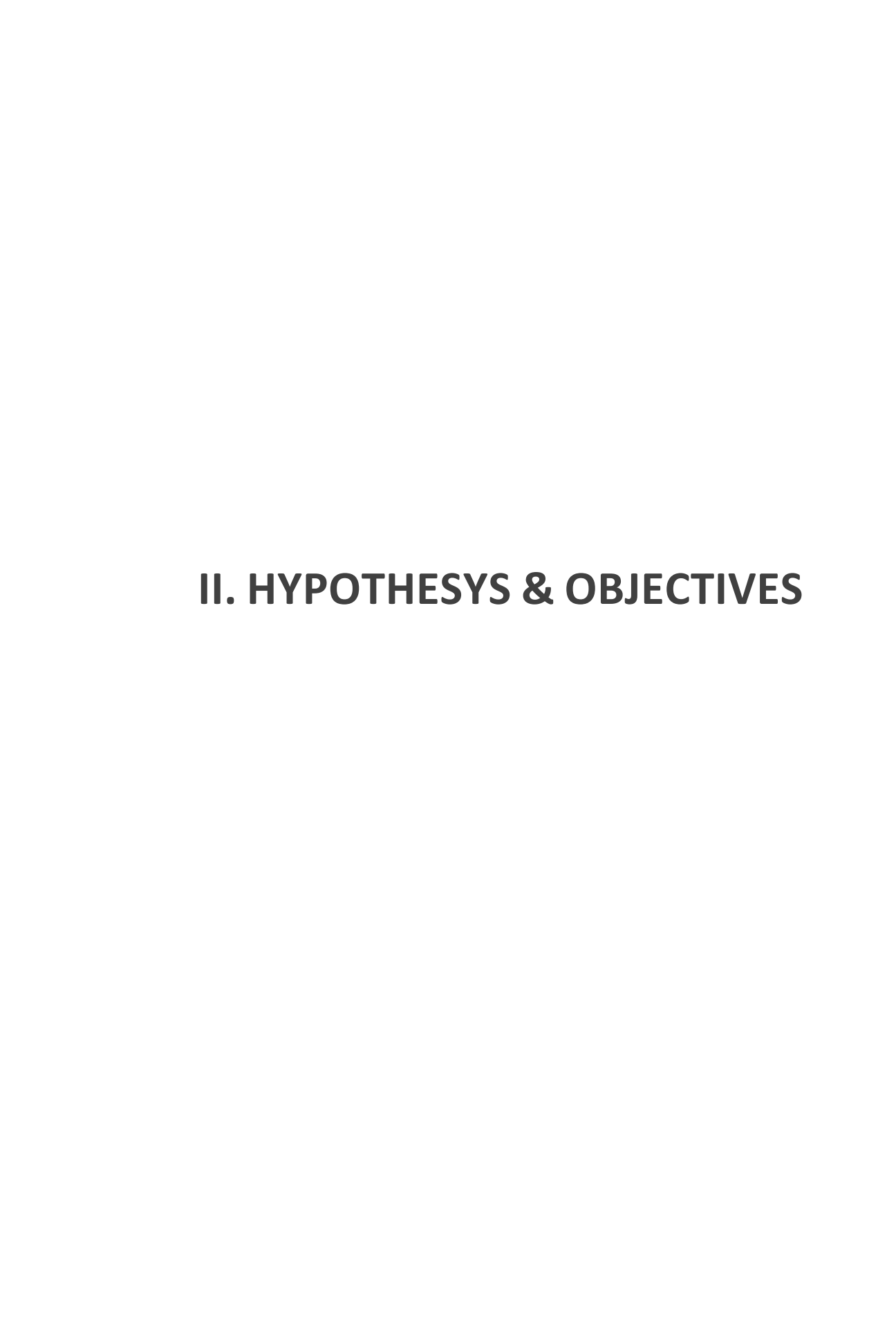
Finally, antipsychotics have been shown to be more effective for treatment of mania compared to mood stabilizers. Specifically, haloperidol, risperidone and olanzapine are the most potent, yet the secondary effects are stronger, and long-term continuation rate is low. On the other hand, second and third generation antipsychotics have shown same efficacy and higher continuation [141].

In treatment resistant conditions, electroconvulsive therapy has been proved to be effective. Moreover, is highly recommended in pregnant women, due to the high teratogenic effect of most mood stabilizers.

Table 4. Clinical recommendation of mood stabilizers and antipsychotics management in bipolar disorder [129]. +: recommended; ++: highly recommended; +++: very highly recommended; -- not much recommended; ---: not recommended; --- not at all recommended.

	Clinical management						
	Mania	Depression	Maintenance				
Mood stabilizers							
Lithium	+++	++	+++				
Valproate	+++	+	++				
Carbamazepine	+++	+	++				
Lamotrigine		++	+++				
Antipsychotics							
Aripiprazole	+++	-	++				
Chlorpromazine	++		+				
Clozapine	+	+	++				

Haloperidol	+++		+
Olanzapine	+++	+++	++
Risperidone	++	-	++
Electroconvulsive therapy	++	++	+



The development of novel pharmacological tools capable of specifically modulating the function of GPCRs represents a key challenge in pharmacology. Among these receptors, the mGlu₅R has garnered significant attention due to its critical role in synaptic plasticity and its involvement in various neurological and psychiatric disorders. Several studies have highlighted the functional interaction between mGlu₅R and A_{2A}R, particularly in the regulation of dopaminergic signaling. This macromolecular assembly represents a promising therapeutic target, as it exhibits unique pharmacological properties distinct from those of the individual receptors. Nanobodies, or single-domain antibodies derived from camelid heavy-chain-only immunoglobulins, have emerged as a powerful tool for selectively modulating GPCR activity. Their small size, high specificity, and ability to stabilize receptor conformations make them ideal candidates for targeting receptor heteromers and other membrane protein complexes. Thus, our main hypothesis is that nanobodies targeting GPCRs are potential pharmacological tools for the modulation of membrane macromolecular assemblies.

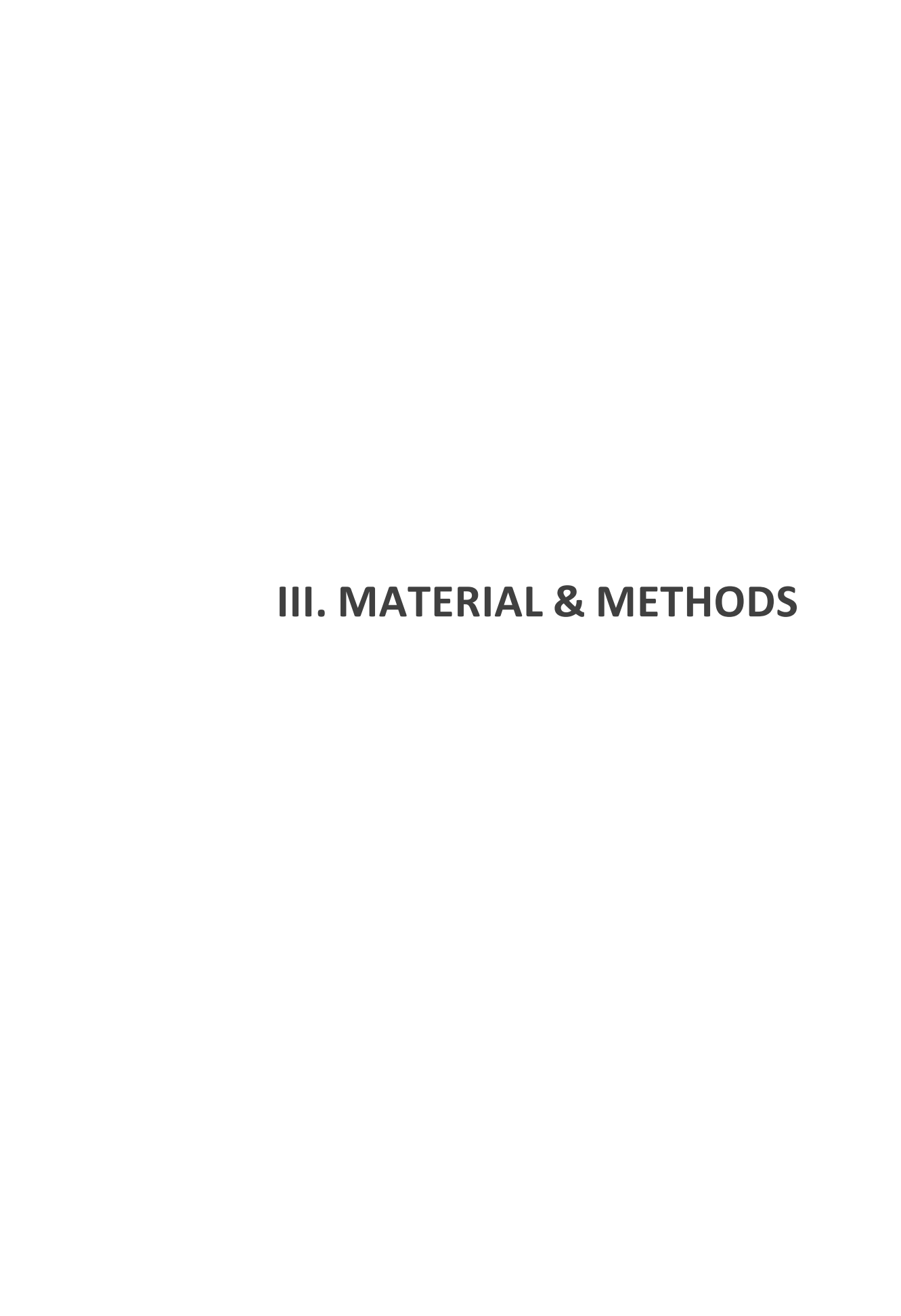
Additionally, this thesis explores the adenosinergic hypothesis as a potential framework for understanding and modulating dopaminergic dysfunction in neuropsychiatric disorders. Adenosine, a key neuromodulator, interacts closely with the dopaminergic system, particularly through adenosine receptors. Given this interplay, purinergic drugs have been proposed as potential therapeutic agents for conditions such as schizophrenia and bipolar disorder, where dopaminergic dysregulation is a hallmark feature. In this context, we hypothesize that purinergic drugs exert clinically relevant effects in schizophrenia and bipolar disorder, with differential impacts on positive, negative and cognitive symptoms.

To evaluate these hypotheses, the specific objectives of this thesis are:

Objective 1: *In vitro* characterization of nanobodies: To assess the binding affinity, selectivity, and pharmacological properties of Nb43 and Nb43-CGS21680 on mGlu $_5$ R and the mGlu $_5$ R -A $_{2A}$ R complex

Objective 2: *In vivo* evaluation of biodistribution and pharmacological activity: To determine the ability of Nb43 and Nb43-CGS21680 to cross the blood-brain barrier and modulate dopaminergic-related behaviors in murine models

Objective 3: Meta-analysis of adenosine metabolism modulators: To systematically review and analyze the efficacy of adenosine metabolism modulators in the treatment of schizophrenia and bipolar disorder



1. NANOBODY PRODUCTION AND PURIFICATION

BL21 (DE3) pLys bacteria were used for the heterologous expression of the nanobodies. This strain contains the DE3 lysogen that carries the gene for T7 RNA polymerase under control of a lacUV5 promoter, allowing the expression of the T7 RNA polymerase to be induced with isopropyl-β-D-1-galactopiranoside (IPTG). Thus, the gene of interest is cloned into the pET vector under the control of T7 transcription and translation regulatory system. The pET26-b(+) plasmid was used in this work, which contains the *pelB* signal sequence for periplasmic expression.

Bacterial transformation with pET26-(b)+ plasmid containing the coding gene for the nanobodies was performed with usual heat-shock protocols. Competent BL21 (DE3) pLys cells (Promega, Madison, WI, USA) were thawed in ice for 10 minutes. Bacteria and DNA samples were mixed in a 1:10 ratio and incubated for 30 minutes on ice. In order to destabilize bacterial membrane, samples were heat shocked at 42°C for 20 seconds in a water bath. Bacteria was again incubated on ice for 10 minutes. Then, recovery was promoted by incubating samples with 1 mL SOC medium (Luria Broth (LB, Sigma Aldrich, St. Louis, MI, USA) medium supplemented with 20 mM glucose, 10 mM MgSO₄ and 10 mM MgCl₂) at 37°C at 500 rpm for one hour. Transformation selection was performed by seeding bacteria in kanamycin (3 mg/kg, Sigma Aldrich) LB agar plates and growing overnight at 37°C.

Colonies were picked and validated for protein expression. High expressing colonies were stored at -80°C in 10% glycerol LB medium.

1.1 Nanobody production

After the nanobody-containing plasmid is established in a BL21 (DE3) lysogen, expression of the target protein is induced by the addition of IPTG to a growing culture. First, a few microliters from a glycerol stock are inoculated into 10 mL

of LB media with the appropriate antibiotic (kanamycin, 3 mg/mL) and grown overnight at 37 $^{\circ}$ C with 220 rpm shaking. The next day, the overgrown culture is escalated to 250 mL LB containing the appropriate antibiotic and it is grown at 37 $^{\circ}$ C with 220 rpm shaking. When OD600 is 0.6-0.7 protein expression is induced by the addition of IPTG (Termo Scientific, Waltham, MA, USA) with a final concentration of 1 mM (250 μ L from a 1 M stock). The culture is then grown overnight at 28 $^{\circ}$ C with 220 rpm shaking.

1.2 Periplasm fraction extraction

Vector pET26-b(+) is characterized by having a *pelB* signal sequence, which targets the expressed proteins to the periplasmic space. The osmotic shock protocol is a simple method for extracting the periplasmic fraction from DE3 lysogens (**Figure 9**).

The culture induced for protein expression is centrifugated at 3000 xg for 10 minutes at 4°C. The cell pellet is thoroughly resuspended in a sucrose solution (30 mM Tris-HCl, 20% sucrose, pH 8; 30 mL/1 L culture) supplemented with protease inhibitor cocktail I (1:1000 dilution, Millipore Sigma, Burlington, MA, USA). The sample is incubated 45 minutes at 4°C in rotation. Then a diluted sucrose solution (1:4) is added (60 mL/L) and sample is incubated one hour more at 4°C in rotation. The shocked cells are precipitated at 12000 xg for 30 minutes at 4°C and the supernatant is recovered as the periplasmic fraction.

1.3 Nanobody purification

Nanobodies are conveniently purified via immobilized metal affinity chromatography (IMAC), e.g. using Ni-NTA (nickel-nitrilotriacetic acid) beads, whereby their C-terminal hexa-histidine tag is captured on immobilized metal ions (Figure 9).

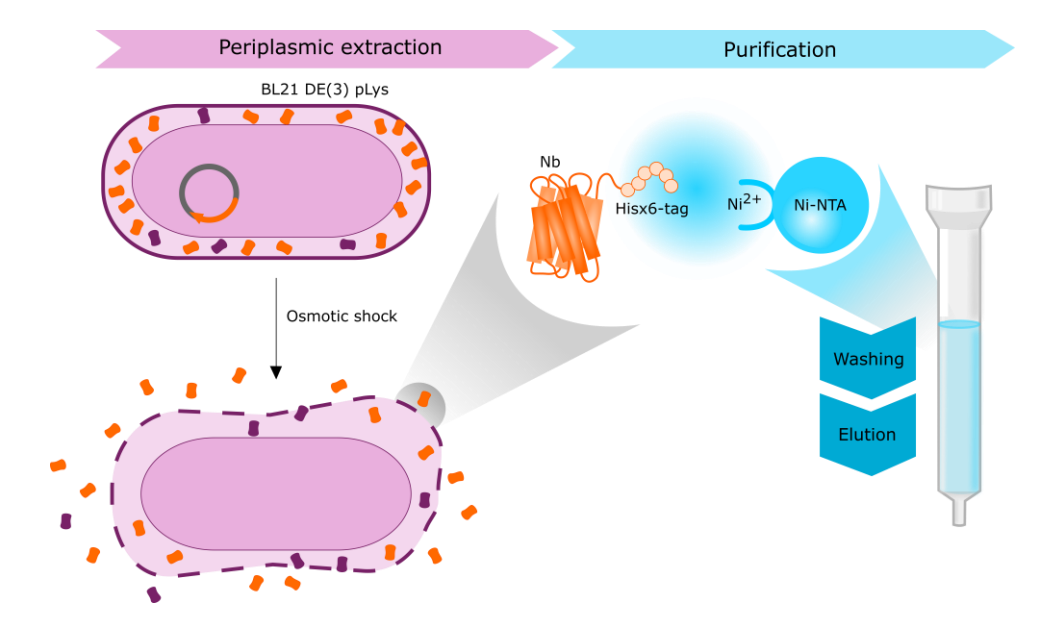


Figure 9. Nanobody expression and purification. Nanobodies are expressed in the periplasm of BL21 DE(3) pLys bacteria. The osmotic shock protocol enables the disruption of the periplasm and this fraction is used for purification using immobilized metal affinity chromatography using Ni-NTA resins.

Ni-NTA resin (Thermo Fisher Scientific) is previously rinsed with equilibration buffer (50 mM NaH₂PO₄, 300 mM NaCl) and then incubated with the periplasmic extract for one hour at 4°C in rotation. Then, the sample is loaded into the drip 5 mL column (Thermo Fisher Scientific) and the flowthrough is discarded. Ni-NTA resin is washed with 7 bed volumes of the washing buffer (50 mM NaH₂PO₄, 300 mM NaCl, 10 mM Imidazole) to discard non-specific bound protein. Nanobody is eluted with the elution buffer (50 mM NaH₂PO₄, 300 mM NaCl, 250 mM Imidazol) and 500 μL fractions are collected.

Protein concentration is determined using 280 nm absorbance (A280) measurements at the ultraviolet (UV) range using the Nanodrop Microvolume ultraviolet (UV)-Vis spectrophotometer (#ND-ONE-W, Thermo Fisher Scientific). Fractions containing protein are collected and the imidazole-containing buffer is exchanged for phosphate buffered saline (PBS, 2 mM KH2PO4, 10 mM Na2HPO4, 137 mM NaCl and 2,7 mM KCl, pH 7.2) using a PD-

10 desalting columns (Cytiva, MA, United States). Protein concentration is again determined using A280 measurements and adjusted to 1 mg/mL. Nanobodies are stored at -20°C.

2. BIOCHEMICAL CHARACTERIZATION OF NANOBODIES

2.1 Bioinformatic predictions

Biochemical properties of the nanobodies were predicted using the ExPaSy ProtParam (SIB Swiss Institute of Bioinformatics, Laussane, Switzerland). ProtParam is a tool which allows the computation of various physical and chemical parameters for a user entered protein sequence (**Table 5**).

Table 5. Biochemical properties of Nb43.

	Molecular weight (KDa)	Molar absorbance	Isoelectric point	Lys content
Nb43	14,252	33,922	8,01	4

2.2 Size exclusion chromatography

Size exclusion chromatography (SEC) is a separation technique that primarily sorts molecules based on their size (hydrodynamic radius) as they pass through a porous medium. In SEC, a sample mixture is passed through a column packed with porous beads. Larger molecules are excluded from entering the pores of the beads and travel through the column more quickly, while smaller molecules penetrate the pores, causing them to take longer to elute.

Purified samples were injected into Superdex 75 Increase 10-300 GL (Cytiva) columns, equilibrated with filtered PBS. Fractions with an absorbance value higher than 0.5 were collected and used for further characterization (Figure 10).

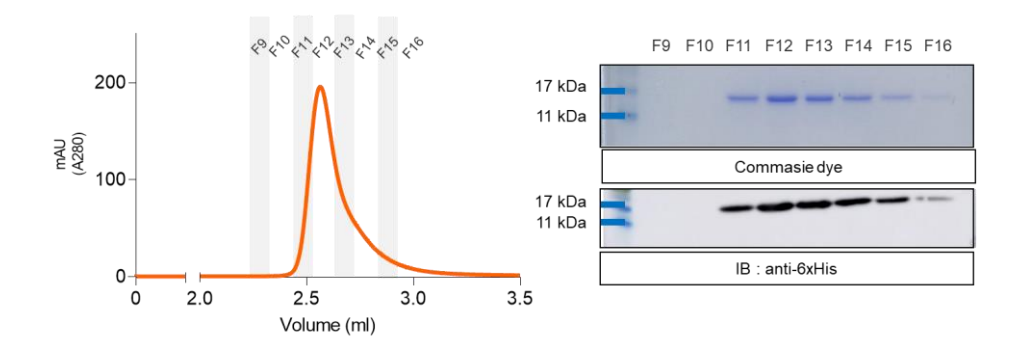


Figure 10. Size exclusion chromatography profile of purified Nb43 and fraction characterization. In the left, Nb43 size exclusion chromatography is shown, and fractions F9-16 were collected for further characterization. In the right, SDS-PAGE acrylamide gels of F9-F16 fractions, as indicated. Coomassie dye was used for visualizing the total amount of protein and immunoblotting (IB) against the Hisx6 tag was used to determinate the specific nanobody amount.

3. Nanobody Labeling

Different strategies were followed for the labeling of the nanobodies. Random labeling with biotin, AlexaFluor647 and DTPA-¹¹¹In was conducted using the naturally occurring lysine's amino groups. On the other hand, site specific labeling was performed with the 99m-Technetium (^{99m}Tc) labeling, using the hexahistidine tag for the labeling (Figure **11**).

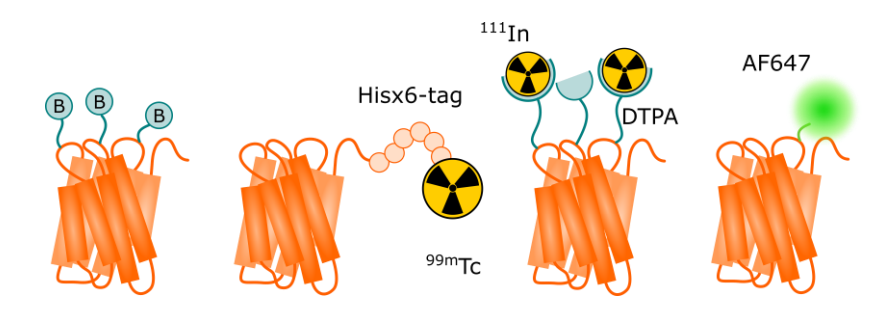


Figure 11. Nanobody labeling strategies. Random labeling (NHS-biotin, NHS-AlexaFluor647 and DTPA) was used against the naturally occurring lysine residues of the nanobody. Sitespecific labeling of the nanobody was used for ^{99m}Tc, using the Hisx6 tag for the labeling.

3.1 Biotinilation

Mix-n-Stain Nanobody labeling kit (Biotium, Fremont, CA, USA) was used for the biotin random labelling. For the labeling, 50 μ g of protein is used in 45 μ L volume (in PBS) for optimal final concentration at 1 μ g / μ L. 5 μ L of Reaction Buffer are added and the final mixture is transferred to the vial containing the lyophilized biotin-NHS. Mixture is incubated for 30 minutes at room temperature in the dark. After the incubation, 5 μ L of Mix-n-Stain Quencher are added and incubated for 5 more minutes.

3.2 AlexaFluor 647 NHS labeling

Succinimidyl-ester (NHS-ester) labeling is a widely used method for covalently attaching fluorescent dyes or other functional groups to proteins, including nanobodies. NHS-ester chemistry targets the primary amine groups, typically found on lysine residues or the N-terminus of nanobodies, forming a stable amide bond. AlexaFluor647-NHS (Invitrogen, Waltham, MA, USA) was used for the fluorescent labeling, using the commercially available protocol. Around 1-2 mg of nanobody are concentrated (200-300 μ L) and supplemented with 100 μ L of 1 M K₂HPO₄. AlexaFluor647-NHS is added in 3 molar excess and incubated for 2 hour in dark at room temperature. After incubation, the reaction sample is immediately injected into the chromatography column Superdex 75 Increase 10-300 GL (Cytiva) (**Figure 12**).

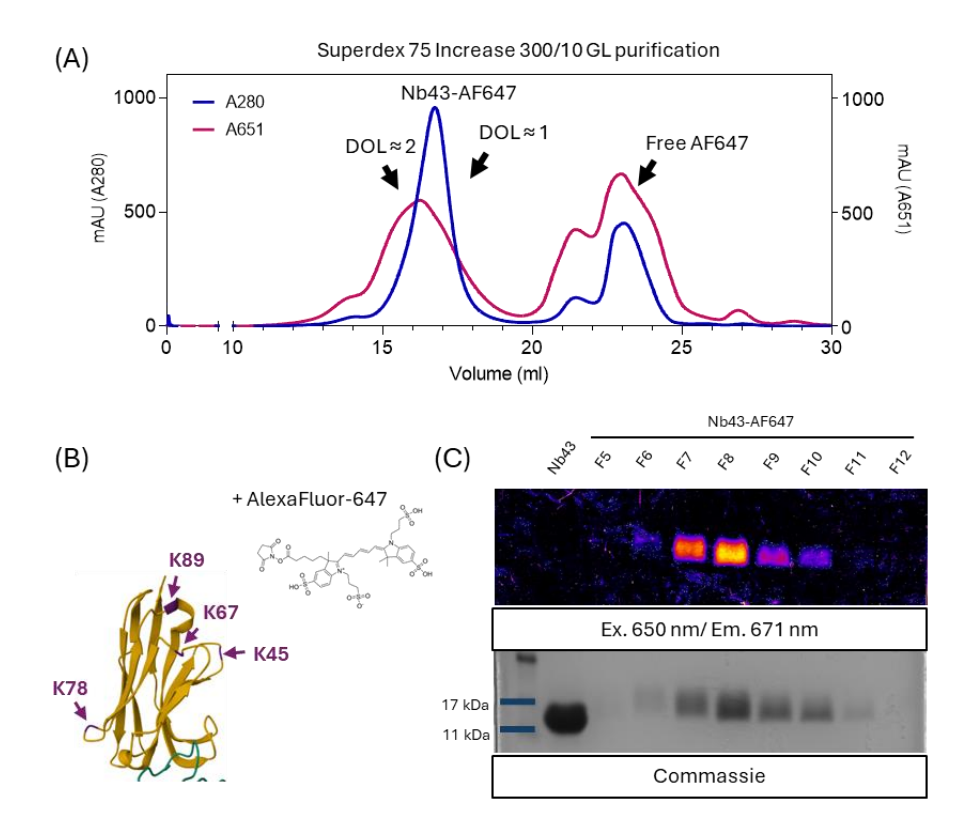


Figure 12. Nobody randomly labeled AlexaFluor-647. (A) Chromatogram of Nb43-AF647 showing absorbance at 280 nm (blue line) and 651 nm (purple line). First peak corresponds to the labelled nanobody and the final peaks correspond to the free dye. **(B)** Structure representation of Nb43 showing the naturally occurring lysine (K) residues and the structure of AlexaFluor647. **(C)** Acrylamide gel of purified fractions of the labelled nanobodies. Nanobody was detected using Commasie Blue and AlexaFluor-647 fluorescent signal. DOL: degree of labeling.

Fractions are collected based on a degree of labeling (DOL) value of ≈ 1 , calculated as follows:

$$DOL = \frac{A_{647}\epsilon_{dye}}{(A_{280} - A_{647})\epsilon_{prot}}$$

 A_{280} : Absorbance of the protein fraction at 280 nm

 A_{647} : Absorbance of the protein fraction at 647 nm

 ϵ_{prot} : Molar extinction coefficient of the pure protein at 280 nm

 ϵ_{dve} : Molar extinction coefficient of the dye at 647 nm

3.3 Radiolabeling with Tc-99m

Nanobodies were labeled with 99mTc at their hexahistidine tail, as previously described. For the labeling, [99mTc(H2O)3(CO)3]+ is synthesized by adding 1 mL of 99mTcO4- (0.74-3.7 GBg) to an Isolink kit (Mallinckrodt Medical BV) containing 4.5 mg of sodium boranocarbonate, 2.85 mg of sodium tetraborate 10H₂O, 8,5 mg of sodium tartrate 2H₂O, and 7,15 mg sodium carbonate, pH 10,5. The vial is incubated at 100°C in boiling bath for 20 minutes. The freshly prepared [99mTc(H₂O)₃(CO)₃]⁺ is allowed to cool at room temperature for 5 min and neutralized with 125 µL of 1 M HCl to pH 7-8. [99mTc(H₂O)₃(CO)₃]⁺ is added to 50 μL of 1 mg/mL of the correspondent nanobody. The mixture is then incubated for 90 minutes at 60 °C in a water bath. NAP-5 column (GE healthcare, Machelen, Belgium) followed by filtration through a 0.22 µm filter (Millipore, Haren, Belgium) is used to purify the 99mTc-Nb complex. The labeling efficiency is determined by instant thin layer chromatography (iTLC) in acetone as mobile phase and analyzed using a radiometric chromatogram scanner (VCS-201; Veenstra, Joure, Friesland, The Netherlands). Only samples with labeling yields higher than 90% are used.

3.4 Radiolabeling with 111 In

For the labeling of nanobodies with ¹¹¹In a metal chelator, namely diethylene triamine pentaacetic acid (DTPA), is conjugated to the nanobody lysine residues. Nanobody's buffer is exchanged using Vivaspin centrifugal concentrators (Vivaproducts, Littleton, MA, USA) to metal free 0.05 M sodium carbonate buffer (pH 8.7). 20 molar excess of the lyophilized p-SCN-CHX-"A-DTPA is added to the nanobody suspension in a final volume of 500 µL and

incubated 2 hours at room temperature in dark. Product is injected immediately into the SEC Superdex 75 Increase 10-300 GL (Cytiva) and eluted with 0.1 M NH_4OAc (pH 7). Fractions with higher molecular weight were collected for further characterization with ^{111}In (**Figure 13A-C**).

For the ¹¹¹In labeling, 50 ug of DTPA-conjugated nanobody (buffered in 0.1 M NH₄OAc) is mixed with [¹¹¹In] HCl. The mixture is incubated for 1 hour and labeling yield is determined by iTLC (**Figure 13D**) in acetone as mobile phase and analyzed using a radiometric chromatogram scanner (VCS-201; Veenstra). Only samples with labeling yields higher than 90% are used. The ¹¹¹In-Nanobody solutions are purified using a NAP-5 column (GE Healthcare) preequilibrated with phosphate buffered saline (PBS). Labelled sample was further characterized by reverse phase chromatography using Superdex 75 Increase 5-150 column, in order to validate the correct labeling and folding of the nanobodies (**Figure 13E**).

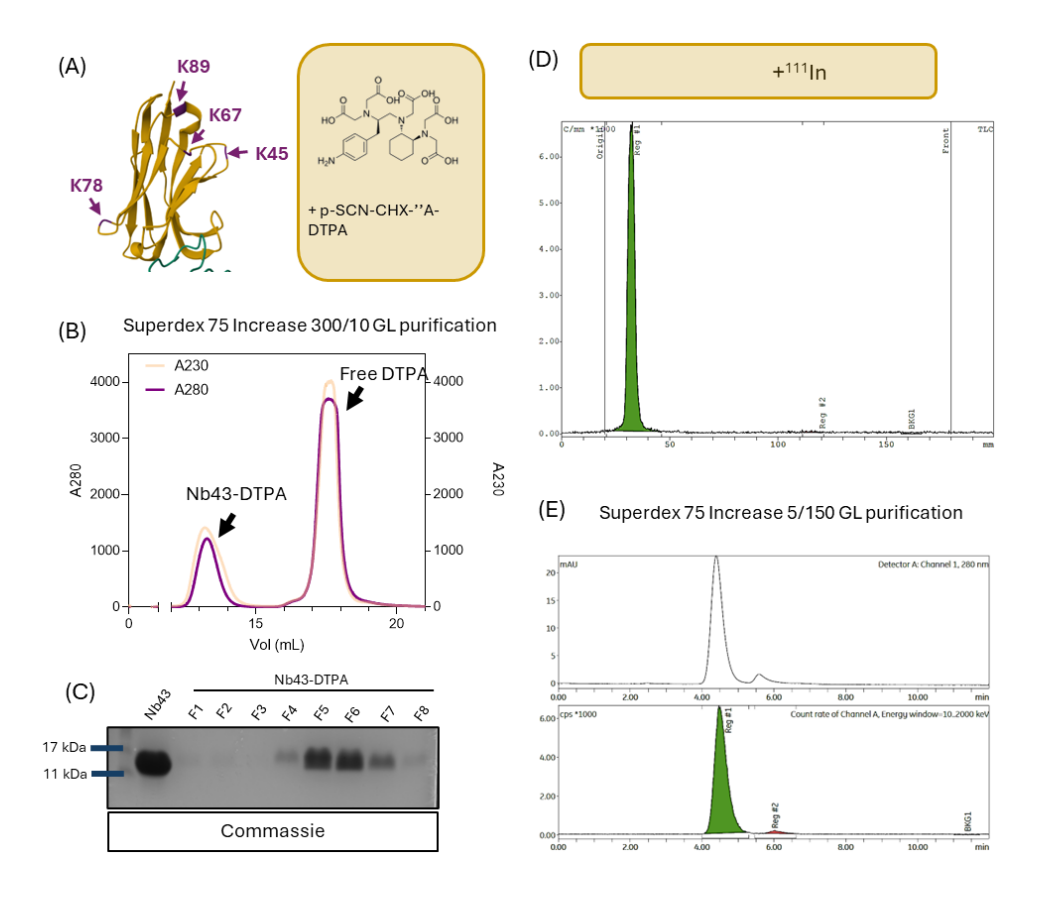


Figure 13. Nanobody labeling process with metal chelator DTPA and ¹¹¹In. (A) Representation of Nb43 structure showing the naturally occurring lysine residues and the molecular structure of DTPA. (B) Chromatogram of Nb43 after DTPA labeling showing the absorvance at 280 and 230 nm. (C) SDS-PAGE of DTPA-labelled Nb43 chromatography fractions detected using Commasie dye. (D) iTLC radiometric scan of ¹¹¹In-labelled Nb43-DTPA showing the labeled Nb43 (green, Reg#1) and free ¹¹¹In (Reg#2). (E) Reverse phase chromatogram showing absorbance at 280 nm (upper panel) and radioactive signal (lower pannel) of 111In-labelled Nb43-DTPA. Second peak (Reg#2) corresponds to free DTPA.

3.5 Nanobody-Drug conjugate

Nb43 was conjugated to CGS21680, a selective A_{2A} receptor agonist, in collaboration with Ross Cheloha (NIH/NIDDK). In parallel, a negative control nanobody, Nb30, was also labeled. Briefly, a 52-atom linker was attached to the C-terminal of Nb43 or Nb30, allowing for the subsequent conjugation of

CGS21680. The ligand was oriented appropriately to ensure its biological activity upon attachment.

4. CELLS AND CONSTRUCTS

In this thesis two cell lines were used, the human embrionary kidney (HEK) 293 cell line and the SHSY-5Y neuroblastoma cell line. The maintenance of these cell lines was done as previously described.

HEK293 and HEK293T cells are cultured in Dulbecco's modified Eagle's medium (DMEM, Sigma Aldrich) supplemented with 100 U/mL streptomycin (Biowest), 100 mg/mL penicillin (Biowest), 1 mM sodium pyruvate (Biowest), 2 mM L-glutamine (Biowest) and 5% (v/v) fetal bovine serum (Invitrogen Corporation, Camarillo, CA, USA) at 37°C and in an atmosphere of 5% CO2. SHSY-5Y cells are cultured equally, with a difference in fetal bovine serum concentration, which is 10% instead of 5%. Subculturing is done when confluence is 100% every 3-4 days.

Stable cell lines are generated using HEK293 cells. For the selection of the cells expressing the construct, antibiotics for the correspondent construct's gene of resistance is used at the indicated concentration.

4.1 Transfection

For the transient expression of proteins in HEK293 or HEK293T cell line, the polyethylamine (PEI, Sigma Aldrich) method was used. PEI is a cationic polymer that allows the delivery of DNA into cultured cells by forming positively charged complexes with negatively charged DNA. These PEI-DNA complexes are endocytosed by cells and the DNA is released intracellularly, leading to transient gene expression.

For this approach, PEI is diluted in NaCl 0,9% solution at 1 mg/mL and mixed with the appropriate quantity of the DNA of interest (**Table 6**). This solution is incubated for 20 minutes at room temperature to stabilize the complexes. The DNA-PEI complexes are added to cells in serum-free medium and incubated for 3 hours. Transgene full expression is assumed within 48 hours post-transfection.

Table 6. Constructs transfected in this thesis.

CONSTRUCT	PLASMID	TAG	REFERENCE
h- mGlu₅R	pCDN3.1	НА	
m- mGlu₅R	pCDN3.1	НА	[153]
A2AR-NLuc	pIRES-Neo	HA, NLuc	[154]
A2AR-SmBiT	pIRES-Neo	HA, SmBiT	[154]
miniGs-LgBiT	pBiT1.1-N	HA, LgBiT	[155]

5. BINDING ASSAYS

5.1 Flow cytometry in vitro

In order to validate the binding ability of the nanobody to its target receptor, flow cytometry experiments were conducted. For this purpose, cells heterologously or endogenously expressing the receptor were used.

For the heterologous expression model, HEK293T cells are transfected using the polyethilienimine (PEI) protocol (explained at 4.1) and the binding assay is conducted two days after transfection. For the endogenous expression model, the SHSY-5Y neuroblastoma cell line is used. Cells are detached using trypsin (Sigma Aldrich) and recovered by centrifugation at 400xg for 5 minutes. Cell pellet is resuspended in 1 mL of blocking buffer (PBS, 0.1% BSA, 2 mM

EDTA) and incubated for 1 hour in rotation. Thereafter, cells are divided and resuspended into different nanobody concentrations. Cells are then incubated for 1 hour at 4 °C in rotation. After nanobody incubation, cells are washed three times with blocking buffer to discard the non-bound nanobody. Cells are resuspended in secondary antibody anti-His6x labelled with phycoerythrin (PE) (Miltenyi, Bergisch Gladbach, Rhineland, Germany) and incubated for 20 minutes at room temperature in dark. Cells are again washed with PBS and transferred to flow cytometry tubes.

Beckman Coulter Gallios flow cytometer (Beckman, Brea, CA, USA) from the "Centres Cientifics I Tecnològics de la Universitat de Barcelona" (CCiT-UB) was used for the acquisition of single cell fluorescent data. Data was analyzed using FlowJo Software (FlowJo LLC, Williamson Way Ashland, OR, USA).

5.2 Flow cytometry ex vivo

Ex vivo model for Nb43 binding was based on mice brain-derived single cell suspensions. To obtain these samples Miltenyi's adult mouse brain dissociation kit (Miltenyi) is used, which is based on the enzymatic and mechanical disaggregation of the mouse brain tissue. Mice brain is extracted and dissected into whole brain or cerebellum and kept in cold Dubelcco's-PBS (D-PBS).

Tissue is washed and transferred to gentleMACS C tubes (Miltenyi). Enzymes P and A are added in their corresponding buffers and samples are mechanically processed with the gentleMACS Octo Dissociator with heaters (Miltenyi) using the pre-stablished protocol $37C_NTDK_1$. After the protocol ends, samples are centrifuged at 400 xg for 3 minutes and the pellet is resuspended in cold D-PBS. Then, samples are applied to sequential MACS SmartStrainers (Miltenyi) of 70 μ m and 30 μ m mesh. Filters are washed with extra 5 mL. Sample is again centrifuged at 300 xg for 10 minutes at 4 $^{\circ}$ C and

pellet is resuspended in 3100 μ L of D-PBS and transferred to a 15 mL tube. Cold Debris Removal Solution (Miltenyi) 900 μ L are added and carefully mixed by pipetting. Then, 4 mL of cold D-PBS are overlaid gently, and two phases are created. Sample is again centrifugated at 3000 xg for 10 minutes at 4°C with full acceleration and full break, and consequently three phases are obtained. The two top phases are discarded by aspiration and sample is filled up to 15 mL with cold PBS. The sample is centrifugated at 1000 xg for 10 minutes at 4°C and supernatant is discarded; brain derived cell suspension is contained in the pellet.

In order to discard brain derived red blood cells (RBC), RBC Lysis buffer is used (0.15 M NH_4Cl , 0.01 M $NaHCO_3$, 0.0001 M EDTA, pH 7.2-7.4). Briefly, cells are resuspended in 1 mL of RBC Lysis buffer and incubated 2 minutes in ice. Immediately after, 10 mL of cold PBS are added and centrifugated at 400 xg for 10 minutes at room temperature.

Sample can be then used for flow cytometry experiment. As previously explained, samples are incubated with blocking buffer for 1 hour in rotation at room temperature. Cell suspension is divided into different condition tubes and centrifugated at 400 xg for 5 minutes at room temperature. Pellet is then resuspended in the corresponding nanobody concentration and incubated for 1 hour in rotation at 4° C. After the incubation, non-bound nanobody is washed with three consecutive cold PBS washes. Immediately after, the samples are fixed with 0.2% PFA for 2 minutes and washed again. Finally, samples are resuspended in 50 μ L of secondary anti-6xHis-PE antibody and incubated for 20 minutes at room temperature in dark. Samples are washed with PBS twice and transferred to flow cytometry tubes for acquisition.

BD FACSCanto II (BD Biosciences, Frankin Lakes, NJ, USA) flow cytometer (Beckman) from the CCiT-UB was used for the acquisition of single cell fluorescent data. Data was analyzed using FlowJo Software (FlowJo LLC).

5.3 Radiolabelled-nanobody binding assay

In order to validate that radiolabeling does not affect the functionality of the receptor, the binding ability of the radiolabeled nanobody is assessed. SHSY-5Y neuroblastoma cells, which endogenously express the mGlu₅R, are plated for 80% confluence the day of the experiment in 24-well plates. On the same day, nanobody is radiolabeled as previously explained. All the steps, otherwise specified, are performed on ice and cells, media and reagents are kept cold through the procedure. The 24-well plates containing the cells are retrieved from cold storage and immediately placed on ice. The supernatant from each well is carefully aspired and each well is incubated with 400 uL of unlabeled targeting nanobody (serially diluted in a 1/3 ratio) or unsupplemented culture medium. Afterwards, every well is added 100 uL of radiolabeled nanobody (1/3 serial dilution) and incubated for 1 hour at 4ºC. After the incubation, cells are washed twice with ice cold PBS. Cells are lysed by adding 1 mL of NaOH per well and incubated at 37°C for 5 minutes. The lysate is collected and an additional 1 mL of 1 M NaOH is added and incubated in agitation for 5 minutes: This fraction is collected at the same tube. Samples are measured using a gamma counter (2480 WIZARD, PerkinElmer, Waltham, MA, USA).

5.4 Immunocytofluorescence

Binding ability of the nanobody was also validated by immunocytofluorescence (IHF) in cells expressing the receptor. For this experiment, cells are seeded in cover glasses pre-treated with poli-ornithine (0.01 mg/mL, Sigma Aldrich) to obtain 50% confluence on the day of the

experiment. On the day of the experiment, cover glasses with the cells are washed with PBS to remove the media and incubated with paraformaldehyde (PFA, 2%, Sigma Aldrich) to fixate the cells. Cover glasses are washed with PBS twice and cells are permeabilized by incubating them with PBS 0,3% Triton-X100 (Sigma Aldrich) for 10 minutes at room temperature. Samples are again washed and incubated with blocking buffer (PBS, 0,05% Triton-X100, 1% bovine serum albumin -BSA-) for one hour at room temperature. Antibodies or nanobodies are incubated overnight at 4°C.

The next day, excess antibody/nanobody is washed with PBS and fluorescently labelled secondary antibodies are incubated for 1 hour at room temperature. Finally, cover glasses are washed with PBS and mounted with polyvinyl alcohol (PVA) medium with 4',6-diamidino-2-phenylindole (DAPI, (0.2 μ g/ μ L in PBS)).

Fluorescence images are acquired using Carl Zeiss LSM880 Confocal microscope (ZEISS, Oberkochen, Germany) from the CCiT-UB.

5.5 Immunohistofluorescence

IHF was for the validation of nanobody binding with spatial resolution within the tissue. Nanobody labelled with biotin (Nb-B) was used for this approach; thus, detection was performed with fluorescently labelled streptavidin (Strep).

In order to preserve the ultrastructure of the tissue, mice are perfused with cold PFA 4% using an automated pump; prior to the PFA perfusion, 50 mL of cold PBS are injected for blood clearing. For this procedure, mice are anesthetized with lethal doses of ketamine/xylazine injected intraperitoneally. Perfusion is done opening the chest and using the heart as the inset/offset of the PBS/PFA flow. After the animal is perfused, the brain is extracted, and brain

slices are obtained using the vibratome (LEICA VT1200S, Leica Welt, Waltzer, Germany). Brain slices are stored at 20°C in Walter criopreserving solution (33% glycerol, 33% polyethyleneglycol, 33% PBS).

For the binding experiment, brain slices are thawed and washed with PBS 3 times for 10 minutes. For permeabilizing the tissue, samples are incubated with PBS 0.3% Triton-100 for 2 hours at room temperature. After 3 washes with PBS, samples are blocked using blocking buffer (PBS, 0.05% Triton, 1% BSA) for 1 hour. Afterwards, the Nb-B (10 μ M) is incubated overnight at 4°C. The next day, excess nanobody is washed with blocking buffer and samples are incubated with Strep-PE (0,5 μ g/mL, Miltenyi) for 20 minutes at room temperature. Samples are washed and mounted using PVA medium containing DAPI (0.2 μ g/ μ L). Fluorescence images are acquired using Carl Zeiss LSM880 Confocal microscope from the CCiT-UB.

6. Intracellular signaling

6.1 NanoBiT

NanoBiT (NanoLuc Binary Technology) is a luminescence-based assay developed for the study of protein-protein interactions and proximity events in living cells. It is based on the reconstitution of NanoLuc luciferase, a small, highly sensitive bioluminescent enzyme, from two non-functional fragments—Large BiT (LgBiT) and Small BiT (SmBiT). These fragments are individually fused to proteins of interest, and their interaction brings the two fragments into close proximity, reconstituting the active enzyme. Once reassembled, NanoLuc catalyzes a luminescent reaction that emits a detectable light signal, which can be quantitatively measured (Figure 14).

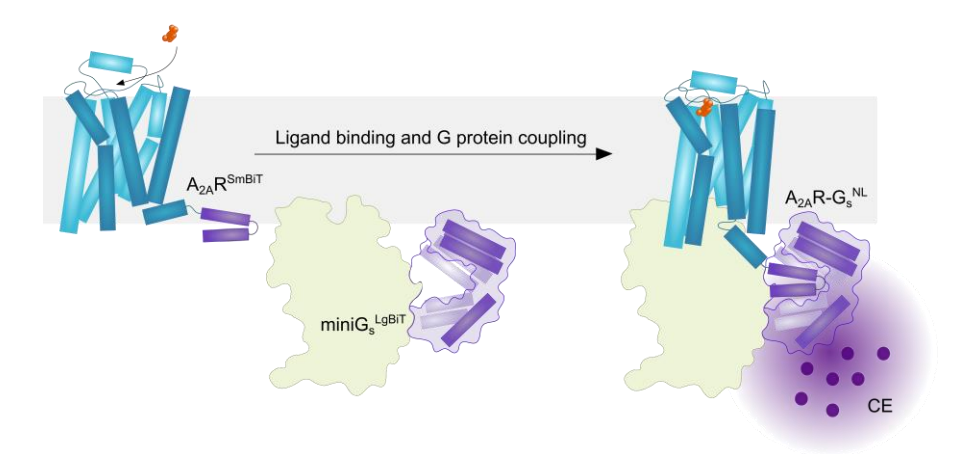


Figure 14. Representation of NanoBiT technology.

Transient transfection of HEK293T cells with corresponding constructs is performed for this experiment and the experiment is conducted 48 hours after. The day of the experiment, transfected cells are dettached with trypsin and plated in white 96-well plates (90.000 cells/90 μ L). Coelenterazine 400a (CE, NanoLight, Pinetop, AZ, USA) 10 μ L are added for final concentration of 2 μ M and bioluminescent signal (λ_{em} : 460-520 nm) is measured for 10-15 minutes until stability is reached. Cells are then challenged with serial dilutions of ligands and the bioluminescent signal is measured for 40-60 minutes every 5 minutes.

The bioluminescent signal (relative luminescent units, RLU) is normalized as follows:

$$RLU = \frac{(RLU_{sample} - RLU_{basal})}{RLU_{basal}}$$

6.2 cAMP assay

Cyclic adenosine monophosphate (cAMP) is a critical second messenger in various cellular signaling pathways and facilitates the study of G protein-coupled receptor (GPCR) activation and signal transduction. In order to

measure cAMP levels, the kit from Perkin Elmer was used, which is based on a competitive immunoassay detected by Homogeneous Time-Resolved Fluorescence (HTRF).

For this experiment, cells in suspension (100.000 cells/mL) are incubated previously in Stimulation Buffer consisting of DMEM containing 0.1% BSA, ADA (0.5 U/mL), and zardaverine (100 μ M) for 1 hour at 37°C in constant agitation (400 rpm). Then, serial dilutions of the ligands are incubated with the cells for 30 minutes at 37°C in agitation (400 rpm) for the stimulation of cAMP production. Finally, 10 μ L of each condition is plated in a white 396-well plate. For the cAMP detection 5 μ L of each reagent from the kit, Ulight and cAMP-Eu, are added following the kits' guidelines. The plate is incubated 1 hour in the dark at room temperature. Time-resolved fluorescence energy tranfers (TR-FRET) was quantified in a POLARStar microplate reader (BMG Labtech, Ortenberg, Germany). Only data suited to the standard range was used for analysis.

6.3 Proximity Ligation Assay

Proximity Ligation Assay (PLA) is a highly sensitive fluorescent-based molecular technique used to detect protein-protein interactions. Specifically, it allows the visualization and quantification of close proximity interactions (within 40 nm) between proteins in their native cellular environment.

In situ PLA was performed in SH-SY5Y cell using the Duolink in situ PLA detection kit (Sigma-Aldrich). For these experiments, cells are seeded in 12 mm diameter cover glasses pre-treated with poly-D-lysine. Cells are grown for two days until the confluence is about 50%. Cells are then washed with PBS and fixed with 2% PFA for 10 minutes at room temperature. PFA is washed with PBS twice and cells are incubated with pre-blocking buffer (20 mM glycine in PBS) for 10 minutes and blocking buffer (0.1% BSA in pre-blocking buffer) for one

hour, subsequently. After blocking the samples, cells are incubated with the corresponding primary antibodies anti- $A_{2A}R$ (sc-32261, Santa Cruz Biotechnology, Dallas, TX, USA) and anti-mGlu₅R (Af300, Watanabe Productions, Shibuya, Tokyo Japan) overnight at 4° C.

The next day, excess of primary antibodies is washed with blocking buffer and cells are incubated 1 hour at 37°C with Duolink PLA anti-rabbit MINUS and anti-mouse PLUS probe, previously mixed and stabilized in commercial blocking buffer. Cells are then washed with Wash A buffer (150 mM NaCl, 10 mM Tris-Base, 0.05% Tween-20, pH 7.4) and incubated with the T4 Ligase (0.025 U/µl, Sigma Aldrich) diluted in the ligation solution (0.25 M NaCl, 5 mM ATP, 0.125% BSA, 0.25% Tween-20) for 30 minutes at 37°C. Thereafter, cells are again washed and incubated with the phi29 DNA polymerase (0.25 U/µl, Sigma Aldrich) diluted in the amplification solution containing the far-red fluorescent probe, which hybridizes to the amplified product. The amplification reaction is incubated for 100 minutes at 37°C and then samples are washed with Wash buffer B (100 mM NaCl, 200 mM Tris, 0.05% Tween-20, pH 7.5) twice and washed once again with 0.01x Wash buffer B before mounting the cover glasses with Vectashield Mounting Medium containing DAPI (VectaLabs, Sydney, Australia).

Images were acquired using Carl Zeiss LSM880 from the CCiT-UB and fluorescent signal was analyzed and quantified using FIJI ImageJ (ImageJ U.S., NIH, Bethesda, MD, USA).

7. ANIMALS

7.1 Radiolabeled nanobody biodistribution

All animal experiments conducted at Vrije Universiteit Brussels (Belgium) were approved by the Brussels Environmental Department (ECD: 24-

272-13). Female wild-type (WT) C57Bl6/J littermate mice were used in these studies. The mice were purchased from Charles River (Wilmington, MA, USA) at 5 weeks of age, quarantined for one week, and subsequently used for experiments. Animals were housed under standard conditions, with *ad libitum* access to food and water, and maintained on a 12-hour light-dark cycle.

For the biodistribution experiments with radiolabeled nanobodies, mice are administered under anesthesia either 99mTc-Nb or 111In-Nb. For 99mTc-Nb, mice receive an intravenous (5 μ g, 19,0125 Bg \pm 1.27) or intranasal (2.5 μ g, 2,958 Bq ± 0.63) injection, and a single SPECT-CT imaging scan is performed 1hour post-administration. For 111In-Nb, mice are administered 5 µg of the tracer intravenously or intranasally, and SPECT-CT imaging is conducted longitudinally at multiple time points (1-, 6-, 24-, and 48-hours post-administration) to monitor biodistribution over time. For both tracers, SPECT-CT imaging is performed with the Vector+ scanner (MILabs B.V., Houten, Netherlands) under isoflurane anesthesia. The single-photon emission computed tomography (SPECT) scan is acquired in spiral mode across six bed positions with a total scan time of 20 minutes (150 seconds per position), while the computed tomography (CT) parameters are set at 60 kV and 615 mA for a 146-second acquisition. Images are analyzed with AMIDE software (Medical Image Data Examiner, UCLA, CA, USA). Following the final imaging point, mice are sacrificed by cervical dislocation, and organs of interest are harvested and assessed for radiotracer uptake using the gamma counter 2480 WIZARD (Perkin Elmer), to determine organ-specific biodistribution. Biodistribution quantification is calculated as the percentage of injected activity (IA%) normalized by the weight of each organ. In order to calculate the activity at the injection time the radioactive decay formula was applied:

$$A = A_0^{\left(\frac{-\ln 2}{T} * \Delta t\right)}$$

 A_0 = Initial activity of the radioisotope

T = Half life of the radioisotope

 Δt = Time range of the decay

7.2 Catalepsy test

Experiments with animals that were conducted at the University of Barcelona were approved by the Catalan Government (CEEA: 108-18). Female WT ICR (CD-1®) littermate mice were used in these studies. The mice were purchased from Charles River at 5-6 weeks of age, quarantined for one week, and subsequently used for experiments. Animals were housed under standard conditions, with *ad libitum* access to food and water, and maintained on a 12-hour light-dark cycle.

The haloperidol-induced catalepsy test is a widely used behavioral assay in rodents to evaluate the motor effects of antipsychotics drugs and to model Parkinsonian-like symptoms. Haloperidol, a potent dopamine D_2 receptor antagonist, induces catalepsy by blocking dopaminergic signaling in the striatum, leading to a state of immobility and rigidity. In this test, mice are administered haloperidol, and the cataleptic behavior is assessed by placing the animal in a specific posture, typically with its forepaws on a raised bar. The duration of the time that the mouse maintains this unnatural position, without attempting to correct its posture, serves as a measure of catalepsy.

In our experimental setup, mice receive the corresponding treatment either intranasally or intracerebroventricularly (icv), followed by the haloperidol-induced catalepsy test conducted three hours post-administration. Haloperidol (1 mg/kg, 5 ml/kg, Tocris, Bristol, UK) is administered 90 minutes before the test to ensure the development of cataleptic behavior.

For the test, mice are placed in an upright position, with their front paws resting on a wooden bar (5 cm high) and their hind paws on the base. The light was kept dim from the moment of haloperidol injection until the end of the test. The duration of immobility is recorded using a stopwatch, with counting stopped under the following conditions:

- 1. Both front paws leave the bar (movement of only one paw does not count).
- 2. Both hind paws leave the base (movement of only one paw does not count).
- 3. The mouse jumps.
- 4. External stimuli interfere with the measurement.

A maximum cutoff time of 180 seconds is set. Five measurements are collected per mouse, with the two lowest values discarded. The final catalepsy score is determined by calculating the mean of the remaining three measurements.

7.2.1 Intranasal administration

Animals are progressively habituated for the intranasal administration for two weeks, following previous protocols [156].

For the intranasal administration mice are held upside down and 2.5 uL drops are placed in each nostril. The inhalation of the drop is ensured before leaving the animal free, and every four drops animals are left free. A total amount of 20 uL is administered, which accounts for 6 nmols of the

correspondent drug (CGS21680 (Abcam, Cambridge, UK), Nb43 or Nb43-CGS21680).

7.2.2 Intracerebroventricular administration

Nanobodies are administered through an implanted cannula in the right ventricle of the mice. Cannula systems are purchased from Bilaney (Düsseldof, Germany) and are implanted through stereotaxic surgery. To this end, mice are anesthesized with isofluorane (4% induction, 1.5% maintenance) and placed in a stereotaxic apparatus with a flat skull. A small hole is drilled into the skull at the right ventricle coordinates, and a cannula is positioned using the reference coordinates (AP:-0.3; ML:-1; DV:-3) from the Paxinos Atlas. The cannula is secured to the skull with dental cement and three anchor screws. A dummy cap is inserted into the cannula to prevent blockage. After surgery, mice are administered analgesic (meloxicam, 2 mg/kg) and antibiotics (enrofluoxacine, 5 mg/kg) subcutaneously for two days.

One week after the cannula implantation, 1.5 nmol the correspondent drugs are administered (CGS21680, Nb43, Nb43-CGS21680 or R3b23) in 5 uL. Briefly, the dummy cap is replaced by an internal probe connected to the tubbing. Using an automatic pump, drugs are administered at a 1 uL/min rate. Thereafter, mice are kept with the internal probe without administering to avoid any reflux by capillarity.

The correct placement of the cannula is confirmed by injecting blue dye through the cannula after the mice are euthanized.

7.3 Locomotion test

Experiments with animals that were conducted at the University of Barcelona were approved by the Catalan Government (CEEA: 108-18). Female WT ICR (CD-1®) littermate mice were used in these studies. The mice were purchased from Charles River at 5-6 weeks of age, quarantined for one week,

and subsequently used for experiments. Animals were housed under standard conditions, with *ad libitum* access to food and water, and maintained on a 12-hour light-dark cycle.

The locomotion test is a widely used behavioral assay to assess spontaneous and drug-induced motor activity in rodents. This test provides valuable insights into neuromotor function, basal activity levels, and psychomotor responses to pharmacological manipulations. Typically conducted in an open-field arena or automated activity chambers, locomotion is measured through distance traveled over a defined period. Changes in locomotor activity can reflect dopaminergic dysfunction, sedation, hyperactivity, or exploratory behavior, making this test particularly relevant in neurological and psychiatric research, including studies on schizophrenia, Parkinson's disease, and psychostimulant effects.

7.3.1 Basal and PCP-induced locomotion

After the administration of the correspondent drug/Nb through the implanted cannula (see section 7.2.2), mice are left in an open field under red light. Mice freely moving in the open field (30cm x 30cm) are recorded for 15 minutes. Open fields are cleaned between animals in order to avoid odour contamination and conditioning.

In the case of phencyclidine (PCP)-induced locomotion, mice are administered PCP (1.5 mg/kg, Tocris) are returned to the open field under red light and recorded for one hour.

Mice are tracked using DeepLabCut [157]. Briefly, DeepLabCut neural network is trained using extracted frames from the recording and manually labeling the base of the mice tail. The neural network is trained with the generated dataset, and the model is evaluated and refined if necessary.

Recordings are analyzed and the position of the mice at each frame is extracted in csv format for further analysis.

MATLAB R2023a (Nattick, MA, USA) is used to process and analyze locomotion data from a behavioral experiment using the coordinates extracted from previous csv file. To ensure data reliability, low-confidence coordinates (likelihood < 0.95) are removed, and missing values are interpolated. Then, the total distance traveled is calculated using Euclidean distance and key movement parameters are derived, such as speed, acceleration. This data is used for plotting trajectories in projected 2D open fields. To ensure accurate distance measurements, a calibration step is included where the user selects two points corresponding to 30 cm in a video frame, allowing the script to compute a conversion factor from pixels to centimeters. The total distance traveled is then converted into real-world units. Additionally, the script analyzes movement over time by segmenting the experiment into one-minute intervals and calculating the distance traveled in each segment.

8. METANALYSIS

The meta-analysis complies with the Preferred Reporting Items for Systematic reviews and Meta-analyses PRISMA guidelines and has been prospectively registered in PROSPERO (CRD42025629627) on December 20, 2024.

Studies included in this meta-analysis were double-blind (DB) randomized controlled trials (RCT) of purinergic drugs (allopurinol, dipyridamole, pentoxifylline, propentofylline) as co-adjuvant treatment in patients with a DMS-IV/V diagnosis of schizophrenia/schizoaffective disorder or mania/bipolar disorder. Trials must have reported at least one Positive and Negative Syndrome Score (PANSS, for schizophrenia patients) and Young Mania Rating Score (YMRS, for bipolar patients).

The systematic search was conducted in PubMed, Web of Science (WoS) and SCOPUS databases using the same keyword pattern while setting a timeframe publication limit from 1990 to 2024. The search procedure details are shown in **Table 7**. All rendered results were imported to EndNote version 20.4 (Clarivate, Philadenphia, PA, USA). Duplicates were automatically eliminated; the remaining manuscripts were manually checked.

The data from the studies was extracted as the change in score from baseline. When the value was not reported, this was calculated manually from the raw data given in the study. When values were not provided, and data was shown in plots, WebPlotDigitizer version 5.2.2024 was used to extract the mean scores and SE at the baseline and the end of the treatment. The quality of the studies was assessed using the Cochrane risk-of-bias tool version 2 (RoB).

The statistical analysis of the metanalysis was done in collaboration with Dr. Sebastian Videla (Bellvitge Hospital, Pharmacology Unit, L'Hospitalet de Llobregat) and Thiago Carnaval. The meta-analysis of the standardized mean differences (SMD) for the PANSS and YMRS results was performed depending on data availability. The effect size was measured using Cohen's d and 95% confidence intervals (95%CI) were calculated. We fitted the restricted maximum likelihood random effects estimator to account for heterogeneity between studies and applied the classic DerSimonian-Laird method based on quantiles of the standard normal distribution to calculate confidence limits. We also used the truncated Knapp-Hartung adjustment to the standard error (SE) to provide alternative conservative confidence limits as a measure of sensitivity. This method has been recommended by the Crochrane Collaboration because it provides maximum efficiency with minimum bias. The I^2 statistic test was performed to quantify heterogeneity between studies. Egger's regression-based test was used to assess possible publication bias. Moreover, we performed sensitivity analyses of the efficacy outcomes by

checking the variation of results after excluding one on one studies (leaving-one-out at a time). Statistical analyses were performed with R version 4.2.2 (R Foundation for Statistical Computing, Vienna, Austria.). Effect estimates were obtained with the package meta, version 6.1-0.

Table 7. Keywords and number of results in Pubmed, WoS and Scopus search

Keywords	Pubmed	WoS	Scopus
("SCH" OR "BD") AND ("Allopurinol"			
OR "Dipyridamole" OR	956	ΕO	127
"Pentoxifylline" OR	856	58	137
"Propentofylline")			

9. STATISTICAL ANALYSIS

Data analysis was performed with Graphpad Prism 9 software. Data are presented as mean standard error of the mean (SEM) with statistical significance set at p <0.05. The sample size (n) in each experimental condition is indicated at the legend of the corresponding figure. Univariate outliers were assessed by the Grubbs' test.

Barlett's test was performed to test for equality of variances between groups. If variances were equal between groups, comparisons were performed using t-test, or one-, or two-way factor analysis of variance (ANOVA), depending on the number of statistical variables in each experimental design. If variances between groups were different, Kruskal-Walli's test was performed instead of the ANOVA test. Dunnet's multiple comparison test was performed for data with gaussian distribution. If data distribution was not Gaussian Holm-Sidàk's post hoc multiple comparison test was performed.

IV. RESULTS

DEVELOPMENT AND CHARACTERIZATION OF NANOBODY-BASED DRUGS: *IN VIVO* STUDIES

Nanobody-based drugs represent a novel class of pharmacological agents derived from single-domain antibodies. Importantly, nanobodies exhibit unique properties such as high specificity and selectivity, stability, and the ability to target challenging epitopes, qualities that make them promising candidates for pharmacotherapy. In the field of neuropharmacology, a major focus lies in the modulation of GPCRs, including $mGlu_5R$ and $A_{2A}R$, which are involved in various neuropsychiatric and neurodegenerative disorders. In this chapter, Nb43, a nanobody targeting $mGlu_5R$, has been characterized for its pharmacological potential *in vitro* and used in the development of a nanobody-based bivalent ligand, Nb43-CGS21680, targeting the $mGlu_5R$ -A_{2A}R heteromers.

1. Characterization of the Nb43 binding to mouse and human mGlu₅R

Nb43 shows higher binding affinity to human mGlu₅R compared to mouse mGlu₅R

The crystal structure of the $mGlu_5R$ -Nb43 complex clearly revealed that Nb43 binds to the extracellular domain of the $mGlu_5R$ receptor [40]. To assess the binding capacity of the nanobody in a more physiological context, Nb43- $mGlu_5R$ interaction was evaluated in HEK293T cells transiently expressing the mouse (m- $mGlu_5R$) or human (h- $mGlu_5R$) $mGlu_5R$ receptor. To this end, cell suspensions expressing the receptor were incubated with increasing concentrations of the Nb43, and nanobody binding was detected with anti-His-PE secondary antibody using flow cytometry. In cells expressing the human

mGlu₃R, increasing concentrations of Nb43 showed a saturating binding curve of the PE-derived fluorescent signal (K_D =3.09 μ M; B_{max} =6.58 μ M). However, in cells expressing the mouse mGlu₅R, Nb43 exhibited a linear binding profile rather than a saturating curve, indicating that, although specific, its binding properties were poor (**Figure 15A**). In addition, confocal immunofluorescence microscopy was used to validate Nb43 binding in HEK293T cells transfected with either human or mouse mGlu₅R, or D2R as a negative control. Notably, cells expressing mGlu₅R, either human or mouse, exhibited a significant fluorescent signal (**Figure 15B**). Moreover, the fluorescence intensity was more pronounced in cells expressing human mGlu₅R compared to the mouse receptor, consistent with the flow cytometry results.

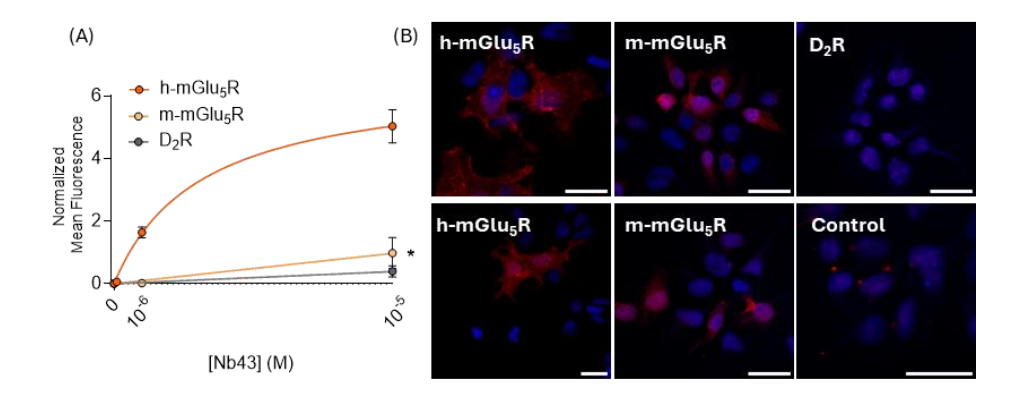


Figure 15. Differential binding ability of Nb43 to human and mouse mGlu $_5$ R in vitro. (A) Binding assay of Nb43 in HEK293T cells transiently expressing human (-h-, dark orange) or mouse (-m-, light orange) mGlu $_5$ R or D $_2$ R (negative control, grey). Nb43 was detected by anti-Hisx6-PE antibodies using flow cytometry. Results show the mean fluorescent signal normalized by the fluorescent signal of the correspondent control without the Nb43. (B) Representative immunofluorescence images of HEK293T cells transiently expressing human or mouse mGlu $_5$ R or D $_2$ R or without Nb43 (control). Nb43 was detected by anti-Hisx6-phycoerythrin (red) and cell nucleus by DAPI (blue) using confocal microscopy. Scale bar represents 25 μ m. For the mouse receptor (compared to to the binding to D2R) *p=0.03; Two-way ANOVA with Tukey's multiple comparison post hoc test.

Nb43 binds to mouse mGlu₅R ex vivo

To further investigate the binding capacity of Nb43 to mouse mGlu₅R, ex vivo experiments were performed on dissociated single cells derived from mouse brain. Two brain fractions were analysed: one containing only the cerebellum and the other comprising the whole brain excluding the cerebellum. The cerebellum, which expresses minimal levels of mGlu₅R compared to the rest of the brain [158], was used as a negative control. To this end, after dissecting the brain tissue, tissue disaggregation and dissociation was done using the mechanical and enzymatic kit from Miltenyi and the GentleMax dissociator. As a result, suspensions of living brain-derived cells were obtained. Lysis of red blood cells and debris removal was required for enriching neuronal and glial populations in the sample. Neuronal and glial cell populations were selected based on size and complexity parameters using the flow cytometer (Figure 16A -P1-). Subsequently, the selected single-cell suspensions were incubated with Nb43 at high concentrations (1 μM and 10 μM) and binding was assessed using anti-His-PE fluorescence via flow cytometry. Importantly, cells derived from brain tissue (excluding cerebellum) displayed a significant increase in fluorescence (F_(2.18)=4.78, p=0.0018), indicating specific binding to mGlu₅R. In contrast, cerebellum derived cell populations, which express minimal mGlu₅R, showed no increase in fluorescence at either concentration $(F_{(2.18)}=4.78, p=0.99)$ (Figure 16B). Overall, these results indicate that Nb43 binds specifically to mouse mGlu₅R, albeit with low affinity.

Immunofluorescence experiments were also performed to assess Nb43 across various brain regions using brain slices from the striatum, hippocampus, cortex and cerebellum. For these experiments, Nb43 was labelled with biotin at the lysine residues and its binding was detected by streptavidin-PE using confocal microscopy. To prevent non-specific binding of the streptavidin-PE to the tissue, the endogenous biotin was blocked prior to the incubation with

Nb43. Interestingly, the streptavidin-PE-derived fluorescence was observed in the hippocampus, striatum, and cortex, revealing distinct fluorescence patterns, highlighting specific cells. In contrast, minimal fluorescence was detected in the cerebellum, consistent with the *ex vivo* single-cell experiments (**Figure 16C**). These results further confirm the specificity of Nb43 binding to mGlu₅R, albeit the low affinity compared to the h- mGlu₅R.

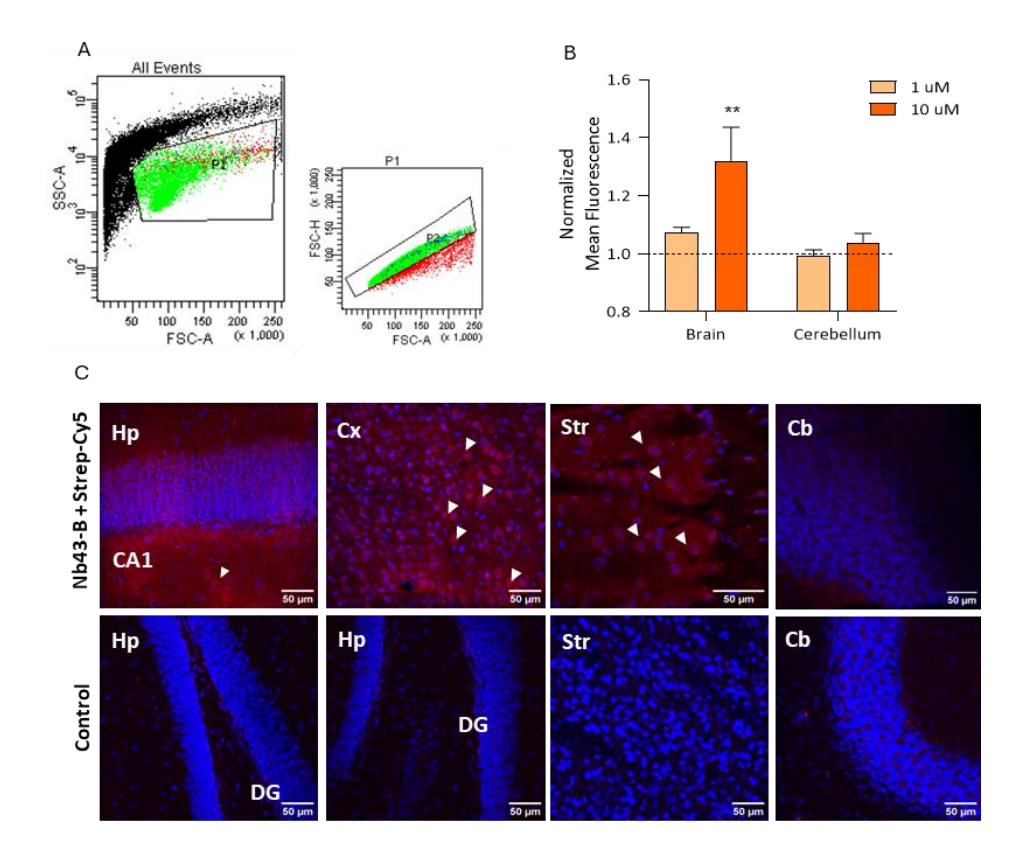


Figure 16. Binding ability of Nb43 to mGlu $_5$ R ex vivo. (A) Flow cytometry panels showing mouse brain-derived single-cell suspension (SCS) populations based on their size (FSC-A) and morphology (SSC-A). (B) Normalized mean fluorescent signal from SCS incubated with increasing concentrations of Nb43 and detected by anti-His-Cy5. SCSs derived from the cerebellum were used as a control, as mGlu $_5$ R expression is significantly lower. At higher concentrations, Nb43 binding is significantly higher compared to the cerebellum (**p<0.01; Two-way ANOVA with post hoc Tukey's multiple comparison test) (C) Immunofluorescence of mouse brain striatum, hippocampus, cortex and cerebellum incubated with Nb43-Biotin and detected by Streptavidin-Cy5. Arrows indicate specific labelled cells. (Hp: hippocampus; DG: dentate gyrus; Cx: Cortex; Str: striatum; Cb: cerebellum).

2. Structural insights on the binding of Nb43 to mGlu₅R Implication of proline 371 and histidine 350 in the binding affinity of Nb43

We observed that Nb43 exhibited significantly reduced binding capacity to the mouse mGlu₅R compared to the human variant (Figure 15). The crystal structure of Nb43 in complex with mGlu₅R reveals the region at the N-terminal domain of mGlu₅R where the nanobody binds. Notably, three amino acid residues near the nanobody's binding interface differ between human and mouse mGlu₅R (Figure 17A): His350, Pro371, and Lys388. Among these, His350 and Pro371, located in the L-M loop, directly interact with CDRs 2 and 3 of the nanobody. In contrast, Lys388 is spatially distant from the binding site, suggesting it may play a negligible role in nanobody recognition (Figure 17B).

Species-specific substitutions at these key positions likely contribute to the observed differences in binding affinity. In mouse mGlu₅R, His350 is replaced by Leu349, potentially weakening polar interactions, as leucine is a hydrophobic aliphatic residue (**Figure 17D**). More critically, Pro371 is substituted by Ala370, which could have a profound impact on binding. Proline's rigid, cyclic structure is known to mediate strong hydrophobic interactions with other hydrophobic residues such as tryptophan (**Figure 17C**). The loss of this interaction may disrupt the stability of the hydrophobic groove at CDR3, a key determinant of nanobody binding.

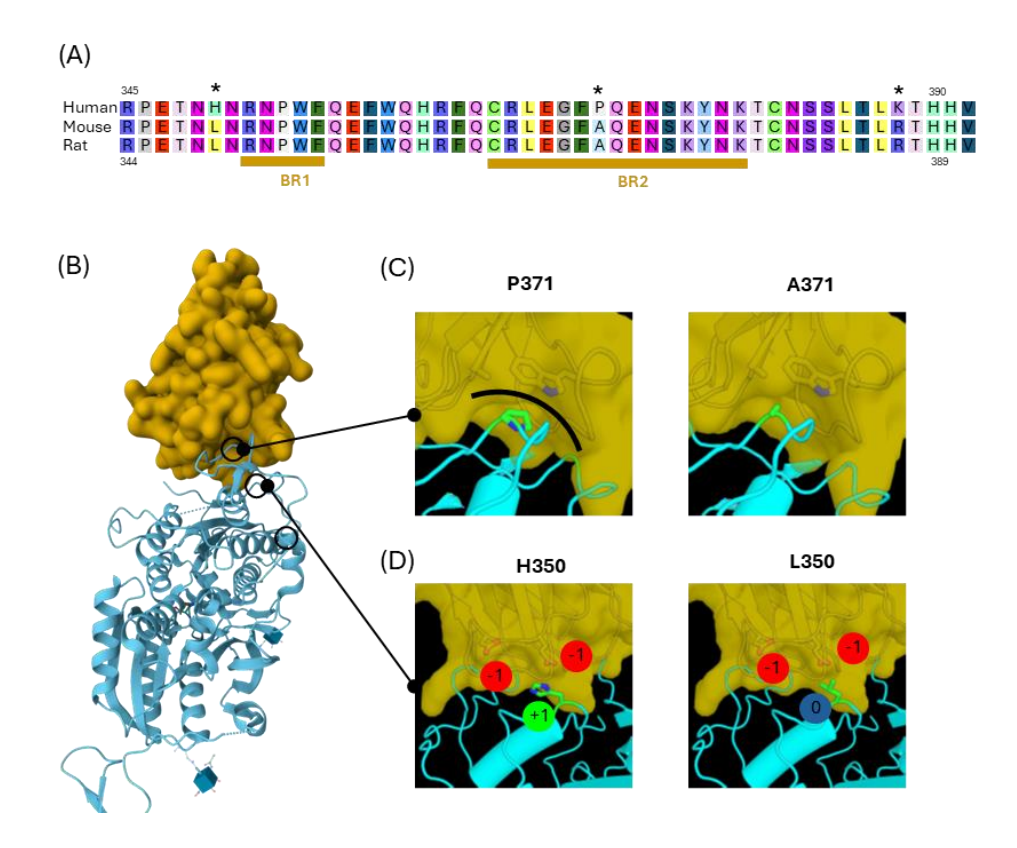


Figure 17. Structural insights on the binding of Nb43 to human and mouse mGlu₅R. (A) Amino acid sequence alignment of the Nb43 binding region (BR) of human, mouse, and rat mGlu₅R. Only three amino acids in the human receptor, H350, P371, and K388 were not conserved in the mouse and rat receptor L349, A370, and R387 (indicated with *). (B) Structure of mGlu₅R Venus Fly Trap (VFT) domain bound to Nb43 (PDB ID:6N50). VFT is represented as a cartoon structure in light blue, and the Nb43 in Gaussian volume in yellow. Circles indicate the position of the non-conserved amino acids. (C) Representation of the P371A substitution (green residue), which results in the loss of polar interaction (black line). (D) Representation of the H350L substitution (green residue), which results in the loss of polar force due to the loss of positive charge. Circles indicate the net charge of the amino acids involved in the interaction.

3. Design and synthesis of a nanobody-based bivalent liquid for targeting $A_{2A}R$ - $mGlu_5R$ heteromers

Functional characterization of the A_{2A}R-mGlu₅R heteromer in living cells

The interaction between $A_{2A}R$ and $mGlu_5R$ has been well established both *in vivo* and *in vitro* experiments. *In vitro*, the interaction between $A_{2A}R$ and $mGlu_5R$ has been demonstrated using fluorescence BRET [159]. In addition, their co-expression and physical interaction in striatal membrane extract has been demonstrated. *In vivo*, the synergistic interaction between both receptors in inhibiting D_2R has been demonstrated in the striatopallidal GABAergic neurons [160], as well as their co-expression and physical interaction in putative synaptic neuronal membranes [159]. In this study, we aimed to further study the interaction between $A_{2A}R$ and $mGlu_5R$ and validate our *in vitro* model.

Physical interaction between receptors has traditionally been studied using biophysical techniques, such as BRET, which often require the heterologous expression of receptors into living cells. Consequently, transiently transfected cells express the receptors of interest at high densities, which could lead to promiscuous interactions. To have a more physiological approach, in this study we used SHSY-5Y neuroblastoma cells which endogenously express A_{2A}R and mGlu₅R (**Supplementary Figure 1**). The physical interaction between both receptors was evaluated by in situ Proximity Ligation Assay (PLA) using specific antibodies against A_{2A}R and mGlu₅R. Confocal microscopy was used to monitor PLA signal, which was detected as discrete far-red fluorescent dots (**Figure 18A**). Quantification of PLA signal showed significantly a greater number of dots per nuclei compared to the control sample (**Figure 18B**) validating the physical interaction between A_{2A}R and mGlu₅R in living cells.

The physical interaction between these receptors has been described to have an impact on neurotransmission [161]. Indeed, mGlu $_5$ R and A $_{2A}$ R were

shown to have a synergistic effect on signaling, which was proposed to be mediated through direct receptor-receptor positive allosteric interactions [162]. In order to assess the functionality and dynamics of this heteromer, Gprotein coupling and intracellular secondary messenger production were monitored upon agonist-induced activation (Figure 18D). NanoLuc Binary Technology (NanoBiT) was first used to evaluate agonist-induced real-time functional coupling of $G_{\alpha s}$ to the $A_{2A}R$ receptor. To this end, $A_{2A}R$ and $G_{\alpha s}$ were tagged to the two halves of a nanoluciferase enzyme, SmallBiT (SmBiT) and LargeBiT (LgBiT) (**Figure 18C**). Engineered A_{2A}R^{SmBiT} and G_{as}LgBiT were heterologously expressed in HEK293T cells. $G_{\alpha s}^{LgBiT}$ protein coupling to $A_{2A}R^{SmBiT}$ was monitored by the reconstituted nanoluciferase-derived bioluminescence upon coelenterazine addition to the cells. As expected, the addition of the A_{2A}R selective agonist CGS21680 resulted in an increase in bioluminescent signal occurred within the first 10 minutes followed by a progressive decay. Interestingly, when mGlu₅R was co-transfected with A_{2A}R^{SmBiT} and protein $G_{\alpha s}^{LgBiT}$, the bioluminescent signal significantly increased, both during peak and decay periods, indicating mGlu₅R positively modulates the G_{αs}-protein coupling to A_{2A}R (Figure 18D). Concentration-response experiments demonstrated that the presence of mGlu₅R enhanced the efficacy of $A_{2A}R^{SmBiT}$ - $G_{\alpha s}^{LgBiT}$ coupling $(F_{(3.57)}=5.161, p=0.0032)$ (Figure 18E). Next, we assessed the impact of A2ARmGlu₅R heteromer formation on A2AR-mediated second messenger cyclic AMP (cAMP). Thus, the second messenger cyclic AMP (cAMP) accumulation was measured in HEK293T cells stably expressing the A_{2A}R upon agonist stimulation. Increasing concentrations of CGS21680 induced a concentration-dependent increase in cAMP levels when A2AR was expressed alone. However, when mGlu₅R was co-transfected, the potency of CGS21680 was significantly higher compared to cells expressing $A_{2A}R$ alone ($F_{(3,29)}$ =4.3, p=0.0125) (**Figure 18F**). Overall, these results are all in line with previous studies and validate the functional and physical interaction in our model.

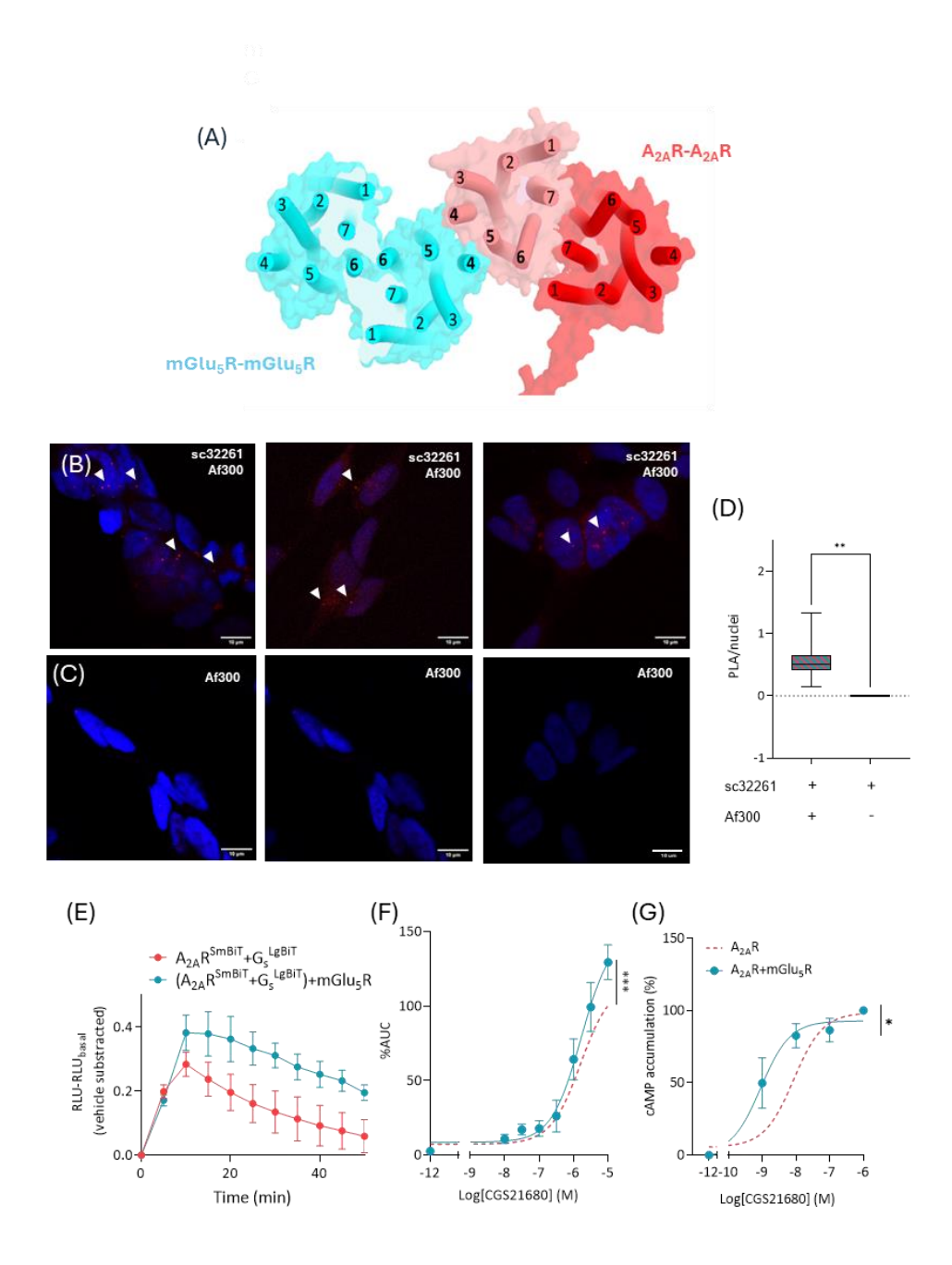


Figure 18. Physical and functional interaction of $A_{2A}R$ and $mGlu_5R$. (A) Computational model of the $A_{2A}R$ -m Glu_5R heterotetramer built by L. Pardo (UAB, Barcelona, Spain). Numbers indicate the transmembrane domains of each receptor. (B) The physical interaction and proximity of $A_{2A}R$ -m Glu_5R in SH-SY5Y was assessed by Proximity Ligation Assay (PLA; see Material and Methods), using specific antibodies against $A_{2A}R$ and m Glu_5R , sc32261 and Af300 respectively. White arrows indicate the PLA fluorescent dots which

represent A_{2A}R and mGlu₅R in proximity. (C) A condition without sc32261 was used as the negative control. Images are representative of three independent experiments. (D) The number of PLA dots was quantified and normalized by the number of nuclei present in the images. (**p<0.01; non-parametric Student's t test) (E) Representative real-time profiles of agonist-induced receptor coupling to G_s. HEK-293T cells expressing A_{2A}R-SmBiT and G_{os}-LgBiT, in the presence or absence of mGlu₅R, were challenged with CGS21680 (10 μM) and the receptor/G-protein coupling was determined by NanoBiT. Data show the NL bioluminescent signal after subtracting the vehicle signal and normalizing by basal signal (before CGS21680 addition). Results are expressed as mean ± SD of one representative experiment. (F) CGS21680-induced concentration-response curves of $A_{2A}R/G_{\alpha s}$ protein coupling in the presence (blue) or absence (red) of mGlu₅R. The area under the curve (AUC) for each CGS-induced real-time NanoBiT profile was quantified and expressed as mean ± SEM of four independent experiments each performed in triplicate. (G) A2AR agonistinduced concentration-response curves of cAMP accumulation in the presence or the absence of mGlu₅R. HEK-293T expressing the indicated receptors were challenged with increasing concentrations of CGS21680 and the cAMP accumulation determined as described in Materials and Methods. Results were normalized by the basal cAMP accumulation in mock transfected cells and expressed as means ± SEM of the four independent experiments each performed in triplicate. (* $F_{(3,29)}$ =4.3, p<0.05; *** $F_{(3,57)}$ = 5.161, p<0.001; extra-sum-of-squares F test).

Design and synthesis of Nb43-CGS21680 targeting A_{2A}R-mGlu₅R heteromer

 $A_{2A}R$ -mGlu₅R heteromers have been shown to have important implications in neurophysiological and neuropathological mechanisms. Indeed, mGlu₅R positive allosteric modulators (PAM) and $A_{2A}R$ agonists have been proposed as potential antipsychotics, which in combination could offer more specificity for the modulation of GABAergic striatopallidal neurons [160]. For this reason, we aimed to engineer a nanobody-based bivalent ligand targeting both receptors, mGlu₅R and $A_{2A}R$, which could selectively activate the heteromeric complex (**Figure 19B**). The design and synthesis of this molecule was done in collaboration with Cheloha, R. (NIH/NIDDK, Baltimore, USA) and was based on Nb43 linked to the selective agonist CGS21680 (**Figure 19A**). The linker was length of 52 atoms. Nb30, a nanobody against the major

histocompatibility complex I was used as a negative control and was also linked to CGS21680 for *in vitro* experiments.

The intrinsic activity of Nb43-CGS21680 was assessed in HEK293 cells stably expressing $A_{2A}R^{NL}$ in the absence or the presence of mGlu₅R. In order to assess the functionality of the bivalent molecule, cAMP accumulation was measured upon ligand stimulation. Interestingly, the potency of CGS21680-mediated cAMP accumulation in cells expressing $A_{2A}R$ -mGlu₅R heteromer was significantly higher to that observed in cells expressing only $A_{2A}R$ (pEC₅₀ = 9.05 vs. pEC₅₀ = 8.07F_(3,29)=4.3, p=0.0125; **Figure 19C**). Importantly, while Nb43-CGS21680 was unable to trigger $A_{2A}R$ signalling in the absence of mGlu₅R, when the mGlu₅R was co-expressed the Nb43-CGS21680 was able to activate $A_{2A}R$ with the same efficacy as CGS21680, but with lower potency (pEC₅₀ = 7.45; **Figure 19C**). These results suggest that Nb43-CGS21680 could specifically target and activate the $A_{2A}R$ in an $A_{2A}R$ -mGlu₅R heteromer-dependent manner. Finally, Nb43-CGS21680 and Nb30-CGS21680 had no efficacy activating the $A_{2A}R^{NL}$ expressing cells ($B_{max Nb43CGS21680}$ (95% IC) = 40.98 (14.08 to AF); $B_{max Nb30CGS21680}$ (95% IC) = 24.77 (18.89 to 31.40)) (**Figure 19C**).

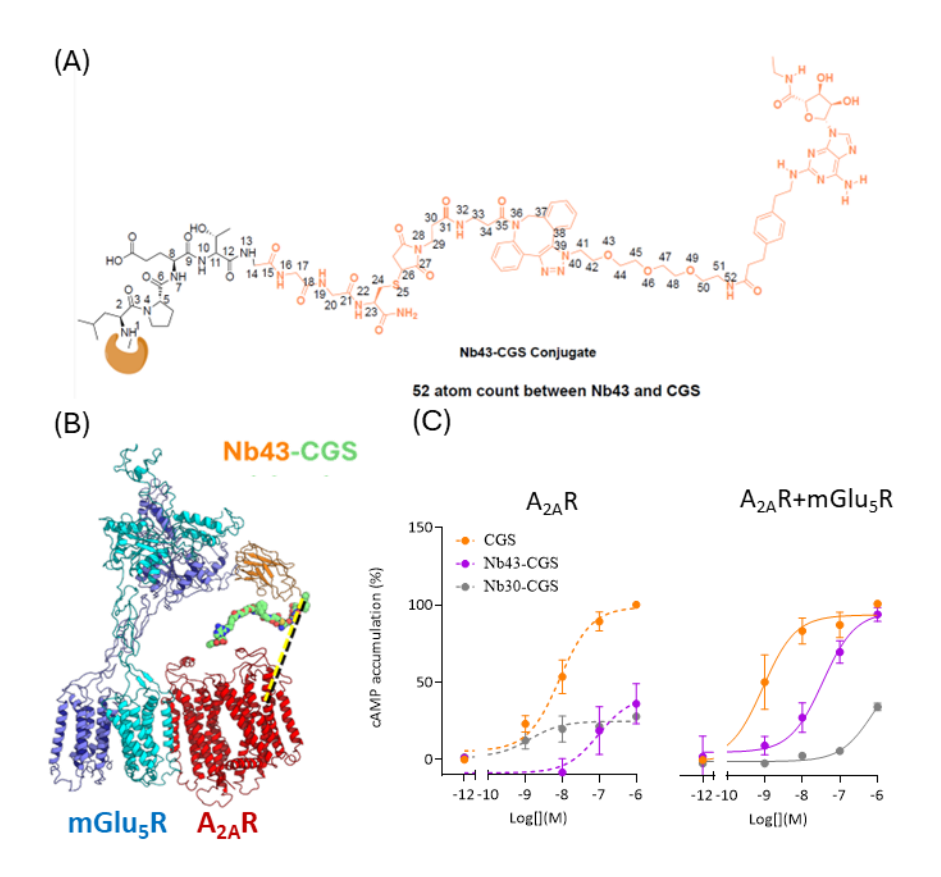


Figure 19. Nb43-CGS2168 potency is increased in the presence of mGlu $_5$ R. (A) Molecular structure of Nb43-CGS21680. Nb43 C-terminal is shown on the left end in dark orange; CGS21680 molecular structure is shown on the right in light orange. Numbers indicate the atoms between Nb43 and the ligand. (B) Computational simulation of the Nb43-CGS21680 interaction in the A_{2A} R-mGlu $_5$ R tetramer context. This model was built by L. Pardo (UAB, Barcelona, Spain) (C) Concentration-response curves of cAMP accumulation induced by CGS21680, Nb43-CGS21680 or Nb30-CGS21680. HEK293 cells stably expressing the A_{2A} R^{NL} were transfected with mock (dashed lines) or mGlu $_5$ R (solid lines) constructs and challenged with increasing concentrations of the agonist or Nb-agonist. Data show the mean \pm SEM of four independent experiments.

EVALUATION OF THE THERAPEUTIC POTENTIAL OF A NANOBODY-BASED DRUG: *IN VIVO* STUDIES

The therapeutic potential of nanobodies targeting GPCRs remains an exciting yet underexplored area of research. Despite their favorable characteristics, such as high specificity and selectivity, structural stability, and small molecular size, their pharmacological efficacy within the central nervous system is still under active investigation, primarily due to the challenge of crossing the blood—brain barrier. To address these limitations, this chapter focuses on evaluating the potential of Nb43 for CNS applications. In particular, non-invasive administration routes, such as intranasal delivery, were explored to bypass the BBB and facilitate direct brain access. To assess the pharmacological properties of Nb43, we examined its effects on mouse behavior using locomotor activity and haloperidol-induced catalepsy assays. These behavioral paradigms allowed the investigation of Nb43-mediated modulation of CNS pathways. Finally, a phencyclidine (PCP)-induced acute psychosis-like model was used to further assess the antipsychotic potential of Nb43 and its derivatives.

1. Behavioral effects of Nb43 and Nb43-CGS21680 at the central nervous system

Modulation of locomotor activity by intracerebroventricular administration of Nb43 and Nb43-CGS21680

In the previous chapter, Nb43 and its bivalent derivative, Nb43-CGS21680, were investigated *in vitro* for their potential pharmacological applications. Their ability to modulate $mGlu_5R$ and $A_{2A}R$ signaling in living cells demonstrated promising prospects for *in vivo* evaluation. Consequently, we

assessed the specific central effects of these nanobodies and their capacity to modulate glutamatergic- and adenosinergic-related behaviors. To ensure direct delivery to the central nervous system, a cannula was surgically implanted into the right lateral ventricle of the mice (see Materials and Methods). Locomotor activity was subsequently monitored as a behavioral readout of striatal mGlu₅R and A_{2A}R modulation. Thus, mice were intracerebroventricularly administered 1 nmol of either vehicle, Nb43, Nb43-CGS21680, CGS21680, or R3b23 (a control nanobody) via the implanted cannula. Following administration, locomotor activity was recorded for 15 minutes in an open field under red light conditions (Figure 20A). As expected, treatment with CGS21680 significantly reduced locomotor activity compared to vehicle treated controls ($F_{(4,15)}$ = 8.5, p=0.0004). Interestingly, mice treated with Nb43 and Nb43-CGS21680 also exhibited a decrease in locomotor activity ($F_{(4,15)}=8.5$, p=0.0039 and p=0.0119, respectively), albeit to a lesser extent than those treated with CGS21680 (Figure 20B-C). In contrast, the administration of R3b23 nanobody did not impact locomotor activity ($F_{(4.15)}$ =8.5, p=0.2629), indicating that the observed behavioral effects of Nb43 and Nb43-CGS21680 were specifically mediated through mGlu₅R targeting.

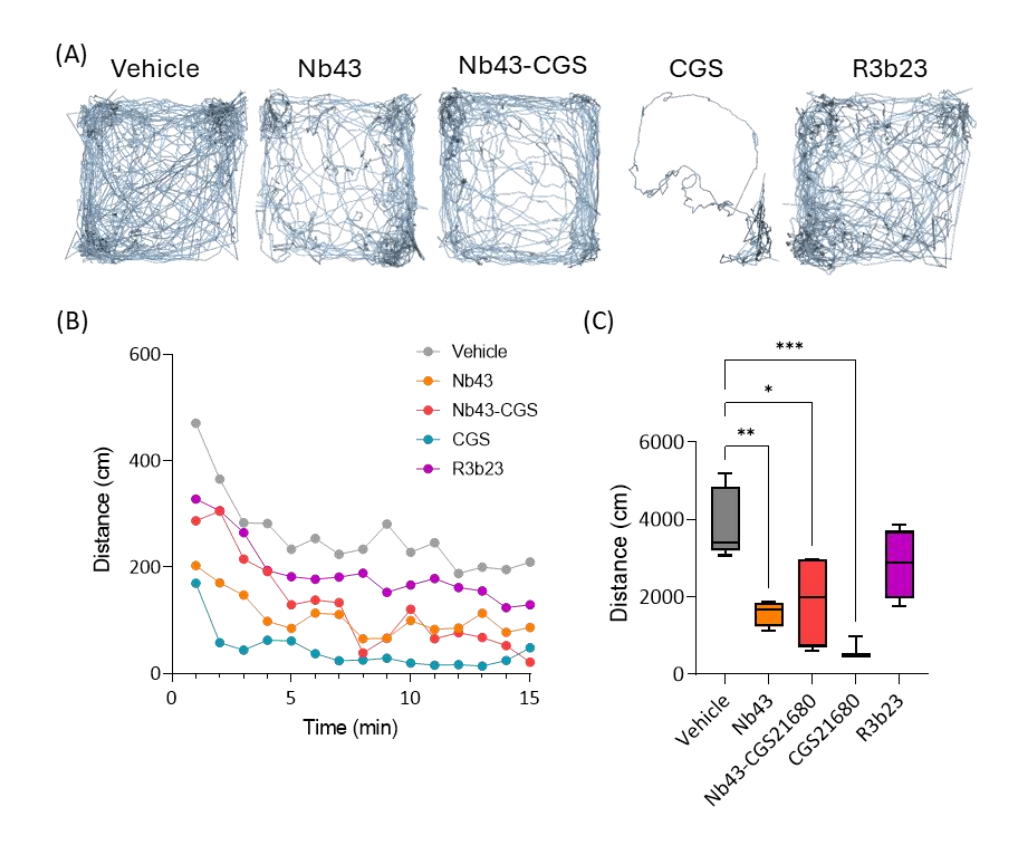


Figure 20. Effect of Nb43 and Nb43-CGS21680 on locomotor activity in mice. (A) Representative 15 min trajectories (see Material and Methods) of open field locomotor activity test of CD-1 mice administered intracerebroventricularly (1 nmol) with vehicle, CGS21680, Nb43, Nb43-CGS21680 or R3b23. (B) Mean travelled distance over time of mice treated with the indicated Nb/drug. (C) Quantification of total horizontal locomotor activity of mice (n=3-5) treated with the indicated Nb/drug. The total distance travelled is expressed as median \pm SEM values (*p<0.05, **p<0.01, ***p<0.001, One way ANOVA test with post hoc Dunnett's multiple comparison test).

Modulation of haloperidol-induced catalepsy by intracerebroventricular administration of Nb43 and Nb43-CGS21680

Catalepsy is a neurological condition marked by a loss of voluntary movements, muscular rigidity of muscles and abnormal maintenance of posture. It is often accompanied by a reduced response to external stimuli and is considered a symptom of certain neurological and psychiatric conditions, such as Parkinson's disease or catatonia. The catalepsy test, usually induced by

a D₂R antagonist such as haloperidol (Halo), is a widely used behavioral assay for assessing dopaminergic transmission. This test is particularly valuable for investigating D₂R-related pharmacological effects. Consequently, mice were administered 1 nmol of vehicle, CGS21680, Nb43, or Nb43-CGS21680 intracerebroventricularly via an implanted cannula to directly target the central nervous system (Figure 21A). before catalepsy was induced using a submaximal dose of haloperidol (1 mg/kg, i.p.) at 3, 24, and 48 hours after intracerebroventricular administration. The cataleptic state, characterized by a prolonged step-down latency measured in seconds, indicative of motor rigidity and loss of voluntary movement, was assessed 90 minutes after haloperidol injection. Interestingly, at 3-hour post-intracerebroventricular administration, mice treated with CGS21680 exhibited a significant increase in step-down latency compared to the vehicle-treated group, indicating a strong inhibitory effect ($F_{(3.17)}$ =14.01, p=0.0002). However, this effect was transient, since no significant differences in step-down latency were observed at 24 or 48 hours, suggesting that CGS21680 is rapidly metabolized or cleared from the central nervous system, as expected. Similarly, Nb43-treated mice showed a marked increase in step-down latency at 3-hour post administration ($F_{(3,17)}=14.01$, p<0.0001) (Figure 21B), indicating its ability to modulate motor function through D₂R-related pathways. This effect was also short-lived, with latency values returning to baseline at 24 and 48 hours, reflecting a limited duration of action. In contrast, mice treated with the Nb43-CGS21680 showed a significant and sustained increase in step-down latency at all measured time points (3 hours: $F_{(3,17)}=14.01$, p=0.0004; 24 hours: $F_{(3,17)}=3.73$, p=0.0281; and 48 hours: $F_{(3,16)}=4.79$, p=0.0194) (**Figure 21B**), suggesting prolonged central activity. The persistence of Nb43-CGS21680's effects highlights its potential for long-term modulation of D_2R pathways.

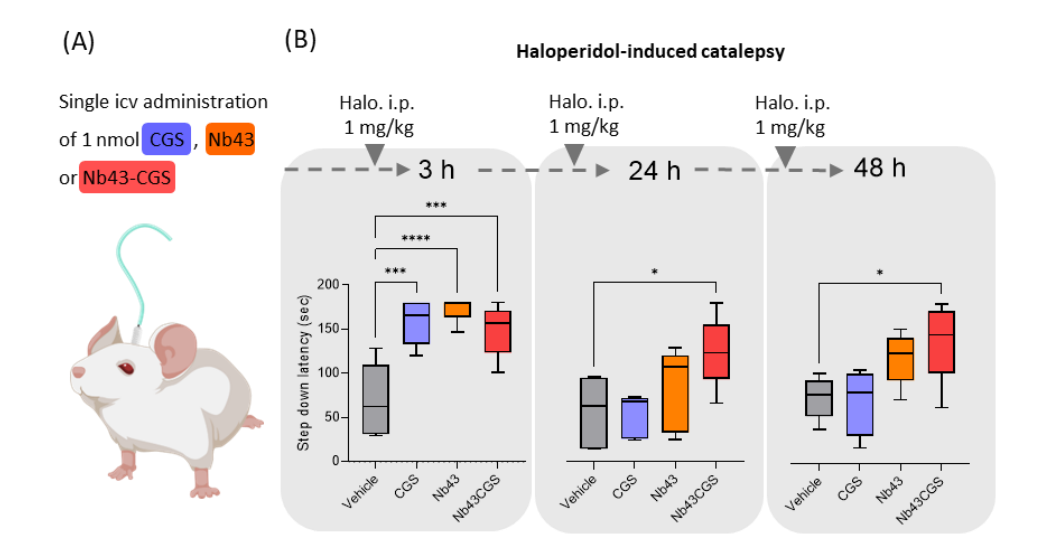


Figure 21. Effect of Nb43 and Nb43-CGS21680 administered intracerebroventricularly on haloperidol-induced catalepsy. (A) Representation of the intracerebroventricular administration through an implanted cannula in awake CD-1 mice. (B) Representation of the step-down latency measurements of the haloperidol-induced test in mice treated with the corresponding treatment (vehicle, CGS21680, Nb43 or Nb43-CGS21680; 1nmol; i.c.v.). Halo was administered (1 mg/kg, i.p.) 90 minutes before the test and the catalepsy measurements were performed at 3, 24 and 48 hours after i.c.v. administration. Results show the median SEM values of n=5-6 animals. (*p<0.05; ***p<0.001; ****p<0.0001; Oneway ANOVA with post hoc Dunnett's or Holm Šidák's multiple comparison test).

2. Biodistribution analysis of Nb43 using SPECT/CT

Comparative biodistribution of ^{99m}Tc-Nb43 following intranasal versus intravenous administration

The ability of nanobodies to cross the blood-brain barrier (BBB) remains a matter of ongoing scientific debate. Despite their low molecular weight and small size, which theoretically should enable easier tissue penetration compared to conventional antibodies, the actual extent to which nanobodies can traverse the BBB and accumulate in the CNS remains unclear. Therefore, it is essential to investigate the biodistribution of each specific nanobody individually, as its behavior can differ depending on its structure,

affinity, and other molecular properties [16,163]. Alternatively, strategies bypassing the BBB, such as intranasal administration, have been proposed [164,165]. This method involves administering drugs through the nasal cavity, which provides a direct access to the brain via the olfactory and trigeminal nerves. Therefore, to evaluate the ability of Nb43 to traverse the blood-brain barrier (BBB) *in vivo*, its biodistribution was assessed following intravenous administration using SPECT/CT imaging. Additionally, intranasal administration of Nb43 was studied to determine whether this route could effectively bypass the BBB and facilitate direct delivery to the central nervous system. To this end, Nb43 and the non-targeting nanobody R3b23 were site-specifically labelled with technetium-99m (99mTc) on their C-terminal hexa-histidine tag (see Material and Methods).

Radiolabeled nanobodies were administered intravenously (0.5 nmol ranging from 45-70 MBq) and SPECT/CT images were acquired one-hour post-administration. Both 99m Tc-Nb43 and 99m Tc-R3b23 showed a high uptake in the kidneys and the bladder (**Figure 22A, Supplementary Figure 2-3**), due to rapid blood clearance [166]. Neither 99m Tc-Nb43 nor 99m Tc-R3b23 showed brain uptake, as confirmed by *ex vivo* γ -counting (<0.05% IA/g) (**Figure 22B, Supplementary Figure 4**). These results suggest that Nb43 cannot traverse the BBB and target mGlu₅R, at least in detectable amounts.

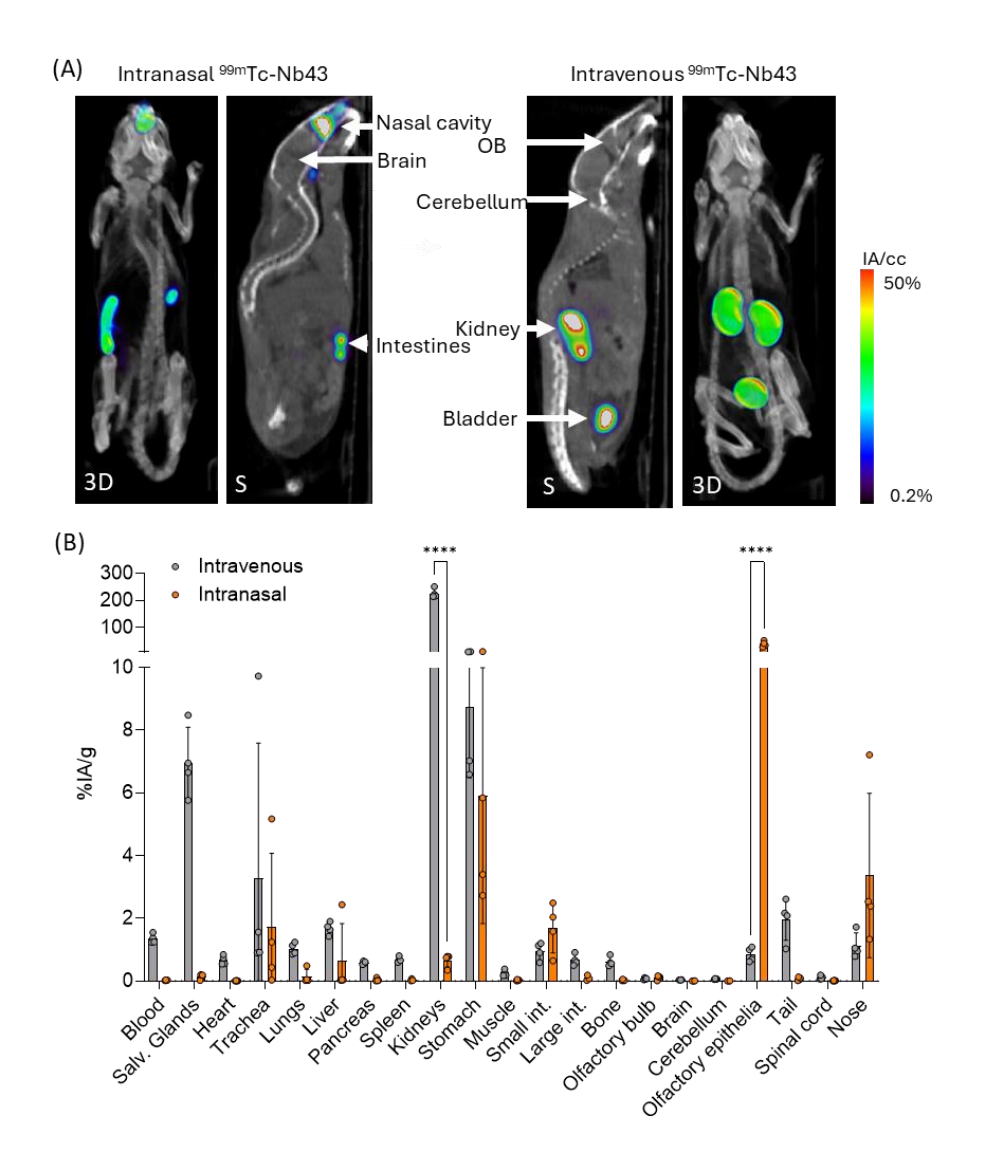


Figure 22. Biodistribution of ^{99m}Tc-Nb43 following intravenous or intranasal administration. (A) ^{99m}Tc -Nb43 was administered either intravenously or intranasally and imaging was conducted 1-hour post-administration. The images show either 3D rendered images (3D) or sagittal images (S) of one representative mouse (CT in grey scale) and radioactivity from the radiolabeled nanobody (rainbow scale). White arrows indicate organs and tissues of interest (OB: olfactory bulb). (B) After the SPECT/CT scan, animals (n=4) were dissected, and organ radioactivity was detected *ex vivo* for activity quantification. Results show the normalized percentage activity of the injected activity (IA) per weight (g) of each organ. (****p<0.001; Two-way ANOVA test with post hoc Šidák's multiple comparison test).

On the other hand, radiolabeled nanobodies were administered intranasally (0.5 nmol ranging from 15-25 MBq) and SPECT/CT images were acquired one-hour post-administration. In contrast to the intravenously administered nanobodies, intranasal administration of the nanobodies did not show high kidney and bladder uptake (**Figure 22A, Supplementary Figure 2-3**), indicating that they do not reach the bloodstream. In contrast, high unspecific accumulation was observed at the olfactory epithelium for both ^{99m}Tc-Nb43 and ^{99m}Tc-R3b23, as confirmed by *ex vivo* γ-counting (39.03±10.24 and 112.5±68.66 %IA/g, respectively) (**Figure 22B, Supplementary Figure 4**). Nevertheless, neither ^{99m}Tc-Nb43 nor ^{99m}Tc-R3b23 showed brain uptake (<0.5% IA/g).

A longitudinal study of the biodistribution of 99mTc-Nb43 following intranasal versus intravenous administration

Intranasal delivery of macromolecules occurs primarily via the olfactory and trigeminal nerves, as well as through perivascular spaces. This route relies on the passive diffusion of molecules, which can result in a slower but sustained accumulation of nanobodies in the brain compared to systemic delivery. Consequently, the kinetics and extent of brain penetration may differ significantly between intranasal and intravenous administration.

To explore the kinetics of this delayed delivery route, a longitudinal study was conducted to compare the biodistribution of nanobodies following intranasal and intravenous administration (**Figure 23A**). To this end, Nb43 and R3b23 were successfully labeled with ¹¹¹In (which has a half-life of 67.2 hours) using a random-labeling with the metal chelator p-SCN-CHX-"A-DTPA (see Material and Methods).

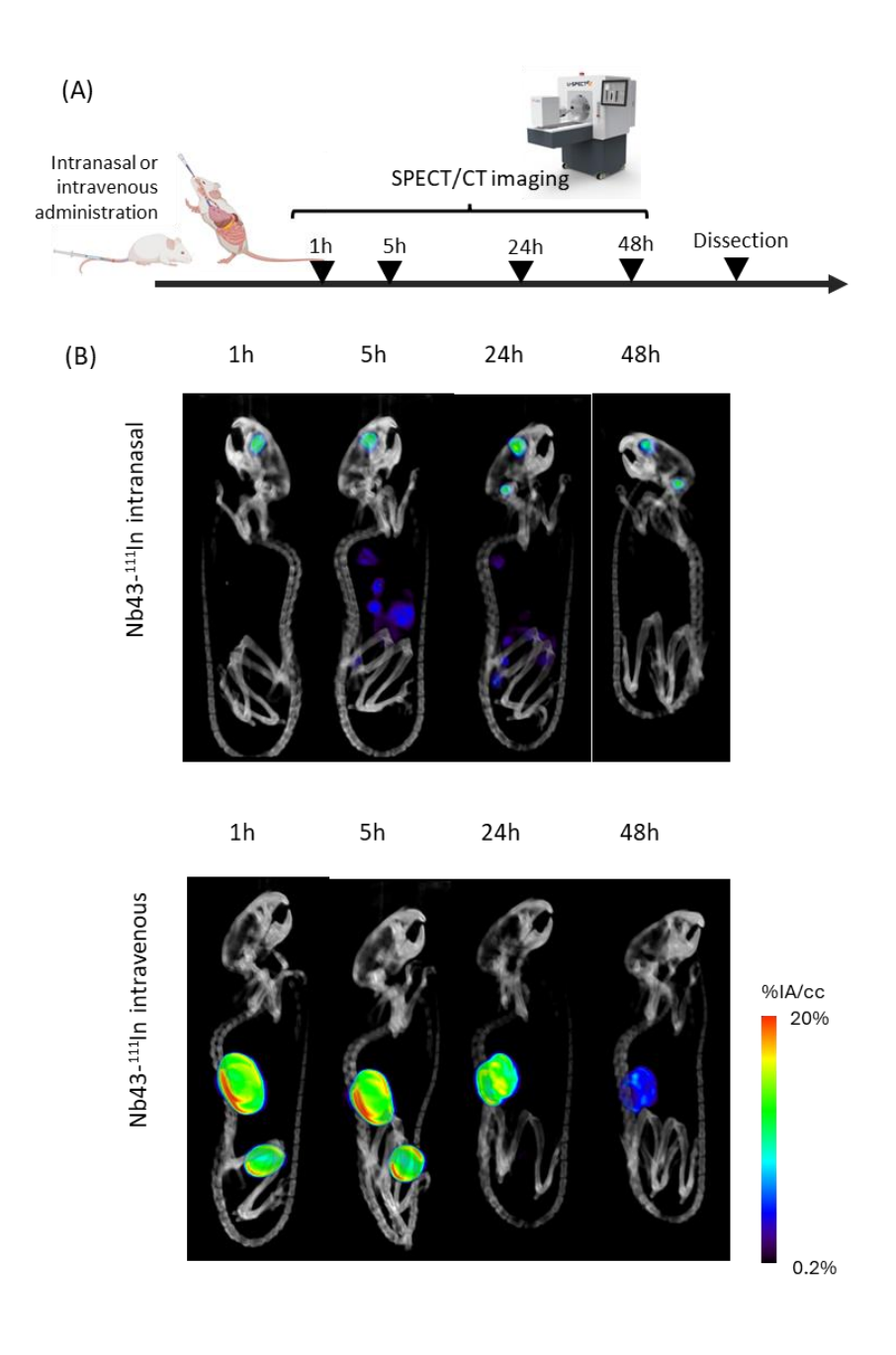


Figure 23. Figure continues in the next page

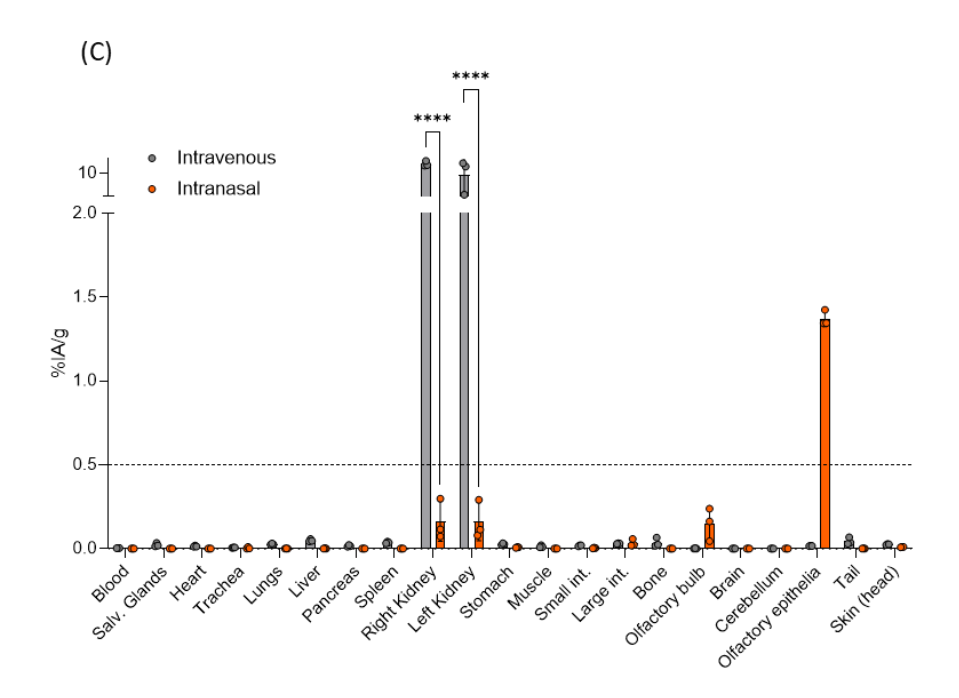


Figure 23. Longitudinal study of ¹¹¹In-Nb43 biodistribution following intravenous or intranasal administration. (A) ¹¹¹In-Nb43 was administered either intravenously or intranasally, and imaging was conducted 1, 5, 24, and 48 hours post administration. After the last SPECT/CT scans, animals (n=3) were dissected, and organ radioactivity was detected *ex vivo* for activity quantification. (B) Images show 3D volume images of mice (computed tomography in grey scale) and radioactivity from the radiolabeled nanobody (rainbow scale) at the indicated time-points. (C) Quantification of biodistribution of ¹¹¹In-Nb43 administered intravenously (grey bars) or intranasally (orange bars). Results show the normalized percentage activity of the injected activity (IA) per weight (g) of each organ. (****p<0.001; Two-way ANOVA test with post hoc multiple comparison Šidák's test)

Briefly, radiolabeled nanobodies were administered either intravenously or intranasally and SPECT/CT images were acquired at 1, 5, 24, and 48 hours post administration. ¹¹¹In-Nb43 and ¹¹¹In-R3b23 administered intravenously (0.5 nmol ranging 3-5 MBq) were characterized by a high uptake in the kidneys and bladder and rapid clearance over time (**Figure 23B, Supplementary Figure 5-8**). At 48 hours post-administration, ¹¹¹In-Nb43 signal was markedly reduced, diminishing the likelihood of effective brain uptake at this time point. On the other hand, intranasally administered ¹¹¹In-Nb43 and

¹¹¹In-R3b23 accumulated at the olfactory epithelium and signal was maintained over time. Interestingly, intranasally delivered nanobodies were cleared through the digestive system. Importantly, although overall brain uptake remained below threshold levels as confirmed by *ex vivo* γ-counting (<0.5%IA/g) (**Figure 23C**), the ¹¹¹In-Nb43 signal was significantly higher when following intranasal administration compared to intravenous administration. These results suggest that although the intranasal administration has limitations for bypassing the BBB, small quantities of nanobody may still reach the CNS.

3. Behavioral effects of intranasally delivered Nb43 and Nb43-CGS21680

Intranasally delivered Nb43 modulates haloperidol-induced catalepsy with long-lasting effects

SPECT/CT results showed no significant brain uptake of Nb43 following either intranasal or intravenous administration. Nevertheless, previous studies have consistently reported central behavioral effects of several nanobodies. For this reason, we aimed to investigate the behavioral effects of intranasally administered Nb43 and its derivative, Nb43-CGS21680. To this end, haloperidol-induced catalepsy test was performed at different time points - 3, 24, and 48 hours, following intranasal administration of either vehicle, CGS21680, Nb43 or Nb43-CGS21680 (**Figure 24A**), as previously described (**Figure 21**). Interestingly, at 3 hours post-administration, mice treated intranasally with CGS21680 showed a significant increase in step-down latency compared to the vehicle-treated group ($F_{(3,17)}$ =1.36146, p=0.0079), indicating a potentiation of haloperidol-induced catalepsy as observed when administered i.c.v. (**Figure 21**). However, this effect was no longer observed at 24- and 48-hour post-treatment. These results suggest that while intranasal administration of CGS21680 can produce a central effect, its delivery to the CNS may be limited

or subject to rapid clearance, thereby reducing its sustained activity. On the other hand, mice treated intranasally with Nb43 showed an increased stepdown latency compared to vehicle-treated group ($F_{(3,17)} = 1.361$, p = 0.0292). This effect was consistently observed at both 24 and 48 hours (p = 0.0441 and p = 0.0452, respectively), indicating a sustained effect on haloperidol-induced catalepsy (**Figure 24B**). Interestingly, mice treated with Nb43-CGS21680 via intranasal administration did not exhibit a significant increase in step-down latency at 3, 24 or 48 hours compared to the vehicle-treated group. Although a slight trend towards an increase was observed, it did not reach statistical significance at any time point (**Figure 24B**).

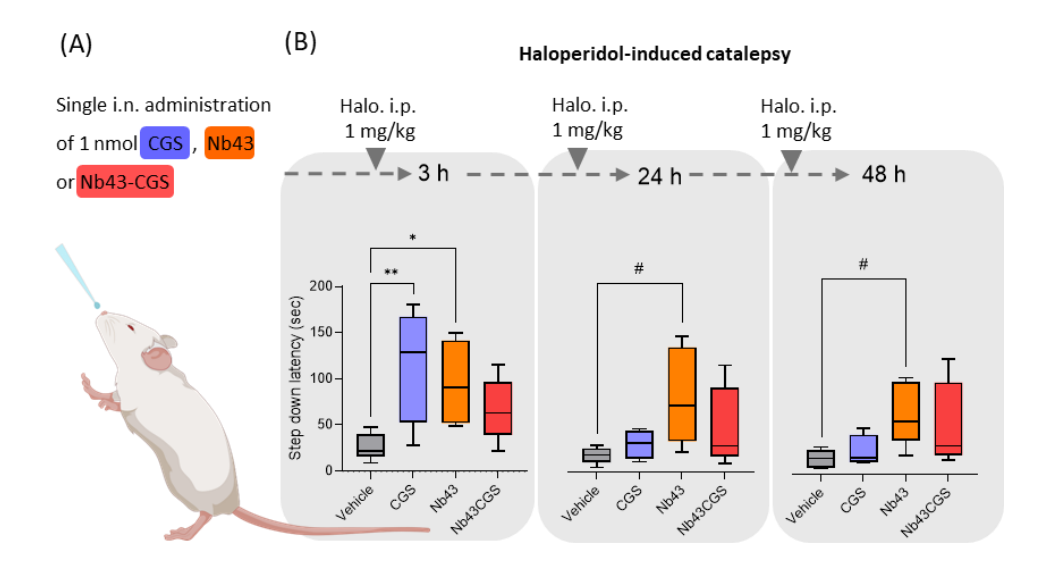


Figure 24. Effect of Nb43 and Nb43-CGS21680 administered intranasally on haloperidol-induced catalepsy. (A) Schematic representation of intranasal administration in awake mice. (B) Step-down latency measurements of the haloperidol-induced catalepsy test following treatment with the indicated compounds. Halo (1 mg/kg, i.p.) was administered 90 minutes before the which was conducted at 3, 24, and 48 hours post-intranasal treatment. Data are presented as median and the SEM values of n=5-6 animals. (*p<0.05; **p<0.01; One-way ANOVA with post hoc Tukey's multiple comparison test; #p<0.05; Kruskal-Wallis test with post hoc multiple comparison Dunn's test)

THE ADENOSINE HYPOTHESIS IN SCHIZOPHRENIA AND BIPOLAR DISORDER: A META-ANALYSIS OF RANDOMIZED CONTROLLED TRIALS OF PURINERGIC DRUGS

Adenosine metabolism and signaling has been implicated in the pathophysiology of schizophrenia and bipolar disorder, suggesting that adenosine modulators may offer therapeutic benefits. This study systematically reviewed and analyzed double-blind, randomized controlled trials evaluating purinergic drugs, including allopurinol, dipyridamole, pentoxifylline and propentofylline, as add-on treatments for these disorders.

1. Study characteristics

Selection of double-blind, randomized controlled trials of purinergic drugs for schizophrenia and bipolar disorder

A total of 1051 records were identified using search criteria (see Material and Methods). Among those, 111 duplicates were discarded, and screening was continued with 940 records. After the first screening 27 articles were evaluated for eligibility and only 14 met the criteria and were included in the analysis (Figure 25).

All included studies combined stable antipsychotic or mood stabilizer treatment with the experimental drug (add-on regimen). Of these, 8 studies focused on patients with schizophrenia or refractory schizophrenia [167–174], while 6 studies were conducted with patients diagnosed with mania or bipolar disorder[175–180] (Figure 25).

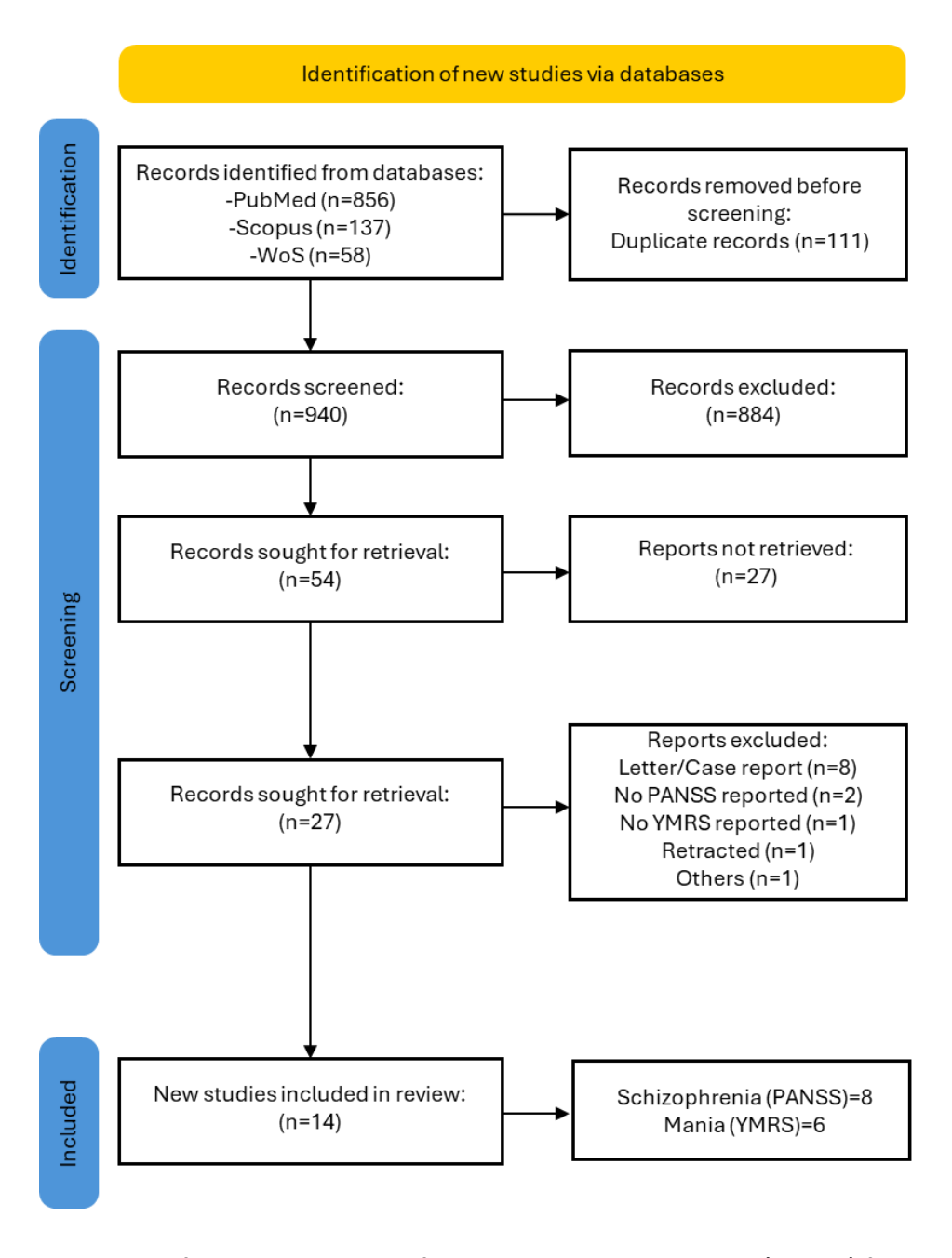


Figure 25. Preferred Reporting Items for Systematic and Meta-analysis (PRISMA) flow diagram of identified studies.

Among the studies conducted with patients with schizophrenia, six studies used a conventional parallel comparison design, and two followed a crossover design. Regarding treatment settings, five were conducted with inpatients, two with outpatients and one included both in- and outpatients (Table 8). Conversely, the studies with patients with mania or bipolar disorder, all employed a conventional parallel comparison design. Finally in terms of treatment settings, four mania/bipolar disorder studies were conducted with inpatients, one with outpatients and one included both in- and outpatients (Table 9).

In studies conducted with patients with schizophrenia, five used allopurinol as an add-on treatment, one used dipyridamole, one used pentoxifylline, and another used propentofylline (**Table 8**). In the studies conducted with patients with mania or bipolar disorder, five used allopurinol as an add-on treatment, while one used both allopurinol and dipyridamole (**Table 9**).

Sample sizes ranged from 23 to 248 patients. The mean (SD) duration of the illness was 67.38 (41.85) months for schizophrenia patients, and 96.48 (13.26) months for bipolar patients. Other characteristics of the studies are shown in **Table 8** and **Table 9**.

Table 8. Summary for the general characteristics of studies conducted with patients with schizophrenia. Allo: allopurinol, DP: dipyridamole, Prop: propentofylline, Pent: pentoxifylline, Pb: Placebo.

Study (year)	Country	Design	Diagnosis	Setting	Groups	n	Sex (M/F)	Mean (SD) Age	Mean (SD) Illness duration (month)	Follow up (weeks)
Akhondzadeh, S. (2005b)* [168]	Iran	DB RCT, Parallel	SCH	Inpatients	Allo Pb	46	33/13	33.82(7.39) 34.95(7.28)	99.90(77.91) 95.18(53.04)	8
Brunstein, M.G. (2005)* [169]	Brazil	DB RCT, Crossover	SCH, SCHAf	Inpatient, outpatient	Allo Pb	23	14/9	35.3(9.1) 42.3(12.9)	18.3(8.7) 24.2(11.3)	6
Dickerson, F.B. (2009)* [172]	USA	DB RCT, Parallel	SCH, SCHAf	Outpatient	Allo Pb	59	39/20	43.1(8.6)	?	8
Modabber, A. (2009) [171]	Iran	DB RCT, Crossover	SCH	Inpatient	Allo Pb	17	?	36.3(8.1) 36.14(7.69)	17.28(7.91) 16.10(7.24)	24
Salimi, S. (2008)* [170]	Iran	DB RCT, Parallel	SCH	Inpatient	Prop Pb	50	31/19	33.12(7.17) 34.24(7.59)	93.12(66.01) 90.00(48.86)	8
Sinichi, F. (2023) [174]	Iran	DB RCT, Parallel	SCH	?	Pent Pb	52	35/17	38.3(10.46) 41.23(8.64)	129.72(76.32) 115.44129.72)	8
Weiser, M. (2012)* [173]	Romania	DB RCT, Parallel	SCH SCHAf	Inpatient, outpatient	Allo Pb	248	128/120	43.5(10.4)	41.8(9.6)	8
Akhondzadeh, S. (2000)* [167]	Iran	DB RCT, Parallel	SCH	Inpatients	DP Pb	31	18/13	?	?	8

Table 9. Summary for the general characteristics of studies conducted with patients with bipolar disorder. Allo: allopurinol, DP: dipyridamole, Pb: placebo.

Study (year)	Country	Design	Diagnosis	Setting	Groups	n	Sex (M/F)	Mean (SD) Age	Mean (SD) Illness duration (month)	Follow up (weeks)
Akhondzadeh, S. (2005a) [179]	Iran	DB RCT, Parallel	М	Inpatient	Allo Pb	82	42/40	29.53(6.72) 28.82(6.86)	?	6
Akhondzadeh, S. (2006)*[176]	Iran	DB RCT, Parallel	М	Inpatient	Allo Pb	82	42/40	29.58(6.75) 28.89(6.89)	?	8
Fan, A. (2012)*[177]	USA	DB RCT, Parallel	М	Outpatient	Allo Pb	27	14/13	39.7(3.3) 46.6(2.6)	?	6
Machado Vieira, R. (2008)* Allo [180]	Brazil	DB RCT, Parallel	BD I	Inpatient	Allo Pb	91	42/53	26.9(8.3) 29.3(8.5)	73.2(63.6) 94.8(90)	4
Machado Vieira, R. (2008)* DP [180]	Brazil	DB RCT, Parallel	BDI	Inpatient	DP Pb	96	43/57	29.3(9.8) 29.3(8.5)	94.8(98.4) 94.8(90)	4
Weiser, M. (2014) [178]	Romania	DB RCT, Parallel	BD I	Inpatient, outpatient	Allo Pb	180	59/121	47.6(12.5) 45.8(11.2)	?	6
Jahangard, L. (2014) [175]	Iran	DB RCT, Parallel	BPI		Allo Pb	57	35/22	35.47(12.5) 33.30(10.33)	103.44(84) 117.84(116.64)	4

2. Efficacy outcomes

In this meta-analysis we assessed the efficacy of the experimental drug as an add-on treatment in patients diagnosed with schizophrenia or mania/bipolar disorder. The primary outcomes included changes in T-PANSS, P-PANSS and N-PANSS for the studies including schizophrenic patients, and changes in YMRS for the studies including bipolar patients.

Purinergic drugs significantly improve total and positive, but not negative, PANSS

The Forest Plots for each score (T-PANSS, P-PANSS, and N-PANSS) are presented in **Figure 26**. All eight studies reported T-PANSS (**Supplementary Table 1**) and were included in the analysis, revealing a statistically significant standardized mean difference (SMD) of -1.96 (95% CI: [-3.68; -0.24], p=0.03). For P-PANSS, all but two studies provided data and were included in the analysis (**Supplementary Table 2**). The results showed a significant reduction (SMD = -1.38; 95% CI: [-2.76; 0.00], p=0.05). Regarding N-PANSS, all but one study reported data (**Supplementary Table 3**). Although no statistically significant difference was observed (SMD = -1.02; 95% CI: [-2.07; 0.02], p=0.06), a trend favoring the experimental group was noted.

The heterogeneity between the studies was significant for all the PANSS scores (T-PANSS I²=95%; P-PANSS I²=96%; T-PANSS I²=95%; p<0.01), probably due to the small sample size of the studies. Leave-One-Out sensitivity analyses were performed for the T-PANSS, P-PANSS, and N-PANSS. The results remained relatively stable across study exclusions, suggesting no single study is overly influential. Notably, the exclusion of the study by Salimi et al. yielded slightly narrower confidence intervals and brought the SMD closer to zero (**Supplementary Figure 10**); however, the overall effect remained significant.

(A) T-PANSS

Study	Mean	Exp SD	Total	Mean	Control SD		Weight	Std. Mean Difference IV, Random, 95% Cl			/lean Diff andom, !		
Akhondzadeh 2000	-48.43	6.8100	16	-37.65	4.2300	14	12.5%	-1.82 [-2.69; -0.95]			-		
Akhondzadeh 2005b	-38.69	19.3500	20	-27.13	15.6900	17	12.7%	-0.64 [-1.30; 0.03]					
Brunstein 2005	-12.00	10.0000	23	3.60	11.3000	23	12.7%	-1.44 [-2.09; -0.78]					
Salimi 2008	-41.35	1.2900	24	-30.81	1.1700	23	11.3%	-8.41 [-10.27; -6.54]	-	•			
Modabber 2009	-17.20	7.0000	10	-3.29	8.7600	9	12.3%	-1.69 [-2.77; -0.61]			-		
Dickerson 2009	-5.12	1.0300	27	-2.72	1.0800	24	12.7%	-2.24 [-2.95; -1.53]			•		
Weiser 2012	-16.50	2.0400	123	-16.60	2.0400	125	12.9%	0.05 [-0.20; 0.30]					
Sinichi 2023	-2.54	5.0800	26	-1.11	4.2200	26	12.8%	-0.30 [-0.85; 0.25]			=		
Total (95% CI)			269			261	100.0%	-1.96 [-3.68; -0.24]			•		
Heterogeneity: Tau2 =	5.9494;	Chi ² = 132	.74, df	= 7 (P <	0.01); $I^2 =$	95%							
Test for overall effect: 2	Z = -2.24	(P = 0.03))						-10	-5	0	5	10
TPANSS										Favors	Exp Fa	vors cor	ntrol

(B) P-PANSS

Study	Mean	Exp SD		Mean	Control SD		Weight	Std. Mean Difference IV, Random, 95% CI	Std. Mean Difference IV, Random, 95% CI
Akhondzadeh 2000	-16.47	2.7800	16	-11.84	2.8600	14	16.4%	-1.60 [-2.44; -0.76]	-
Akhondzadeh 2005b	-14.21	7.5100	20	-9.60	5.7400	17	16.8%	-0.67 [-1.33; -0.00]	-
Brunstein 2005	-5.00	4.5000	23	0.80	5.1000	23	16.9%	-1.19 [-1.82; -0.55]	
Salimi 2008	-14.09	0.5700	24	-11.21	0.6100	23	15.6%	-4.80 [-5.96; -3.64]	
Modabber 2009	-5.50	1.9700	10			9	0.0%		
Dickerson 2009			27			24	0.0%		i
Weiser 2012	-5.60	0.5600	123	-5.90	0.6000	125	17.4%	0.52 [0.26; 0.77]	
Sinichi 2023	-2.70	1.8100	26	-1.04	1.9400	26	17.0%	-0.87 [-1.44; -0.30]	-
Total (95% CI)			269				100.0%	-1.38 [-2.76; 0.00]	•
Heterogeneity: Tau ² =	2.8563;	Chi ² = 11	8.18, d	f = 5 (P	< 0.01);	$ ^2 = 96\%$	%		1 1 1 1 1
Test for overall effect: 2	Z = -1.95	(P = 0.0)	15)						-4 -2 0 2 4
PPANSS									Favors Exp Favors cor

(C) N-PANSS

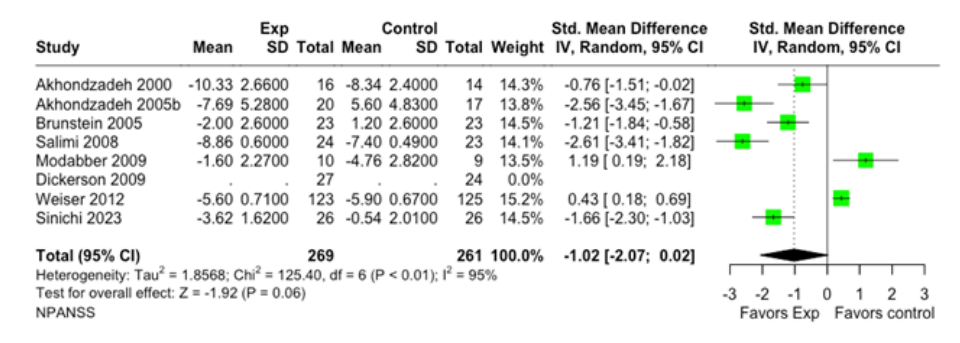


Figure 26. Forest Plots for the (A) T-PANSS, (B) P-PANSS and (C) N-PANSS.

Purinergic drugs significantly improve YMRS scores

The Forest Plot for the YMRS score is shown in **Figure 27**. All studies reported this result and were included in the analysis (**Supplementary Table 4**). The standardized mean difference was statistically significant (SMD=-1.21; 95%CI: [-2.20; -0.22]; p=0.02), favoring the experimental group treated with allopurinol or dipyridamole. Between-study heterogeneity was high (I^2 =94%). The leave-one-out method was again used for performing sensitivity analyses for the YMR. SMD values remained somewhat similar across study exclusions, suggesting that the overall effect estimate is robust (**Supplementary Figure 11**)

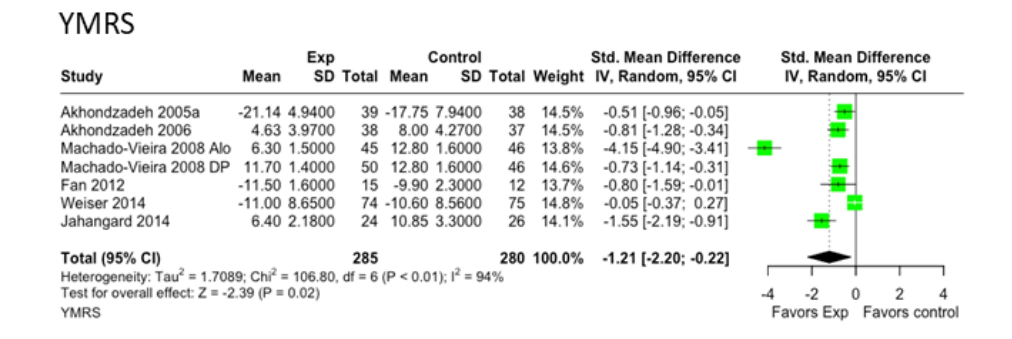


Figure 27. Forest Plot for the YMRS



Novel Pharmacological Strategies based on Nanobodies Targeting GPCRs

In this study, we provided a compelling analysis of the potential pharmacological use of nanobodies targeting GPCRs, focusing on the nanobody Nb43 against the mGlu5 receptor. Nb43 was selected due to its unique ability to bind to the N-terminal extracellular domain of the receptor [40]. Notably, nanobodies targeting the extracellular domains of GPCRs are rare, likely due to the high sequence conservation and low immunogenicity of these receptor domains, which attenuate the immune response in heterologous host species [35]. Despite these challenges, nanobodies that interact with extracellular domains hold significant therapeutic promise, as they can often modulate receptor activity without requiring intracellular access.

Nanobodies are typically characterized by their high binding affinities, often in the nanomolar range [10,181] . However, our findings revealed that Nb43 exhibits a dissociation constant (K_D) of 3.06 μM for the human mGlu₅R receptor in a heterologous expression system, indicating a relatively low binding affinity for a nanobody. Importantly, while the binding affinity of Nb43 had not been previously reported [40,182], its lower affinity may be inferred from the experiments conducted by Koehl et al., where Nb43 was employed at relatively high concentrations (1–10 μM) to investigate receptor cooperativity and allosterism [40].

Nb43 was originally developed against human mGlu₅R, thus it is not surprising that Nb43 exhibits significantly reduced binding capacity for the mouse mGlu₅R receptor, despite a 98% sequence similarity in their N-terminal

domains. Interestingly, computational analysis identified two unique amino acid substitutions, HIS350LEU and PRO371ALA, as potential contributors to this loss in binding affinity. This observation suggests that Nb43 naturally evolved to target these less conserved residues of the human receptor, highlighting the selectivity of nanobodies for distinct epitopes and their potential to target specific receptors with exceptional precision, even among closely related orthologs.

It is worth noting that despite the reduced binding affinity of Nb43 for the mouse mGlu₅R compared to its human counterpart, we were able to demonstrate **specific binding of Nb43 to the mouse receptor both** *in vitro* and *ex vivo*. Future studies could explore whether modifications to Nb43, such as affinity maturation through mutagenesis or phage display [183], might enhance its binding to mouse mGlu₅R without compromising its selectivity. Alternatively, the development of bivalent or bispecific nanobody constructs has been shown to increase the binding strength and therapeutic potential, particularly in targeting receptor heteromers or complexes [184]. Given the dimeric nature of mGlu₅R [185], it makes sense to design a bivalent nanobody, consisting of two Nb43 promoters connected by a flexible linker to enhance binding affinity and stability.

Despite these species-specificity considerations, we have developed the **first Nb43-Drug conjugate by linking the selective** $A_{2A}R$ **agonist CGS21680 to the C-terminal end of the Nb43**, an innovative concept grounded in evidence supporting the formation of a heteromeric complex between mGlu₅R and $A_{2A}R$, which plays a critical role in neuronal signaling [159]. Indeed, there is substantial evidence supporting the co-expression and synergistic signaling of mGlu₅R and $A_{2A}R$, both *in vitro* and *in vivo* [159,160,186]. Here, we further validated the mGlu₅R- $A_{2A}R$ heteromer formation in living cells using complementary approaches, thus providing evidence of the **close interaction**

between mGlu₅R and A₂AR in SH-SY5Y neuroblastoma cells, which endogenously express both receptors. While previous studies have relied on bioluminescence-based techniques, such as BRET, which require the heterologous expression of recombinant proteins [159], our approach used the Proximity Ligation Assay (PLA). This method offers a distinct advantage by enabling the detection of receptor-receptor interactions in their native cellular context, without the need for heterologous overexpression [187]. However, the PLA approach relies on the use of antibodies against the proteins of interest, which may be limited by the specificity of the antibodies and therefore require appropriate controls to validate the PLA result. The formation of GPCR heteromers often entails functional consequences for receptor(s) signaling. In fact, we demonstrated that mGlu₅R positively modulates A2AR signaling in an agonist-dependent context, consistent with previous findings from our research group. These heteromeric interactions represent novel therapeutic opportunities, since the resulting pharmacological entities may exhibit distinct signaling properties from their homomeric counterparts.

Interestingly, several ligands targeting $A_{2A}R$ and $mGlu_5R$ have been proposed for the treatment of psychotic disorders [160] and Parkinson's disease [162]. Interestingly, the described synergistic functional interaction based on $A_{2A}R$ - $mGlu_5R$ heteromer, particularly in the modulation of GABAergic striatopallidal transmission [188], could support the development of bivalent $A_{2A}R$ - $mGlu_5R$ ligands that exploit this pharmacological synergism. Thus, motivated by this rationale, we designed and synthesized Nb43–CGS21680 to specifically target the membrane heteromeric complex $A_{2A}R$ - $mGlu_5R$ complex, which is thought to modulate dopaminergic activity in the ventral striatum [162]. Our *in vitro* experiments demonstrated that Nb43-CGS21680 exhibited significant efficacy in activating $A_{2A}R$, but only in the presence of $mGlu_5R$, indicating that it specifically targets and modulates the heteromeric complex. However, the

potency of Nb43-CGS21680 was relatively modest (pEC₅₀ 7.45) compared to the CGS21680 alone (pEC₅₀ 9.04), a limitation that could be addressed through optimization of the linker design [189]. First, the linker between Nb43 and CGS21680 is currently of 52 atoms, which could be slightly shorter according to the computational estimated distance between the binding region of Nb43 and the orthosteric binding site of CGS21680, within the mGlu₅R-A_{2A}R heteromeric context. Current computational calculations suggest that a longer linker would be more appropriate, although some bending of the N-terminal domain of mGlu5R could be tolerated. Adjusting the linker length to better match this spatial requirement could improve the alignment and efficacy of the conjugate, enhancing its ability to activate the receptor complex with greater potency. Second, the conjugation of CGS21680 to the Nb43 linker was constrained by the limited chemical space available on CGS21680 for covalent attachment, thereby reducing opportunities for chemical exploration aimed at mitigating the expected loss of affinity typically associated with the conjugation of small molecules [190]. To address this, a comprehensive study of potential modifications of the molecule is warranted to assess the binding affinity of the resulting bivalent compounds.

Despite these limitations *in vitro*, we sought to investigate the potential of Nb43 and Nb43-CGS21680 in a physiological context by assessing its effects *in vivo*. To evaluate whether Nb43 and its derivatives could modulate dopaminergic transmission, behavioral assays were performed after their intracerebroventricular administration. The results of both the locomotion and the haloperidol-induced catalepsy tests provide converging evidence that Nb43 and Nb43-CGS21680 modulate dopaminergic transmission, although through complementary mechanisms to those of CGS21680 alone. The reduction in locomotion induced by Nb43 and Nb43-CGS21680, along with their ability to enhance haloperidol-induced catalepsy, strongly suggests that these constructs

negatively regulate dopaminergic activity. The lack of effect observed with R3b23 reinforces the specificity of Nb43-mediated modulation.

Despite these similarities, the nuanced differences in the effects of CGS21680, Nb43, and Nb43-CGS21680 highlight distinct underlying mechanisms. CGS21680 produced robust hypolocomotion and potentiated haloperidolinduced catalepsy, effects consistent with the well-known paradigm of A2ARmediated transinhibition of D₂R signaling [191]. In fact, the effects of CGS21680 were no longer observed after 24-48 hours, consistent with its rapid clearance/metabolism expected for small-molecule drug pharmacokinetics [192]. Similarly, Nb43, which acts as an mGlu₅R positive allosteric modulator (PAM) [40], also reduced locomotion -albeit with lower efficacy compared to CGS21680 alone- and increased haloperidol-induced catalepsy. This is consistent with previous reports showing that mGlu₅R negative allosteric modulators (NAMs) induce locomotor activity in mice depending on the target region of the brain [193]. The dorsolateral striatum (DLS), a region associated with motor control, has been shown to mediate increased locomotion upon mGlu₅R inhibition. Since Nb43 is a PAM, its reduction in locomotion may stem from enhancing mGlu₅R activity in this region, counterbalancing striatal D₂R inhibition. Importantly, this mGlu₅R-mediated transinhibition of D₂R signaling is A_{2A}R-dependent [162], suggesting a complementary mechanism of action to that proposed for CGS21680.

Finally, Nb43-CGS21680 exhibited prolonged effects on the catalepsy test, persisting for up to 48 hours. This prolonged effect suggests that conjugation of CGS21680 to Nb43 enhances receptor modulation in a more sustained manner, possibly due to the expected Nb43-mediated increase in residence time of CGS21680 within the mGlu₅R-A_{2A}R heteromer vicinity. Alternatively, the persistence of catalepsy with Nb43-CGS21680, but not with CGS21680 alone, raises the possibility that the nanobody conjugate stabilizes heteromeric

receptor interactions, prolonging their functional consequences. This is particularly relevant given that $mGlu_5R-A_{2A}R$ heteromers have been implicated in fine-tuning dopaminergic signaling in the striatum [160,162] Indeed, future studies using $A_{2A}R$ or $mGlu_5R$ transmembrane peptides to disrupt the heteromer could help determine whether the sustained effects of Nb43–CGS21680 arise from its selective targeting of $mGlu_5R-A_{2A}R$ complexes, rather than individual receptors [194]. Together, these behavioral findings reinforce the hypothesis that Nb43 and its conjugate exert their effects through a complex interplay between $mGlu_5R$ and $A_{2A}R$. While CGS21680 directly activates $A_{2A}R$ to produce anti-dopaminergic effects, Nb43-CGS21680 appear to act within the framework of the heteromer, leading to sustained modulation of dopaminergic signaling.

The ability of nanobodies to reach the central nervous system (CNS) remains uncertain. While their small size compared to conventional antibodies may facilitate BBB penetration, additional factors, such as isoelectric point, have been identified as crucial for targeting the brain [16]. Ultimately, the ability of each nanobody to traverse the BBB must be evaluated individually. Here, by using molecular imaging techniques we were unable to detect Nb43 in the CNS following intravenous administration. To date a few nanobodies have been reported to penetrate the BBB, through different mechanisms. For instance, the disruption of the BBB has been shown to facilitate the passive leakage of the nanobodies into the brain, typically due to pathophysiological conditions (i.e., cancer, inflammation or infections [195–197]) (intraparenchymal physicochemical approaches catheters [198] hyperosmotic strategies [199,200]). Interestingly, nanobodies targeting receptors in the BBB engage active transport mechanisms, such as transcytosis. Ultimately, strategies such as tagging cell-penetrating peptides or increasing

the nanobody's isoelectric point have been explored to enhance adsorption and BBB passage [201,202].

Interestingly, intranasal administration has been proposed as a non-invasive route to bypass the BBB for antibody delivery [203–205]. However, our molecular imaging studies revealed that only limited amounts of Nb43 reached the CNS via intranasal administration, in agreement with the ongoing debate over its effectiveness. Some studies have reported successful delivery of full-length antibodies, such as anti-Nogo-A [206], to various brain regions, while others found that small peptides, like orexin, do not reach the CNS [207]. Notably, many studies claiming success of intranasal delivery rely on highly sensitive detection methods, such as mass spectrometry and ELISAs [206,208], rather than *in vivo* imaging techniques like PET or SPECT. Additionally, behavioral assessments have been used as indirect measures of CNS penetration [19].

In this thesis, we evaluated the behavioral effects of Nb43 and its derivative, Nb43-CGS21680, after intranasal administration. Interestingly, **Nb43, but not Nb43-CGS21680**, **significantly enhanced haloperidol-induced catalepsy**, suggesting that Nb43 reached the CNS. This effect could be attributed to the interaction of Nb43 with the olfactory bulb, the most anterior brain region, which expresses mGlu₅R and plays a role in locomotion and balance and could be modulating the cataleptic behavior [193]. Our longitudinal imaging studies support this hypothesis, demonstrating that Nb43 accumulated in the olfactory bulb in small but detectable amounts. However, since it was not feasible to assess Nb43-CGS21680 in molecular imaging, it remains unclear whether this conjugate reaches the olfactory bulb. It is possible that Nb43-CGS21680 possesses unfavorable physicochemical properties that interfere with its accumulation in the olfactory epithelium, thereby hindering its delivery to the CNS and limiting its behavioral effects.

To date, only one nanobody targeting a GPCR has been reported to modulate GPCR function in the CNS. DN13, a nanobody with PAM activity against mGluR2, was evaluated for its role in fear conditioning modulation [39]. Although numerous nanobodies against GPCRs of the nervous system have been described, their therapeutic potential remains largely unexplored. In this thesis we emphasize the need for exploring nanobodies as pharmacological entities, focusing on GPCRs and the centrals nervous system.

EFFICACY OF PURINERGIC DRUGS IN SCHIZOPHRENIA AND BIPOLAR DISORDER

In this thesis, we conducted a comprehensive meta-analysis evaluating the efficacy and safety of purinergic drugs as adjunctive treatments for patients with schizophrenia, schizoaffective disorder, or bipolar disorder. A previous meta-analysis by Hirota et al. (2013) reported only a marginal effect of purinergic drugs in both schizophrenia and bipolar disorder populations. Given the availability of new clinical trials since then, our goal was to update and expand upon the previous findings to assess whether more recent data offer stronger evidence of their efficacy.

Our meta-analysis included eight studies on patients with schizophrenia and six studies on patients with bipolar disorder, incorporating two additional schizophrenia studies and three additional bipolar disorder studies compared to the previous meta-analysis by Hirota et al..

The analysis of schizophrenia studies showed that purinergic drugs significantly improved total and positive PANSS scores but did not yield a significant improvement in negative PANSS scores. These findings align with the previous meta-analysis by Hirota et al. Notably, the additional studies included in this meta-analysis did not report any improvement in negative symptoms, and only Sinichi et al. (2023) found a significant improvement in positive PANSS scores. In contrast, in patients with bipolar disorder, purinergic drugs demonstrated efficacy in reducing YMRS scores, consistent with the findings of Hirota et al. However, a key difference in this updated analysis is the substantial increase in heterogeneity. While Hirota et al. reported a

heterogeneity of 15%, our meta-analysis found a heterogeneity of 94%, indicating that the included studies increased the variability of the study. This variability between the studies could be explained by the small number of studies included in the meta-analysis and the small size of the number of patients.

In our study, we included various purinergic drugs with distinct pharmacodynamic and pharmacokinetic properties. We selected allopurinol, dipyridamole, pentoxifylline, and propentofylline, as these xanthine derivatives are known to increase plasma levels of adenosine or its metabolites (e.g., cAMP, AMP, inosine) [209–212]. Among them, propentofylline exhibits unique pharmacodynamic properties despite its structural similarity to other xanthines. Notably, it acts as a weak adenosine A₁ receptor (A₁R) agonist [212,213], which could explain the significant improvement in schizophrenia symptoms reported in Salimi et al. (2008). Additionally, propentofylline has neuroprotective effects, reducing inflammation and microgliosis, and has been shown to ameliorate chronic pain and dementia [212,214].

However, allopurinol has been the most extensively studied purinergic drug as an adjuvant in schizophrenia and bipolar disorder treatment. Numerous case reports and cohort studies (excluded from this meta-analysis) describe significant improvements in positive and negative symptomatology in treatment-resistant schizophrenia [215–218]. Clinically, allopurinol is a xanthine oxidase inhibitor primarily used for gout management and stroke prevention. By reducing uric acid levels, allopurinol indirectly affects purinergic signaling and increases extracellular adenosine concentrations. This mechanism is thought to underlie its potential antipsychotic effects, particularly its ability to reduce dopamine hyperactivity in the mesolimbic system [219]. Additionally, studies suggest that elevated uric acid levels may be

associated with oxidative stress and neuroinflammation in schizophrenia, further supporting allopurinol's therapeutic potential [220,221].

In contrast, dipyridamole has been less explored as an adjunctive treatment for schizophrenia. This meta-analysis included only one study on dipyridamole, which reported improvements in positive and total symptoms, but no effect on negative symptoms. Dipyridamole is an antiplatelet agent that inhibits adenosine uptake and deamination, thereby increasing extracellular adenosine levels [222]. This elevation of synaptic adenosine could enhance A₁R-mediated inhibition of dopamine transmission, contributing to its potential antipsychotic effects [213,223]. However, unlike allopurinol, dipyridamole has not been extensively studied in psychiatric disorders, and its clinical relevance in schizophrenia remains uncertain.

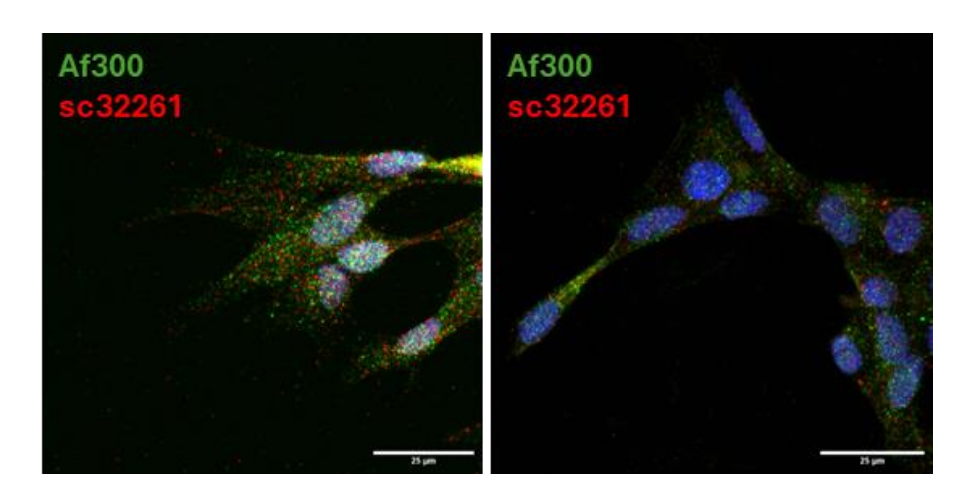


This thesis explored the pharmacological potential of nanobodies and modulators of purine metabolism as therapeutic tools for neurological conditions associated with glutamate and adenosine transmission. Based on the findings, the following conclusions can be drawn:

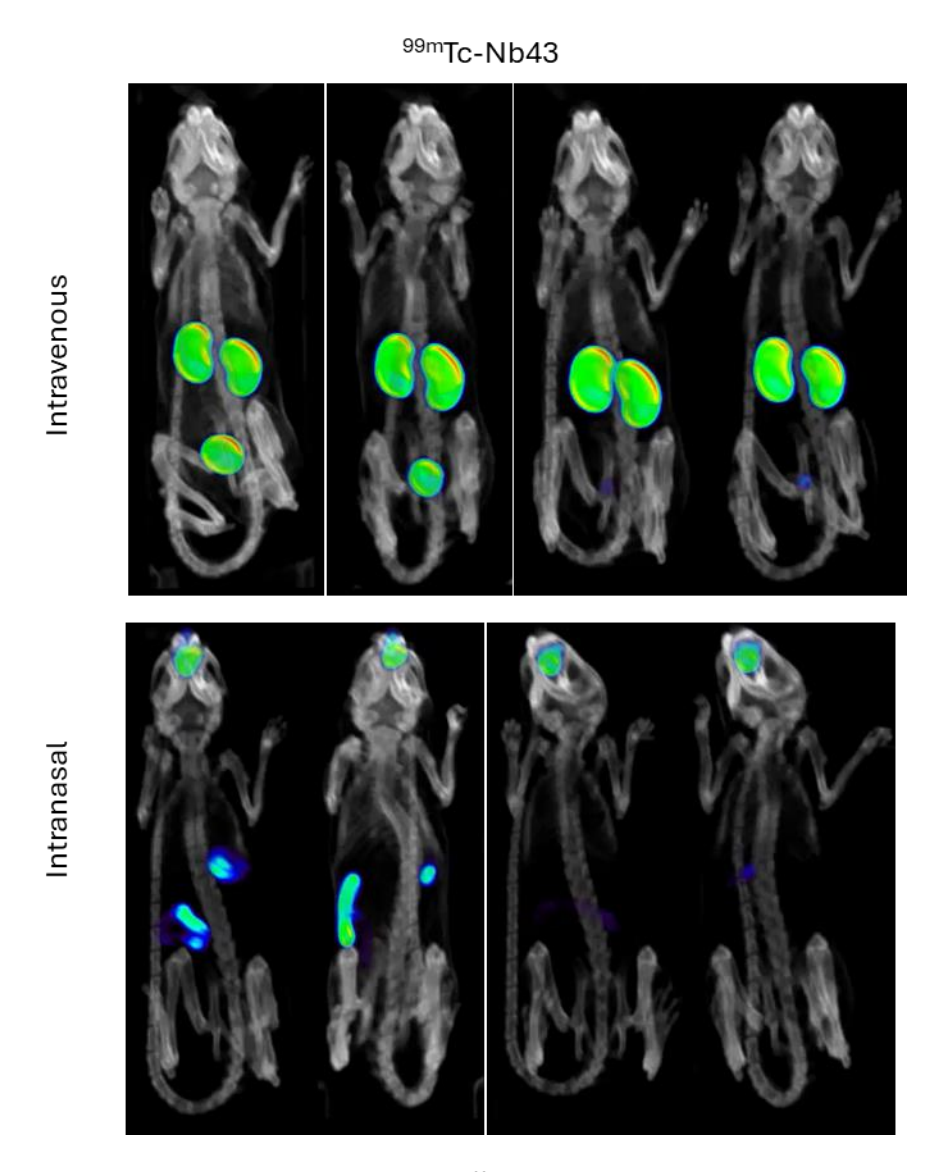
- Nb43 specifically detects human and mouse mGlu₅R under physiological conditions (i.e. in vitro and ex vivo), although it seems to target more effectively the human receptor.
- 2. We have developed an Nb-DC that incorporates a small ligand (i.e. CGS21680), which specifically modulates the $A_{2A}R$ -mGlu₅R heteromer in cultured cells.
- mGlu₅R-A₂AR heteromers represent a potential pharmacological target as they present unique pharmacological properties compared to their individual monomers.
- 4. Intracerebroventricular administration of Nb43-CGS21680 produces a long-lasting (≥48h) modulatory effect on dopamine-associated behavior in mice, compared to the acute (3h) effects of Nb43 or CGS21680 alone.
- 5. SPECT-based biodistribution analysis of Nb43 after intravenous administration reveals no detectable presence in the mouse brain, suggesting poor penetration of the BBB.
- Intranasal administration of Nb43 results in its prolonged accumulation (≥48h) in the olfactory epithelium, with only subthreshold detection in the olfactory bulb (brain), suggesting limited BBB penetration.
- 7. Intranasal administration of Nb43 induces prolonged (≥48h) antidopaminergic behavioral effects, evidenced by pro-cataleptic activity in mice, likely mediated by mGlu₅R-A_{2A}R-D₂R heteromeric interactions.

- 8. Nb43-CGS21680 does not show a modulatory effect on dopamine-associated behavior in mice after intranasal administration, compared to Nb43, suggesting that CGS21680 hinders BBB penetration.
- Our meta-analysis confirmed that adenosine metabolism modulators show potential therapeutic effects in schizophrenia and bipolar disorder, particularly in the treatment of positive symptomatology.



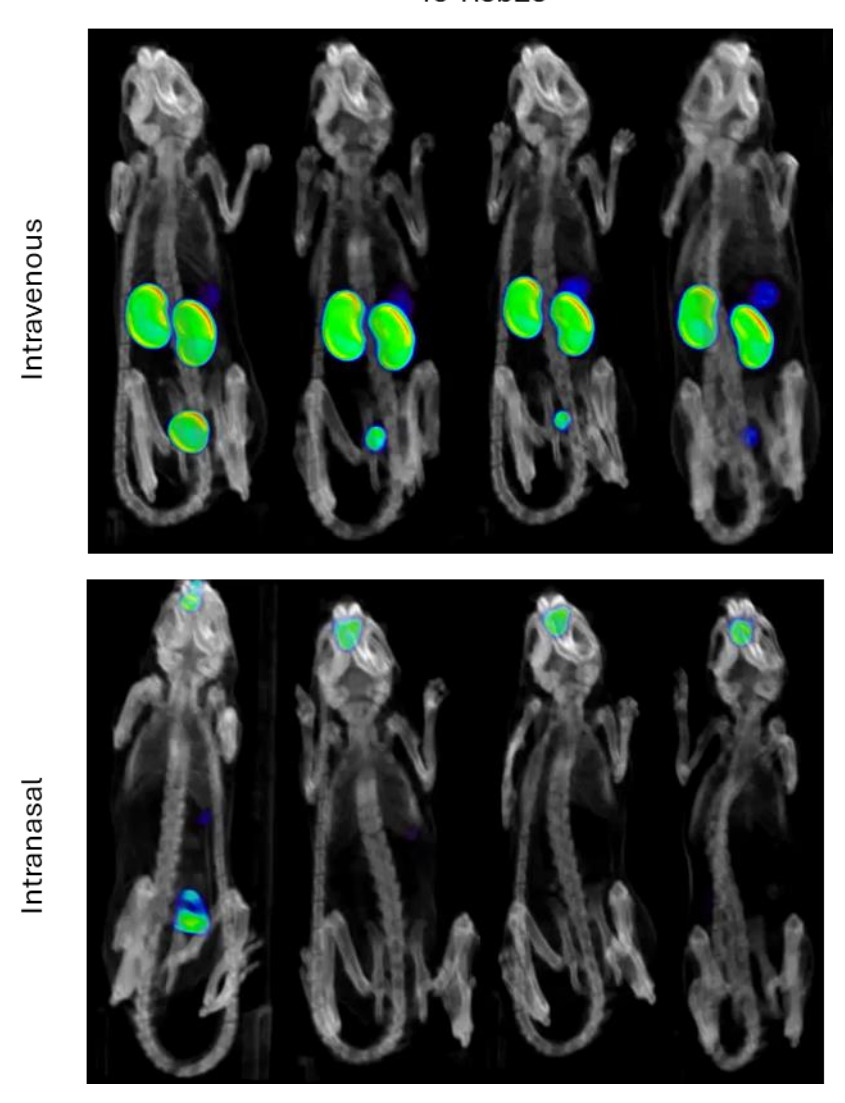


Supplementary Figure 1. mGlu $_5$ R and A $_{2A}$ R expression in SH-SY5Y neuroblastoma cell line. Expression of the receptors was detected using immunocytofluorescence in SH-SY5Y cells using mouse anti-A $_{2A}$ R and rabbit anti-mGlu $_5$ R antibodies (sc32261 and Af300, respectively). Antibodies were detected with secondary antibodies anti-mouse-Alexa647 and anti-rabbit-Alexa488. Scale bar represents 25 μ m.

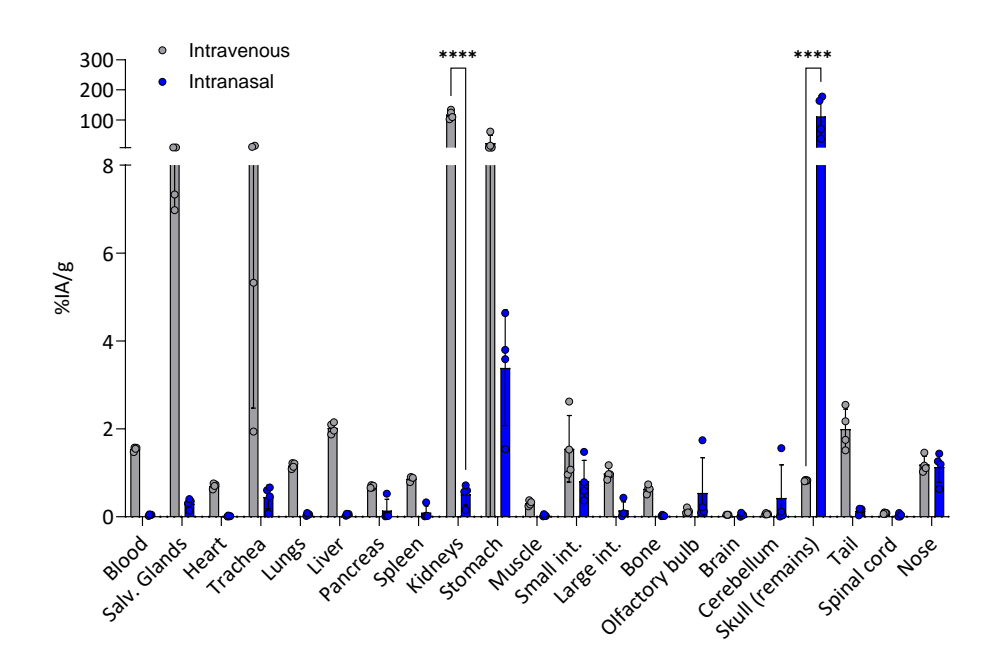


Supplementary Figure 2 Biodistribution of ^{99m}Tc-Nb43 following intravenous or intranasal administration. ^{99m}Tc -Nb43 was administered either intravenously (upper images) or intranasally (lower images) and imaging was conducted 1-hour post-administration. The Images show 3D rendered images of all mice included in the study (CT in grey scale) and radioactivity from the radiolabeled nanobody (rainbow scale).

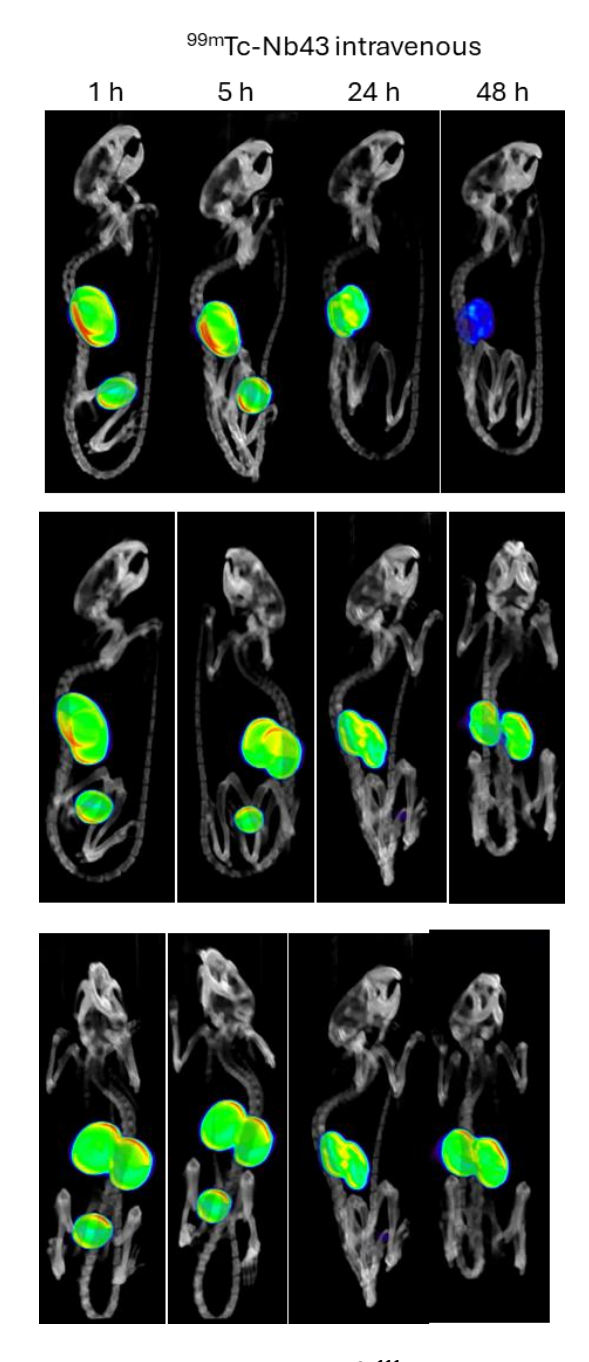
^{99m}Tc-R3b23



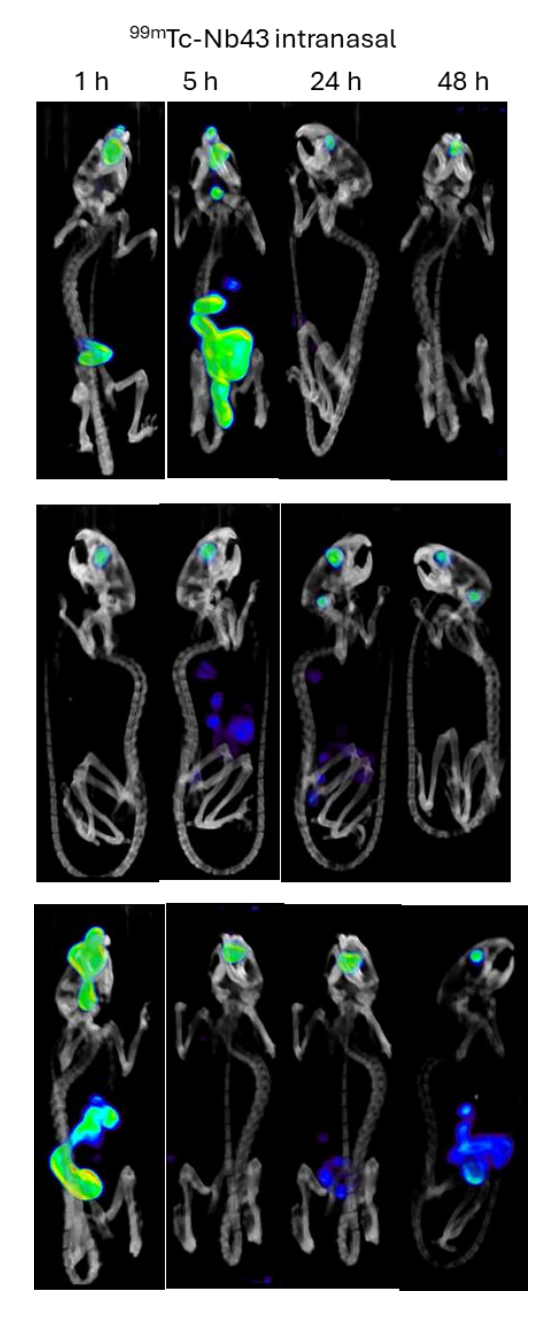
Supplementary Figure 3 Biodistribution of ^{99m}**Tc-R3b23 following intravenous or intranasal administration.** ^{99m}**Tc -R3b23** was administered either intravenously (upper images) or intranasally (lower images) and imaging was conducted 1-hour post-administration. The Images show 3D rendered images of all mice included in the study (CT in grey scale) and radioactivity from the radiolabeled nanobody (rainbow scale).



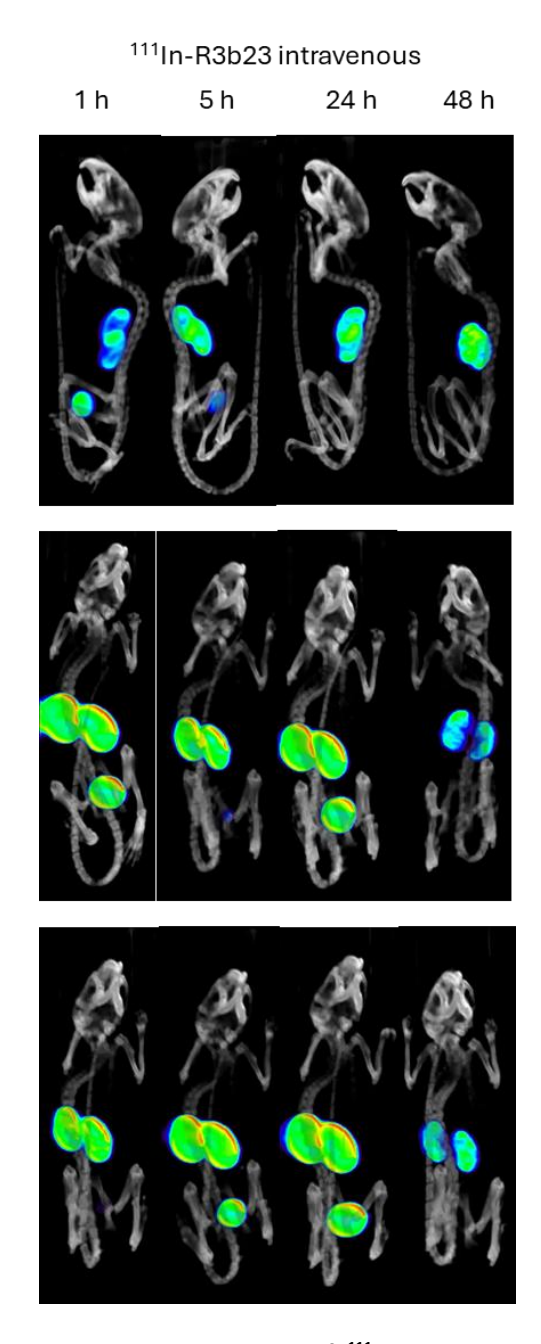
Supplementary Figure 4. Quantitative biodistribution of ^{99m}Tc-R3b23 following intravenous or intranasal administration. ^{99m}Tc -R3b23 was administered either intravenously or intranasally, and after the SPECT/CT scan, animals (n=4) were dissected, and organ radioactivity was detected *ex vivo* for activity quantification. Results show the normalized percentage activity of the injected activity (IA) per weight (g) of each organ. (****p<0.001; Two-way ANOVA test with post hoc Šidák's multiple comparison test).



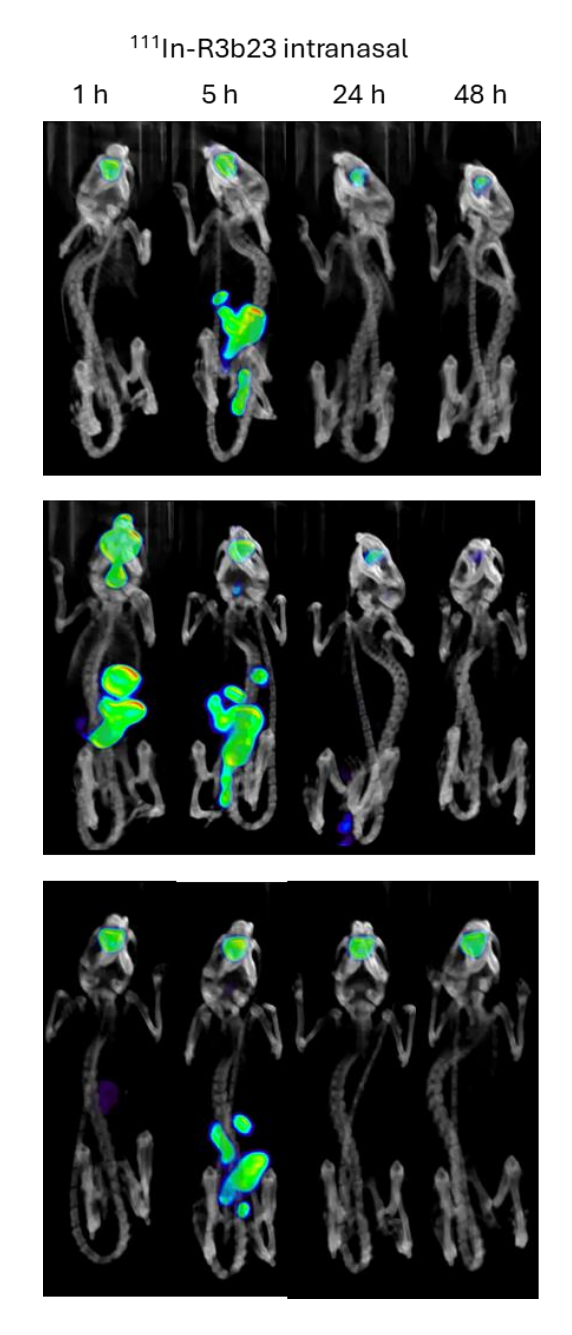
Supplementary Figure 5. Longitudinal study of ¹¹¹In-Nb43 biodistribution following intravenous administration. Images show 3D rendered images of all mice (n=3) administered ^{111In}-Nb43 intravenously and scanned by SPECT/CT at 1-, 5-, 24-, and 24-hours post administration. CT is represented in grey scale and radiolabeled nanobody in rainbow scale.



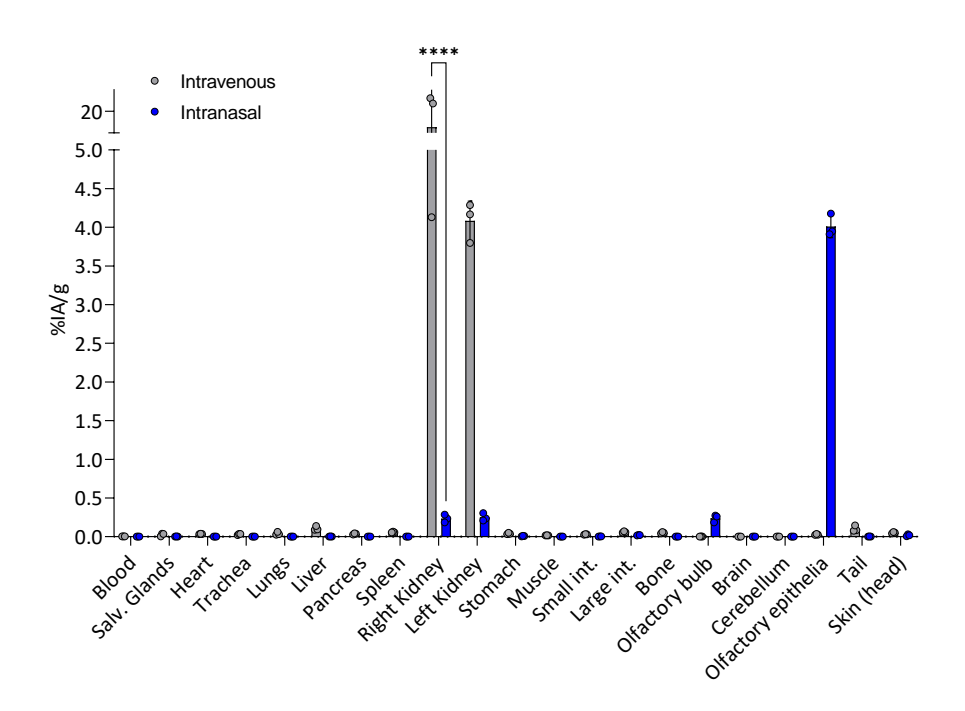
Supplementary Figure 6. Longitudinal study of ¹¹¹In-Nb43 biodistribution following intranasal administration. Images show 3D rendered images of all mice (n=3) administered ^{111In}-Nb43 intranasally and scanned by SPECT/CT at 1-, 5-, 24-, and 24-hours post administration. CT is represented in grey scale and radiolabeled nanobody in rainbow scale.



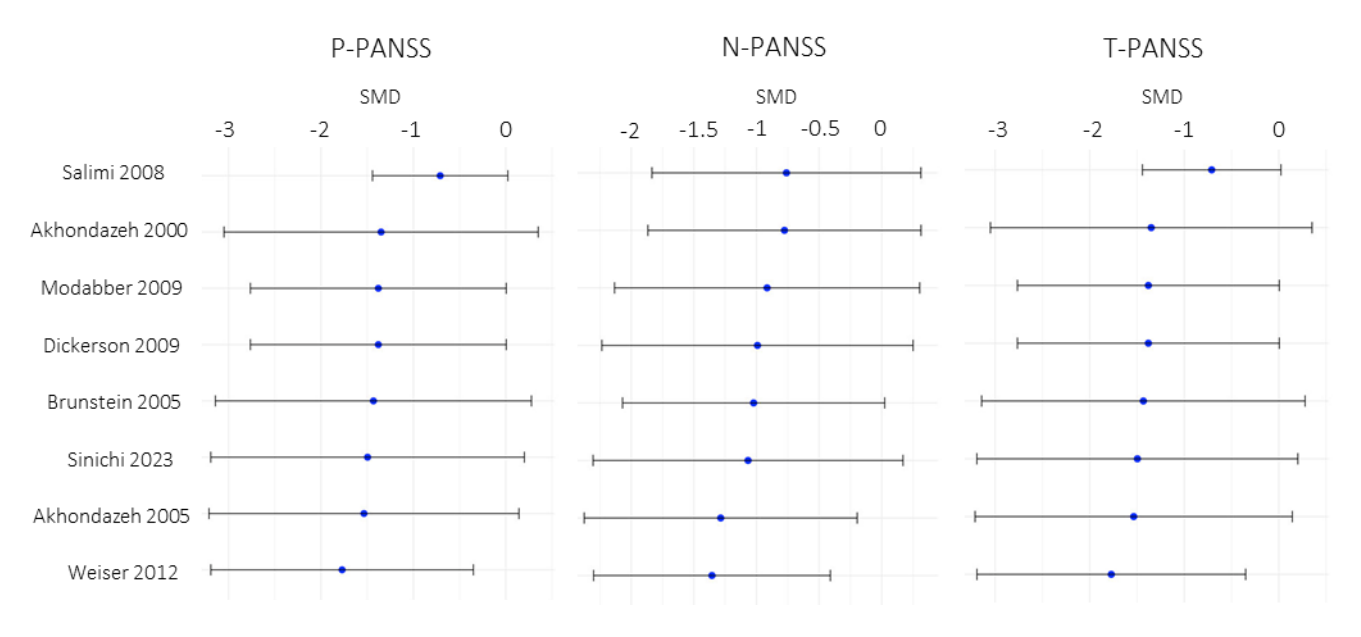
Supplementary Figure 7. Longitudinal study of ¹¹¹In-R3b23 biodistribution following intravenous administration. Images show 3D rendered images of all mice (n=3) administered ^{111In}-R3b23 intravenously and scanned by SPECT/CT at 1-, 5-, 24-, and 24-hours post administration. CT is represented in grey scale and radiolabeled nanobody in rainbow scale.



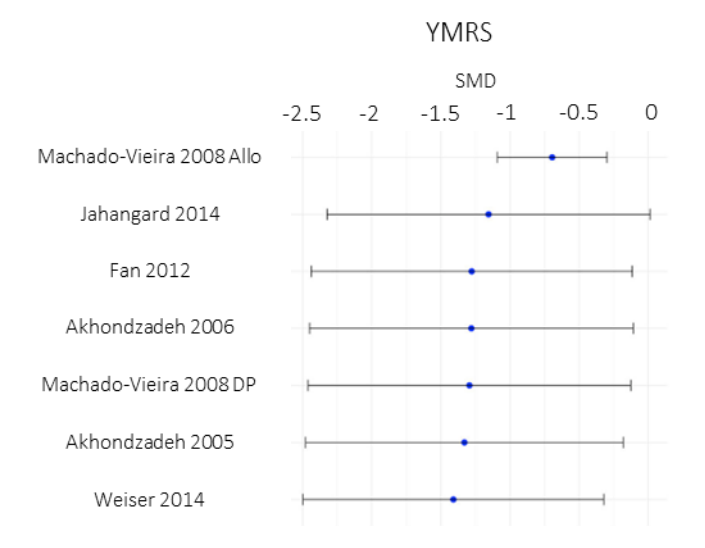
Supplementary Figure 8. Longitudinal study of ¹¹¹In-R3b23 biodistribution following intranasal administration. Images show 3D rendered images of all mice (n=3) administered ^{111In}-R3b23 intranasally and scanned by SPECT/CT at 1-, 5-, 24-, and 24-hours post administration. CT is represented in grey scale and radiolabeled nanobody in rainbow scale.



Supplementary Figure 9. Quantitative biodistribution of ^{99m}Tc-R3b23 following intravenous or intranasal administration. ^{99m}Tc -R3b23 was administered either intravenously or intranasally, and after the last SPECT/CT scan 48-hours post administration, animals (n=3) were dissected, and organ radioactivity was detected *ex vivo* for activity quantification. Results show the normalized percentage activity of the injected activity (IA) per weight (g) of each organ. (****p<0.001; Two-way ANOVA test with post hoc Šidák's multiple comparison test).



Supplementary Figure 10. Sensitivity analysis (Leave-One-Out method) for P-PANSS, N-PANSS and T-PANSS conducted with studies including patients with schizophrenia.



Supplementary Figure 11. Sensitivity analysis (Leave-One-Out method) for YMRS conducted with studies including patients with bipolar disorder.

Supplementary Table 1. Reported T-PANSS differences for the selected studies.

Ref.	Mean drugs	SD	N	Mean control	SD	N
Akhondzadeh, S. (2005b)*	-38.69	19.35	20	-27.13	15.69	17
Brunstein, M.G. (2005)*	-12	10	12	3.6	11.3	11
Dickerson, F.B. (2009)*	-5.12	1.03	27	-2.72	1.08	24
Modabber, A. (2009)	-17.2	7.00	10	-3.29	8.76	9
Salimi, S. (2008)*	-41.35	1.29	24	-30.81	1.17	23
Sinichi, F. (2023)	-2.54	5.08	26	-1.11	4.22	26
Weiser, M. (2012)*	-16.5	2.04	123	-16.6	2.04	125
Akhondzadeh, S. (2000)*	-48.43	6.81	16	-37.65	4.23	14

Supplementary Table 2. Reported P-PANSS differences for the selected studies.

Ref.	Mean drugs	SD	N	Mean control	SD	N
Akhondzadeh, S. (2005b)*	-14.21	7.51	20	-9.60	5.74	17
Brunstein, M.G. (2005)*	-5	4.5	12	0.8	5.1	11
Dickerson, F.B. (2009)*						
Modabber, A. (2009)	-5.5	1.97	10			9
Salimi, S. (2008)*	-14.09	0.57	24	-11.21	0.61	23
Sinichi, F. (2023)	-2.7	1.81	26	-1.04	1.94	26
Weiser, M. (2012)*	-5.6	0.56	123	-5.9	0.60	125
Akhondzadeh, S. (2000)*	-16.47	2.78	16	-11.84	2.86	14

Supplementary Table 3. Reported N-PANSS differences for the selected studies.

Ref.	Mean drugs	SD	N	Mean control	SD	N
Akhondzadeh, S. (2005b)*	-14.21	7.51	20	-9.60	5.74	17
Brunstein, M.G. (2005)*	-5	4.5	12	0.8	5.1	11
Dickerson, F.B. (2009)*						
Modabber, A. (2009)	-5.5	1.97	10			9
Salimi, S. (2008)*	-14.09	0.57	24	-11.21	0.61	23
Sinichi, F. (2023)	-2.7	1.81	26	-1.04	1.94	26
Weiser, M. (2012)*	-5.6	0.56	123	-5.9	0.60	125
Akhondzadeh, S. (2000)*	-16.47	2.78	16	-11.84	2.86	14

Supplementary Table 4. Reported YMRS differences for the selected studies.

Ref.	Mean drugs	SD	N	Mean control	SD	N
Akhondzadeh, S. (2005a)	-21.14	4.94	39	-17.75	7.94	38
Akhondzadeh, S. (2006)*	4.63	3.97	38	8.00	4.27	37
Fan, A. (2012)*	-11.5	1.6	15	-9.9	2.3	12
Machado Vieira, R. (2008)* Allo	6.3	1.5	45	12.8	1.6	46
Machado Vieira, R. (2008)*DP	11.7	1.4	50	12.8	1.6	46
Weiser, M. (2014)	-11.0	8.65	74	-10.6	8.56	75
Jahangard, L. (2014)	6.40	2.18	24	10.85	3.30	26



- [1] Muyldermans S. Single domain camel antibodies: current status. Reviews in Molecular Biotechnology 2001;74:277–302. https://doi.org/10.1016/S1389-0352(01)00021-6.
- [2] Asefy Z, Hoseinnejhad S, Ceferov Z. Nanoparticles approaches in neurodegenerative diseases diagnosis and treatment. Neurological Sciences 2021;42:2653–60. https://doi.org/10.1007/s10072-021-05234-x.
- [3] Cong Y, Devoogdt N, Lambin P, Dubois LJ, Yaromina A. Promising Diagnostic and Therapeutic Approaches Based on VHHs for Cancer Management. Cancers (Basel) 2024;16:371. https://doi.org/10.3390/cancers16020371.
- [4] Pothin E, Lesuisse D, Lafaye P. Brain Delivery of Single-Domain Antibodies: A Focus on VHH and VNAR. Pharmaceutics 2020;12:937. https://doi.org/10.3390/pharmaceutics12100937.
- [5] Muyldermans S. Applications of Nanobodies. Annu Rev Anim Biosci 2021;9:401–21. https://doi.org/10.1146/annurev-animal-021419-083831.
- [6] Zeghal M, Matte K, Venes A, Patel S, Laroche G, Sarvan S, et al. Development of a V5-tag-directed nanobody and its implementation as an intracellular biosensor of GPCR signaling. J Biol Chem 2023;299:105107. https://doi.org/10.1016/j.jbc.2023.105107.
- [7] Braun MB, Traenkle B, Koch PA, Emele F, Weiss F, Poetz O, et al. Peptides in headlock--a novel high-affinity and versatile peptide-binding nanobody for proteomics and microscopy. Sci Rep 2016;6:19211. https://doi.org/10.1038/srep19211.
- [8] Vu KB, Ghahroudi MA, Wyns L, Muyldermans S. Comparison of Ilama VH sequences from conventional and heavy chain antibodies. Mol Immunol 1997;34:1121–31. https://doi.org/10.1016/S0161-5890(97)00146-6.
- [9] Mitchell LS, Colwell LJ. Analysis of nanobody paratopes reveals greater diversity than classical antibodies. Protein Eng Des Sel 2018;31:267–75. https://doi.org/10.1093/protein/gzy017.

- [10] Muyldermans S. Nanobodies: Natural Single-Domain Antibodies. Annu Rev Biochem 2013;82:775–97. https://doi.org/10.1146/annurev-biochem-063011-092449.
- [11] Bao G, Tang M, Zhao J, Zhu X. Nanobody: a promising toolkit for molecular imaging and disease therapy. EJNMMI Res 2021;11:6. https://doi.org/10.1186/s13550-021-00750-5.
- [12] Piché M-S, Mounho-Zamora B, LeSauteur L, Burns-Naas LA. Immunotoxicology Testing of Monoclonal Antibodies in Macaca fascicularis. The Nonhuman Primate in Nonclinical Drug Development and Safety Assessment, Elsevier; 2015, p. 519–42. https://doi.org/10.1016/B978-0-12-417144-2.00027-5.
- [13] Schoen P, Jacobs S, Verschueren K, Ottevaere I, Sobry S, Holz J-B. Anti-RANKL nanobody ALX-0141 shows sustained biomarker inhibition in a Phase I study in healthy postmenopausal Women. Bone Abstracts 2013. https://doi.org/10.1530/boneabs.1.PP135.
- [14] Keyaerts M, Xavier C, Heemskerk J, Devoogdt N, Everaert H, Ackaert C, et al. Phase I Study of ⁶⁸ Ga-HER2-Nanobody for PET/CT Assessment of HER2 Expression in Breast Carcinoma. Journal of Nuclear Medicine 2016;57:27–33. https://doi.org/10.2967/jnumed.115.162024.
- [15] Zheng F, Pang Y, Li L, Pang Y, Zhang J, Wang X, et al. Applications of nanobodies in brain diseases. Front Immunol 2022;13:978513. https://doi.org/10.3389/fimmu.2022.978513.
- [16] Ruiz-López E, Schuhmacher AJ. Transportation of Single-Domain Antibodies through the Blood–Brain Barrier. Biomolecules 2021;11:1131. https://doi.org/10.3390/biom11081131.
- [17] Kadry H, Noorani B, Cucullo L. A blood–brain barrier overview on structure, function, impairment, and biomarkers of integrity. Fluids Barriers CNS 2020;17:69. https://doi.org/10.1186/s12987-020-00230-3.
- [18] Muruganandam A, Tanha J, Narang S, Stanimirovic D. Selection of phage-displayed llama single-domain antibodies that transmigrate across human blood-brain barrier endothelium. The FASEB Journal 2002;16:1–22. https://doi.org/10.1096/fj.01-0343fje.

- [19] Wouters Y, Jaspers T, De Strooper B, Dewilde M. Identification and in vivo characterization of a brain-penetrating nanobody. Fluids Barriers CNS 2020;17:62. https://doi.org/10.1186/s12987-020-00226-z.
- [20] Frecot DI, Froehlich T, Rothbauer U. 30 years of nanobodies an ongoing success story of small binders in biological research. J Cell Sci 2023;136:jcs261395. https://doi.org/10.1242/jcs.261395.
- [21] Manglik A, Kobilka BK, Steyaert J. Nanobodies to Study G Protein–Coupled Receptor Structure and Function. Annu Rev Pharmacol Toxicol 2017;57:19–37. https://doi.org/10.1146/annurev-pharmtox-010716-104710.
- [22] Burgstaller S, Wagner TR, Bischof H, Bueckle S, Padamsey A, Frecot D, et al. Monitoring extracellular ion and metabolite dynamics with recombinant nanobody-fused biosensors. IScience 2022;25:104907. https://doi.org/10.1016/j.isci.2022.104907.
- [23] Park KS, Park T-I, Lee JE, Hwang S-Y, Choi A, Pack SP. Aptamers and Nanobodies as New Bioprobes for SARS-CoV-2 Diagnostic and Therapeutic System Applications. Biosensors (Basel) 2024;14:146. https://doi.org/10.3390/bios14030146.
- [24] Kim H, Baek I-Y, Seong J. Genetically encoded fluorescent biosensors for GPCR research. Front Cell Dev Biol 2022;10. https://doi.org/10.3389/fcell.2022.1007893.
- [25] Gondry O, Caveliers V, Xavier C, Raes L, Vanhoeij M, Verfaillie G, et al. Phase II Trial Assessing the Repeatability and Tumor Uptake of [68 Ga]Ga-HER2 Single-Domain Antibody PET/CT in Patients with Breast Carcinoma. Journal of Nuclear Medicine 2024;65:178–84. https://doi.org/10.2967/jnumed.123.266254.
- [26] Scully M, Cataland SR, Peyvandi F, Coppo P, Knöbl P, Kremer Hovinga JA, et al. Caplacizumab Treatment for Acquired Thrombotic Thrombocytopenic Purpura. New England Journal of Medicine 2019;380:335–46. https://doi.org/10.1056/NEJMoa1806311.
- [27] Tan X-T, Huang S-W, Lin Y-C, Lin F-Y, Cho D-Y, Chiu S-C. A New PD-L1 Nanobody Enhances Cell Death in Lung Cancer *In Vitro* and *In Vivo*.

- Anticancer Res 2025;45:535–47. https://doi.org/10.21873/anticanres.17442.
- [28] McIlroy PR, Pham LTM, Sheffield T, Stefan MA, Thatcher CE, Jaryenneh J, et al. Nanobody screening and machine learning guided identification of cross-variant anti-SARS-CoV-2 neutralizing heavy-chain only antibodies. PLoS Pathog 2025;21:e1012903. https://doi.org/10.1371/journal.ppat.1012903.
- [29] Lu J, Jiang F, Lu A, Zhang G. Linkers Having a Crucial Role in Antibody-Drug Conjugates. Int J Mol Sci 2016;17:561. https://doi.org/10.3390/ijms17040561.
- [30] Regard JB, Sato IT, Coughlin SR. Anatomical Profiling of G Protein-Coupled Receptor Expression. Cell 2008;135:561–71. https://doi.org/10.1016/j.cell.2008.08.040.
- [31] Heukers R, De Groof TWM, Smit MJ. Nanobodies detecting and modulating GPCRs outside in and inside out. Curr Opin Cell Biol 2019;57:115–22. https://doi.org/10.1016/j.ceb.2019.01.003.
- [32] De Groof TWM, Bobkov V, Heukers R, Smit MJ. Nanobodies: New avenues for imaging, stabilizing and modulating GPCRs. Mol Cell Endocrinol 2019;484:15–24. https://doi.org/10.1016/j.mce.2019.01.021.
- [33] Laeremans T, Sands ZA, Claes P, De Blieck A, De Cesco S, Triest S, et al. Accelerating GPCR Drug Discovery With Conformation-Stabilizing VHHs. Front Mol Biosci 2022;9. https://doi.org/10.3389/fmolb.2022.863099.
- [34] Rasmussen SGF, Choi H-J, Fung JJ, Pardon E, Casarosa P, Chae PS, et al. Structure of a nanobody-stabilized active state of the β2 adrenoceptor. Nature 2011;469:175–80. https://doi.org/10.1038/nature09648.
- [35] Raynaud P, Gauthier C, Jugnarain V, Jean-Alphonse F, Reiter E, Bruneau G, et al. Intracellular VHHs to monitor and modulate GPCR signaling. Front Endocrinol (Lausanne) 2022;13. https://doi.org/10.3389/fendo.2022.1048601.
- [36] Van Hout A, Klarenbeek A, Bobkov V, Doijen J, Arimont M, Zhao C, et al. CXCR4-targeting nanobodies differentially inhibit CXCR4 function and

- HIV entry. Biochem Pharmacol 2018;158:402–12. https://doi.org/10.1016/j.bcp.2018.10.015.
- [37] Maussang D, Mujić-Delić A, Descamps FJ, Stortelers C, Vanlandschoot P, Stigter-van Walsum M, et al. Llama-derived Single Variable Domains (Nanobodies) Directed against Chemokine Receptor CXCR7 Reduce Head and Neck Cancer Cell Growth in Vivo. Journal of Biological Chemistry 2013;288:29562–72. https://doi.org/10.1074/jbc.M113.498436.
- [38] Bradley ME, Dombrecht B, Manini J, Willis J, Vlerick D, De Taeye S, et al. Potent and Efficacious Inhibition of CXCR2 Signaling by Biparatopic Nanobodies Combining Two Distinct Modes of Action. Mol Pharmacol 2015;87:251–62. https://doi.org/10.1124/mol.114.094821.
- [39] Scholler P, Nevoltris D, de Bundel D, Bossi S, Moreno-Delgado D, Rovira X, et al. Allosteric nanobodies uncover a role of hippocampal mGlu2 receptor homodimers in contextual fear consolidation. Nat Commun 2017;8:1967. https://doi.org/10.1038/s41467-017-01489-1.
- [40] Koehl A, Hu H, Feng D, Sun B, Zhang Y, Robertson MJ, et al. Structural insights into the activation of metabotropic glutamate receptors. Nature 2019;566:79–84. https://doi.org/10.1038/s41586-019-0881-4.
- [41] Pierce KL, Premont RT, Lefkowitz RJ. Seven-transmembrane receptors. Nat Rev Mol Cell Biol 2002;3:639–50. https://doi.org/10.1038/nrm908.
- [42] Hauser AS, Attwood MM, Rask-Andersen M, Schiöth HB, Gloriam DE. Trends in GPCR drug discovery: new agents, targets and indications. Nat Rev Drug Discov 2017;16:829–42. https://doi.org/10.1038/nrd.2017.178.
- [43] Lagerström MC, Schiöth HB. Structural diversity of G protein-coupled receptors and significance for drug discovery. Nat Rev Drug Discov 2008;7:339–57. https://doi.org/10.1038/nrd2518.
- [44] Fredriksson R, Lagerström MC, Lundin L-G, Schiöth HB. The G-Protein-Coupled Receptors in the Human Genome Form Five Main Families. Phylogenetic Analysis, Paralogon Groups, and Fingerprints. Mol Pharmacol 2003;63:1256–72. https://doi.org/10.1124/mol.63.6.1256.

- [45] Yang D, Zhou Q, Labroska V, Qin S, Darbalaei S, Wu Y, et al. G protein-coupled receptors: structure- and function-based drug discovery. Signal Transduct Target Ther 2021;6:7. https://doi.org/10.1038/s41392-020-00435-w.
- [46] Latorraca NR, Venkatakrishnan AJ, Dror RO. GPCR Dynamics: Structures in Motion. Chem Rev 2017;117:139–55. https://doi.org/10.1021/acs.chemrev.6b00177.
- [47] Roth NS, Lefkowitz RJ, Caron MG. Structure and Function of the Adrenergic Receptor Family, 1991, p. 223–38. https://doi.org/10.1007/978-1-4684-6015-5_20.
- [48] Kobilka B. The Structural Basis of G-Protein-Coupled Receptor Signaling (Nobel Lecture). Angewandte Chemie International Edition 2013;52:6380–8. https://doi.org/10.1002/anie.201302116.
- [49] Calebiro D, Koszegi Z, Lanoiselée Y, Miljus T, O'Brien S. G protein-coupled receptor-G protein interactions: a single-molecule perspective. Physiol Rev 2021;101:857–906. https://doi.org/10.1152/physrev.00021.2020.
- [50] Jiang H, Galtes D, Wang J, Rockman HA. G protein-coupled receptor signaling: transducers and effectors. American Journal of Physiology-Cell Physiology 2022;323:C731–48. https://doi.org/10.1152/ajpcell.00210.2022.
- [51] Syrovatkina V, Alegre KO, Dey R, Huang X-Y. Regulation, Signaling, and Physiological Functions of G-Proteins. J Mol Biol 2016;428:3850–68. https://doi.org/10.1016/j.jmb.2016.08.002.
- [52] Yan K, Gao L-N, Cui Y-L, Zhang Y, Zhou X. The cyclic AMP signaling pathway: Exploring targets for successful drug discovery (Review). Mol Med Rep 2016;13:3715–23. https://doi.org/10.3892/mmr.2016.5005.
- [53] Mizuno N, Itoh H. Functions and Regulatory Mechanisms of Gq-Signaling Pathways. Neurosignals 2009;17:42–54. https://doi.org/10.1159/000186689.

- [54] Berridge MJ. The Inositol Trisphosphate/Calcium Signaling Pathway in Health and Disease. Physiol Rev 2016;96:1261–96. https://doi.org/10.1152/physrev.00006.2016.
- [55] Smrcka A V. G protein βγ subunits: Central mediators of G protein-coupled receptor signaling. Cellular and Molecular Life Sciences 2008;65:2191–214. https://doi.org/10.1007/s00018-008-8006-5.
- [56] Gurevich E V., Gurevich V V. GRKs as Modulators of Neurotransmitter Receptors. Cells 2020;10:52. https://doi.org/10.3390/cells10010052.
- [57] Reiter E, Lefkowitz RJ. GRKs and β -arrestins: roles in receptor silencing, trafficking and signaling. Trends in Endocrinology & Metabolism 2006;17:159–65. https://doi.org/10.1016/j.tem.2006.03.008.
- [58] Kolb P, Kenakin T, Alexander SPH, Bermudez M, Bohn LM, Breinholt CS, et al. Community guidelines for GPCR ligand bias: IUPHAR review 32. Br J Pharmacol 2022;179:3651–74. https://doi.org/10.1111/bph.15811.
- [59] Ferré S, Ciruela F, Dessauer CW, González-Maeso J, Hébert TE, Jockers R, et al. G protein-coupled receptor-effector macromolecular membrane assemblies (GEMMAs). Pharmacol Ther 2022;231:107977. https://doi.org/10.1016/j.pharmthera.2021.107977.
- [60] Ferré S, Baler R, Bouvier M, Caron MG, Devi LA, Durroux T, et al. Building a new conceptual framework for receptor heteromers. Nat Chem Biol 2009;5:131–4. https://doi.org/10.1038/nchembio0309-131.
- [61] Angers S, Salahpour A, Bouvier M. Biochemical and biophysical demonstration of GPCR oligomerization in mammalian cells. Life Sci 2001;68:2243–50. https://doi.org/10.1016/S0024-3205(01)01012-8.
- [62] Gahbauer S, Böckmann RA. Membrane-Mediated Oligomerization of G Protein Coupled Receptors and Its Implications for GPCR Function. Front Physiol 2016;7. https://doi.org/10.3389/fphys.2016.00494.
- [63] Dale NC, Johnstone EKM, Pfleger KDG. GPCR heteromers: An overview of their classification, function and physiological relevance. Front Endocrinol (Lausanne) 2022;13. https://doi.org/10.3389/fendo.2022.931573.

- [64] Devi LA. Heterodimerization of G-protein-coupled receptors: pharmacology, signaling and trafficking. Trends Pharmacol Sci 2001;22:532–7. https://doi.org/10.1016/S0165-6147(00)01799-5.
- [65] Meiser J, Weindl D, Hiller K. Complexity of dopamine metabolism. Cell Communication and Signaling 2013;11:34. https://doi.org/10.1186/1478-811X-11-34.
- [66] Yeragani V, Tancer M, Chokka P, Baker G. Arvid Carlsson, and the story of dopamine. Indian J Psychiatry 2010;52:87. https://doi.org/10.4103/0019-5545.58907.
- [67] Chinta SJ, Andersen JK. Dopaminergic neurons. Int J Biochem Cell Biol 2005;37:942–6. https://doi.org/10.1016/j.biocel.2004.09.009.
- [68] Speranza L, di Porzio U, Viggiano D, de Donato A, Volpicelli F. Dopamine: The Neuromodulator of Long-Term Synaptic Plasticity, Reward and Movement Control. Cells 2021;10:735. https://doi.org/10.3390/cells10040735.
- [69] Meiser J, Weindl D, Hiller K. Complexity of dopamine metabolism. Cell Commun Signal 2013;11:34. https://doi.org/10.1186/1478-811X-11-34.
- [70] Martel JC, Gatti McArthur S. Dopamine Receptor Subtypes, Physiology and Pharmacology: New Ligands and Concepts in Schizophrenia. Front Pharmacol 2020;11. https://doi.org/10.3389/fphar.2020.01003.
- [71] De Mei C, Ramos M, Iitaka C, Borrelli E. Getting specialized: presynaptic and postsynaptic dopamine D2 receptors. Curr Opin Pharmacol 2009;9:53–8. https://doi.org/10.1016/j.coph.2008.12.002.
- [72] Gurevich E V., Gainetdinov RR, Gurevich V V. G protein-coupled receptor kinases as regulators of dopamine receptor functions. Pharmacol Res 2016;111:1–16. https://doi.org/10.1016/j.phrs.2016.05.010.
- [73] Simpson EH, Gallo EF, Balsam PD, Javitch JA, Kellendonk C. How changes in dopamine D2 receptor levels alter striatal circuit function and motivation. Mol Psychiatry 2022;27:436–44. https://doi.org/10.1038/s41380-021-01253-4.

- [74] Krnjevic K. Glutamate and γ-Aminobutyric Acid in Brain. Nature 1970;228:119–24. https://doi.org/10.1038/228119a0.
- [75] Fonnum F. Glutamate: A Neurotransmitter in Mammalian Brain. J Neurochem 1984;42:1–11. https://doi.org/10.1111/j.1471-4159.1984.tb09689.x.
- [76] Andersen J V., Markussen KH, Jakobsen E, Schousboe A, Waagepetersen HS, Rosenberg PA, et al. Glutamate metabolism and recycling at the excitatory synapse in health and neurodegeneration. Neuropharmacology 2021;196:108719. https://doi.org/10.1016/j.neuropharm.2021.108719.
- [77] Norenberg MD, Martinez-Hernandez A. Fine structural localization of glutamine synthetase in astrocytes of rat brain. Brain Res 1979;161:303–10. https://doi.org/10.1016/0006-8993(79)90071-4.
- [78] Bak LK, Schousboe A, Waagepetersen HS. The glutamate/GABA-glutamine cycle: aspects of transport, neurotransmitter homeostasis and ammonia transfer. J Neurochem 2006;98:641–53. https://doi.org/10.1111/j.1471-4159.2006.03913.x.
- [79] Kvamme E, Torgner IAa, Roberg B. Kinetics and localization of brain phosphate activated glutaminase. J Neurosci Res 2001;66:951–8. https://doi.org/10.1002/jnr.10041.
- [80] Nakanishi S, Nakajima Y, Masu M, Yoshiki Ueda, Nakahara K, Watanabe D, et al. Glutamate receptors: brain function and signal transduction. Brain Res Rev 1998;26:230–5. https://doi.org/10.1016/S0165-0173(97)00033-7.
- [81] Traynelis SF, Wollmuth LP, McBain CJ, Menniti FS, Vance KM, Ogden KK, et al. Glutamate Receptor Ion Channels: Structure, Regulation, and Function. Pharmacol Rev 2010;62:405–96. https://doi.org/10.1124/pr.109.002451.
- [82] Niswender CM, Conn PJ. Metabotropic Glutamate Receptors: Physiology, Pharmacology, and Disease. Annu Rev Pharmacol Toxicol 2010;50:295–322. https://doi.org/10.1146/annurev.pharmtox.011008.145533.

- [83] Cleva RM, Olive MF. Positive Allosteric Modulators of Type 5 Metabotropic Glutamate Receptors (mGluR5) and Their Therapeutic Potential for the Treatment of CNS Disorders. Molecules 2011;16:2097– 106. https://doi.org/10.3390/molecules16032097.
- [84] Haas LT, Salazar S V., Smith LM, Zhao HR, Cox TO, Herber CS, et al. Silent Allosteric Modulation of mGluR5 Maintains Glutamate Signaling while Rescuing Alzheimer's Mouse Phenotypes. Cell Rep 2017;20:76–88. https://doi.org/10.1016/j.celrep.2017.06.023.
- [85] Xu J, Zhu Y, Contractor A, Heinemann SF. mGluR5 Has a Critical Role in Inhibitory Learning. The Journal of Neuroscience 2009;29:3676–84. https://doi.org/10.1523/JNEUROSCI.5716-08.2009.
- [86] Vincent K, Cornea VM, Jong Y-JI, Laferrière A, Kumar N, Mickeviciute A, et al. Intracellular mGluR5 plays a critical role in neuropathic pain. Nat Commun 2016;7:10604. https://doi.org/10.1038/ncomms10604.
- [87] Su L-D, Wang N, Han J, Shen Y. Group 1 Metabotropic Glutamate Receptors in Neurological and Psychiatric Diseases: Mechanisms and Prospective. The Neuroscientist 2022;28:453–68. https://doi.org/10.1177/10738584211021018.
- [88] Chen J-F, Lee C, Chern Y. Adenosine Receptor Neurobiology: Overview, 2014, p. 1–49. https://doi.org/10.1016/B978-0-12-801022-8.00001-5.
- [89] Burnstock G. Historical review: ATP as a neurotransmitter. Trends Pharmacol Sci 2006;27:166–76. https://doi.org/10.1016/j.tips.2006.01.005.
- [90] Chen J-F, Eltzschig HK, Fredholm BB. Adenosine receptors as drug targets what are the challenges? Nat Rev Drug Discov 2013;12:265—86. https://doi.org/10.1038/nrd3955.
- [91] Fredholm BB, IJzerman AP, Jacobson KA, Klotz KN, Linden J. International Union of Pharmacology. XXV. Nomenclature and classification of adenosine receptors. Pharmacol Rev 2001;53:527–52.
- [92] Borroto-Escuela DO, Narváez M, Navarro G, Franco R, Fuxe K. Heteroreceptor Complexes Implicated in Parkinson's Disease. G-Protein-Coupled Receptor Dimers, Cham: Springer International

- Publishing; 2017, p. 477–501. https://doi.org/10.1007/978-3-319-60174-8_20.
- [93] Borroto-Escuela DO, Hinz S, Navarro G, Franco R, Müller CE, Fuxe K. Understanding the Role of Adenosine A2AR Heteroreceptor Complexes in Neurodegeneration and Neuroinflammation. Front Neurosci 2018;12. https://doi.org/10.3389/fnins.2018.00043.
- [94] Patel V. Universal Health Coverage for Schizophrenia: A Global Mental Health Priority. Schizophr Bull 2016;42:885–90. https://doi.org/10.1093/schbul/sbv107.
- [95] Marder SR, Cannon TD. Schizophrenia. New England Journal of Medicine 2019;381:1753–61. https://doi.org/10.1056/NEJMra1808803.
- [96] Biological insights from 108 schizophrenia-associated genetic loci. Nature 2014;511:421–7. https://doi.org/10.1038/nature13595.
- [97] Salleh MR. The genetics of schizophrenia. Malays J Med Sci 2004;11:3–11.
- [98] van de Leemput J, Hess JL, Glatt SJ, Tsuang MT. Genetics of Schizophrenia, 2016, p. 99–141. https://doi.org/10.1016/bs.adgen.2016.08.001.
- [99] Stilo SA, Murray RM. Non-Genetic Factors in Schizophrenia. Curr Psychiatry Rep 2019;21:100. https://doi.org/10.1007/s11920-019-1091-3.
- [100] VANDERGAAG M, HOFFMAN T, REMIJSEN M, HIJMAN R, DEHAAN L, VANMEIJEL B, et al. The five-factor model of the Positive and Negative Syndrome Scale II: A ten-fold cross-validation of a revised model. Schizophr Res 2006;85:280–7. https://doi.org/10.1016/j.schres.2006.03.021.
- [101] Stahl SM. Beyond the dopamine hypothesis of schizophrenia to three neural networks of psychosis: dopamine, serotonin, and glutamate. CNS Spectr 2018;23:187–91. https://doi.org/10.1017/S1092852918001013.

- [102] Nord M, Farde L. Antipsychotic Occupancy of Dopamine Receptors in Schizophrenia. CNS Neurosci Ther 2011;17:97–103. https://doi.org/10.1111/j.1755-5949.2010.00222.x.
- [103] Lako IM, van den Heuvel ER, Knegtering H, Bruggeman R, Taxis K. Estimating Dopamine D2 Receptor Occupancy for Doses of 8 Antipsychotics. J Clin Psychopharmacol 2013;33:675–81. https://doi.org/10.1097/JCP.0b013e3182983ffa.
- [104] Grace AA. Dysregulation of the dopamine system in the pathophysiology of schizophrenia and depression. Nat Rev Neurosci 2016;17:524–32. https://doi.org/10.1038/nrn.2016.57.
- [105] McCutcheon RA, Krystal JH, Howes OD. Dopamine and glutamate in schizophrenia: biology, symptoms and treatment. World Psychiatry 2020;19:15–33. https://doi.org/10.1002/wps.20693.
- [106] Howes OD, Kapur S. The Dopamine Hypothesis of Schizophrenia: Version III--The Final Common Pathway. Schizophr Bull 2009;35:549–62. https://doi.org/10.1093/schbul/sbp006.
- [107] McCutcheon R, Beck K, Jauhar S, Howes OD. Defining the Locus of Dopaminergic Dysfunction in Schizophrenia: A Meta-analysis and Test of the Mesolimbic Hypothesis. Schizophr Bull 2018;44:1301–11. https://doi.org/10.1093/schbul/sbx180.
- [108] Kapur S. Psychosis as a State of Aberrant Salience: A Framework Linking Biology, Phenomenology, and Pharmacology in Schizophrenia. American Journal of Psychiatry 2003;160:13–23. https://doi.org/10.1176/appi.ajp.160.1.13.
- [109] Ward RD, Kellendonk C, Kandel ER, Balsam PD. Timing as a window on cognition in schizophrenia. Neuropharmacology 2012;62:1175–81. https://doi.org/10.1016/j.neuropharm.2011.04.014.
- [110] Howes O, McCutcheon R, Stone J. Glutamate and dopamine in schizophrenia: An update for the 21 st century. Journal of Psychopharmacology 2015;29:97–115. https://doi.org/10.1177/0269881114563634.

- [111] Kitzinger H, Arnold DG, Cartwright RW, Shapiro D. A Preliminary Study of the Effects of Glutamic Acid on Catatonic Schizophrenics. Rorschach Res Exch J Proj Tech 1949;13:210–8. https://doi.org/10.1080/10683402.1949.10381459.
- [112] Daniel C. Javitt, Stephen R. Zukin. Recent advances in the phencyclidine model of schizophrenia. American Journal of Psychiatry 1991;148:1301–8. https://doi.org/10.1176/ajp.148.10.1301.
- [113] Egerton A, Grace AA, Stone J, Bossong MG, Sand M, McGuire P. Glutamate in schizophrenia: Neurodevelopmental perspectives and drug development. Schizophr Res 2020;223:59–70. https://doi.org/10.1016/j.schres.2020.09.013.
- [114] Castañé A, Santana N, Artigas F. PCP-based mice models of schizophrenia: differential behavioral, neurochemical and cellular effects of acute and subchronic treatments. Psychopharmacology (Berl) 2015;232:4085–97. https://doi.org/10.1007/s00213-015-3946-6.
- [115] Corina Bondi, Marguerite Matthews, Bita Moghaddam. Glutamatergic Animal Models of Schizophrenia. Curr Pharm Des 2012;18:1593–604. https://doi.org/10.2174/138161212799958576.
- [116] Frohlich J, Van Horn JD. Reviewing the ketamine model for schizophrenia. Journal of Psychopharmacology 2014;28:287–302. https://doi.org/10.1177/0269881113512909.
- [117] Poltavskaya EG, Kornetova EG, Freidin MB, Pozhidaev I V., Paderina DZ, Bocharova A V., et al. The Role of Glutamatergic Gene Polymorphisms in the Clinical Phenotypes of Schizophrenia. Genes (Basel) 2023;14:575. https://doi.org/10.3390/genes14030575.
- [118] Glessner JT, Reilly MP, Kim CE, Takahashi N, Albano A, Hou C, et al. Strong synaptic transmission impact by copy number variations in schizophrenia. Proceedings of the National Academy of Sciences 2010;107:10584–9. https://doi.org/10.1073/pnas.1000274107.
- [119] Snyder MA, Gao W-J. NMDA hypofunction as a convergence point for progression and symptoms of schizophrenia. Front Cell Neurosci 2013;7. https://doi.org/10.3389/fncel.2013.00031.

- [120] Boszormenyi-Nagy I, Gerty F-J, Kueber J. Correlation between an anomaly of the intracellular metabolism of adenosine nucleotides and schizophrenia. J Nerv Ment Dis 1956;124:413–6. https://doi.org/10.1097/00005053-195610000-00013.
- [121] Gottlieb JS. Energy Transfer Systems in Schizophrenia. AMA Arch Neurol Psychiatry 1959;81:504. https://doi.org/10.1001/archneurpsyc.1959.02340160102014.
- [122] Gottlieb JS. Production of High-Energy Phosphate Bonds in Schizophrenia. Arch Gen Psychiatry 1959;1:243. https://doi.org/10.1001/archpsyc.1959.03590030027002.
- [123] Arnold OH, Hofmann G. Correlations between clinical and biochemical data in schizophrenia. Behavioral Neuropsychiatry 1972;3:18–24.
- [124] Ferré S. Adenosine-dopamine interactions in the ventral striatum. Psychopharmacology (Berl) 1997;133:107–20. https://doi.org/10.1007/s002130050380.
- [125] Singer P, Yee BK. The adenosine hypothesis of schizophrenia into its third decade: From neurochemical imbalance to early life etiological risks. Front Cell Neurosci 2023;17. https://doi.org/10.3389/fncel.2023.1120532.
- [126] Lara DR, Dall'Igna OP, Ghisolfi ES, Brunstein MG. Involvement of adenosine in the neurobiology of schizophrenia and its therapeutic implications. Prog Neuropsychopharmacol Biol Psychiatry 2006;30:617–29. https://doi.org/10.1016/j.pnpbp.2006.02.002.
- [127] Hirota T, Kishi T. Adenosine hypothesis in schizophrenia and bipolar disorder: A systematic review and meta-analysis of randomized controlled trial of adjuvant purinergic modulators. Schizophr Res 2013;149:88–95. https://doi.org/10.1016/j.schres.2013.06.038.
- [128] Lara DR, Dall'Igna OP, Ghisolfi ES, Brunstein MG. Involvement of adenosine in the neurobiology of schizophrenia and its therapeutic implications. Prog Neuropsychopharmacol Biol Psychiatry 2006;30:617–29. https://doi.org/10.1016/j.pnpbp.2006.02.002.
- [129] Katzung BG. Basic & clinical pharmacology. McGraw-Hill; 2018.

- [130] Trifu S, Trifu AD. Receptor profiles of atypical antipsychotic molecules. Bull, Series B n.d.;82:2020.
- [131] Leucht S, Corves C, Arbter D, Engel RR, Li C, Davis JM. Second-generation versus first-generation antipsychotic drugs for schizophrenia: a meta-analysis. The Lancet 2009;373:31–41. https://doi.org/10.1016/S0140-6736(08)61764-X.
- [132] Mauri MC, Paletta S, Maffini M, Colasanti A, Dragogna F, Pace C Di, et al. Clinical pharmacology of atypical antipsychotics: an update. vol. 13. 2014.
- [133] de Bartolomeis A, Tomasetti C, Iasevoli F. Update on the Mechanism of Action of Aripiprazole: Translational Insights into Antipsychotic Strategies Beyond Dopamine Receptor Antagonism. CNS Drugs 2015;29:773–99. https://doi.org/10.1007/s40263-015-0278-3.
- [134] Lieberman JA. Dopamine Partial Agonists. CNS Drugs 2004;18:251–67. https://doi.org/10.2165/00023210-200418040-00005.
- [135] Matosin N, Newell KA. Metabotropic glutamate receptor 5 in the pathology and treatment of schizophrenia. Neurosci Biobehav Rev 2013;37:256–68. https://doi.org/10.1016/j.neubiorev.2012.12.005.
- [136] Meltzer HY, Gadaleta E. Contrasting Typical and Atypical Antipsychotic Drugs. Focus (Madison) 2021;19:3–13. https://doi.org/10.1176/appi.focus.20200051.
- [137] Siafis S, Tzachanis D, Samara M, Papazisis G. Antipsychotic Drugs: From Receptor-binding Profiles to Metabolic Side Effects. Curr Neuropharmacol 2018;16:1210–23. https://doi.org/10.2174/1570159X15666170630163616.
- [138] Smith DJ, Whitham EA, Ghaemi SN. Bipolar disorder, 2012, p. 251–63. https://doi.org/10.1016/B978-0-444-52002-9.00015-2.
- [139] Harrison PJ, Geddes JR, Tunbridge EM. The Emerging Neurobiology of Bipolar Disorder. Trends Neurosci 2018;41:18–30. https://doi.org/10.1016/j.tins.2017.10.006.

- [140] Solé B, Jiménez E, Torrent C, Reinares M, Bonnin C del M, Torres I, et al. Cognitive Impairment in Bipolar Disorder: Treatment and Prevention Strategies. International Journal of Neuropsychopharmacology 2017;20:670–80. https://doi.org/10.1093/ijnp/pyx032.
- [141] Grande I, Berk M, Birmaher B, Vieta E. Bipolar disorder. The Lancet 2016;387:1561–72. https://doi.org/10.1016/S0140-6736(15)00241-X.
- [142] Ben-Menachem E. Pregabalin Pharmacology and Its Relevance to Clinical Practice. Epilepsia 2004;45:13–8. https://doi.org/10.1111/j.0013-9580.2004.455003.x.
- [143] Geddes JR, Calabrese JR, Goodwin GM. Lamotrigine for treatment of bipolar depression: independent meta-analysis and meta-regression of individual patient data from five randomised trials. British Journal of Psychiatry 2009;194:4–9. https://doi.org/10.1192/bjp.bp.107.048504.
- [144] Mesbah R, Koenders MA, van der Wee NJA, Giltay EJ, van Hemert AM, de Leeuw M. Association Between the Fronto-Limbic Network and Cognitive and Emotional Functioning in Individuals With Bipolar Disorder. JAMA Psychiatry 2023;80:432. https://doi.org/10.1001/jamapsychiatry.2023.0131.
- [145] Perrottelli A, Marzocchi FF, Caporusso E, Giordano GM, Giuliani L, Melillo A, et al. Advances in the understanding of the pathophysiology of schizophrenia and bipolar disorder through induced pluripotent stem cell models. J Psychiatry Neurosci 2024;49:E109–25. https://doi.org/10.1503/jpn.230112.
- [146] Pereira AC, Oliveira J, Silva S, Madeira N, Pereira CMF, Cruz MT. Inflammation in Bipolar Disorder (BD): Identification of new therapeutic targets. Pharmacol Res 2021;163:105325. https://doi.org/10.1016/j.phrs.2020.105325.
- [147] Berk M, Kapczinski F, Andreazza AC, Dean OM, Giorlando F, Maes M, et al. Pathways underlying neuroprogression in bipolar disorder: Focus on inflammation, oxidative stress and neurotrophic factors. Neurosci Biobehav Rev 2011;35:804–17. https://doi.org/10.1016/j.neubiorev.2010.10.001.

- [148] Cuomo A, Koukouna D, Spiti A, Barillà G, Goracci A, Bolognesi S, et al. Biomarkers, Inflammation, and Bipolar Disorder: Association Between the Improvement of Bipolar Disorder Severity and the Improvement in C-Reactive Protein Levels After 7 Days of Inpatient Treatment. Front Psychiatry 2021;12. https://doi.org/10.3389/fpsyt.2021.803034.
- [149] Harwood AJ, Agam G. Search for a common mechanism of mood stabilizers. Biochem Pharmacol 2003;66:179–89. https://doi.org/10.1016/S0006-2952(03)00187-4.
- [150] Malhi GS, Tanious M, Das P, Coulston CM, Berk M. Potential Mechanisms of Action of Lithium in Bipolar Disorder. CNS Drugs 2013;27:135–53. https://doi.org/10.1007/s40263-013-0039-0.
- [151] Alda M. Lithium in the treatment of bipolar disorder: pharmacology and pharmacogenetics. Mol Psychiatry 2015;20:661–70. https://doi.org/10.1038/mp.2015.4.
- [152] Grunze HCR. Anticonvulsants in bipolar disorder. Journal of Mental Health 2010;19:127–41. https://doi.org/10.3109/09638230903469186.
- [153] Fernández-Dueñas V, Qian M, Argerich J, Amaral C, Risseeuw MDP, Van Calenbergh S, et al. Design, Synthesis and Characterization of a New Series of Fluorescent Metabotropic Glutamate Receptor Type 5 Negative Allosteric Modulators. Molecules 2020;25:1532. https://doi.org/10.3390/molecules25071532.
- [154] Sarasola LI, del Torrent CL, Pérez-Arévalo A, Argerich J, Casajuana-Martín N, Chevigné A, et al. The ADORA1 mutation linked to early-onset Parkinson's disease alters adenosine A<inf>1</inf>-A<inf>2A</inf> receptor heteromer formation and function. Biomedicine and Pharmacotherapy 2022;156. https://doi.org/10.1016/j.biopha.2022.113896.
- [155] Wan Q, Okashah N, Inoue A, Nehmé R, Carpenter B, Tate CG, et al. Mini G protein probes for active G protein–coupled receptors (GPCRs) in live cells. Journal of Biological Chemistry 2018;293:7466–73. https://doi.org/10.1074/jbc.RA118.001975.

- [156] Hanson LR, Fine JM, Svitak AL, Faltesek KA. Intranasal Administration of CNS Therapeutics to Awake Mice. Journal of Visualized Experiments 2013. https://doi.org/10.3791/4440.
- [157] Mathis A, Mamidanna P, Cury KM, Abe T, Murthy VN, Mathis MW, et al. DeepLabCut: markerless pose estimation of user-defined body parts with deep learning. Nat Neurosci 2018;21:1281–9. https://doi.org/10.1038/s41593-018-0209-y.
- [158] Abe T, Sugihara H, Nawa H, Shigemoto R, Mizuno N, Nakanishi S. Molecular characterization of a novel metabotropic glutamate receptor mGluR5 coupled to inositol phosphate/Ca2+ signal transduction. Journal of Biological Chemistry 1992;267:13361–8. https://doi.org/10.1016/S0021-9258(18)42219-3.
- [159] Cabello N, Gandía J, Bertarelli DCG, Watanabe M, Lluís C, Franco R, et al. Metabotropic glutamate type 5, dopamine D 2 and adenosine A 2a receptors form higher-order oligomers in living cells. J Neurochem 2009;109:1497–507. https://doi.org/10.1111/j.1471-4159.2009.06078.x.
- [160] Díaz-Cabiale Z, Vivó M, Del Arco A, O'Connor WT, Harte MK, Müller CE, et al. Metabotropic glutamate mGlu5 receptor-mediated modulation of the ventral striopallidal GABA pathway in rats. Interactions with adenosine A2A and dopamine D2 receptors. Neurosci Lett 2002;324:154–8. https://doi.org/10.1016/S0304-3940(02)00179-9.
- [161] Díaz-Cabiale Z, Vivó M, Del Arco A, O'Connor WT, Harte MK, Müller CE, et al. Metabotropic glutamate mGlu5 receptor-mediated modulation of the ventral striopallidal GABA pathway in rats. Interactions with adenosine A2A and dopamine D2 receptors. Neurosci Lett 2002;324:154–8. https://doi.org/10.1016/S0304-3940(02)00179-9.
- [162] Romero-Fernandez W, Taura JJ, Crans RAJ, Lopez-Cano M, Fores-Pons R, Narváez M, et al. The mGlu5 Receptor Protomer-Mediated Dopamine D2 Receptor Trans-Inhibition Is Dependent on the Adenosine A2A Receptor Protomer: Implications for Parkinson's Disease. Mol Neurobiol 2022;59:5955–69. https://doi.org/10.1007/s12035-022-02946-9.

- [163] Tashima T, Tournier N. Non-Invasive Device-Mediated Drug Delivery to the Brain across the Blood–Brain Barrier. Pharmaceutics 2024;16:361. https://doi.org/10.3390/pharmaceutics16030361.
- [164] Soleimanizadeh A, Dinter H, Schindowski K. Central Nervous System Delivery of Antibodies and Their Single-Domain Antibodies and Variable Fragment Derivatives with Focus on Intranasal Nose to Brain Administration. Antibodies 2021;10:47. https://doi.org/10.3390/antib10040047.
- [165] Kumar NN, Lochhead JJ, Pizzo ME, Nehra G, Boroumand S, Greene G, et al. Delivery of immunoglobulin G antibodies to the rat nervous system following intranasal administration: Distribution, dose-response, and mechanisms of delivery. Journal of Controlled Release 2018;286:467–84. https://doi.org/10.1016/j.jconrel.2018.08.006.
- [166] Debie P, Devoogdt N, Hernot S. Targeted Nanobody-Based Molecular Tracers for Nuclear Imaging and Image-Guided Surgery. Antibodies 2019;8:12. https://doi.org/10.3390/antib8010012.
- [167] Akhondzadeh, Shasavand, Jamilian, Shabestari, Kamalipour. Dipyridamole in the treatment of schizophrenia: adenosine-dopamine receptor interactions. J Clin Pharm Ther 2000;25:131–7. https://doi.org/10.1046/j.1365-2710.2000.00273.x.
- [168] Akhondzadeh S, Safarcherati A, Amini H. Beneficial antipsychotic effects of allopurinol as add-on therapy for schizophrenia: a double blind, randomized and placebo controlled trial. Prog Neuropsychopharmacol Biol Psychiatry 2005;29:253–9. https://doi.org/10.1016/j.pnpbp.2004.11.008.
- [169] Brunstein MG, Ghisolfi ES, Ramos FLP, Lara DR. A Clinical Trial of Adjuvant Allopurinol Therapy for Moderately Refractory Schizophrenia. J Clin Psychiatry 2005;66:213–9. https://doi.org/10.4088/JCP.v66n0209.
- [170] Salimi S, Fotouhi A, Ghoreishi A, Derakhshan M-K, Khodaie-Ardakani M-R, Mohammadi M-R, et al. A placebo controlled study of the propentofylline added to risperidone in chronic schizophrenia. Prog

- Neuropsychopharmacol Biol Psychiatry 2008;32:726–32. https://doi.org/10.1016/j.pnpbp.2007.11.021.
- [171] Modabber A, Tahaie S, Pharm N. Allopurinol as an adjuvant therapy for refractory schizophrenia. vol. 25. 2009.
- [172] Dickerson FB, Stallings CR, Origoni AE, Sullens A, Khushalani S, Sandson N, et al. A double-blind trial of adjunctive allopurinol for schizophrenia. Schizophr Res 2009;109:66–9. https://doi.org/10.1016/j.schres.2008.12.028.
- [173] Weiser M, Gershon AA, Rubinstein K, Petcu C, Ladea M, Sima D, et al. A randomized controlled trial of allopurinol vs. placebo added on to antipsychotics in patients with schizophrenia or schizoaffective disorder. Schizophr Res 2012;138:35–8. https://doi.org/10.1016/j.schres.2012.02.014.
- [174] Sinichi F, Farid Hosseini F, Fayyazi-Bordbar M, Sinichi M, Jamali J, Mohammadpour A. Pentoxifylline as adjunctive therapy in cognitive deficits and symptoms of schizophrenia: A randomized double-blind placebo-controlled clinical trial. Journal of Psychopharmacology 2023;37:1003–10. https://doi.org/10.1177/02698811231186760.
- [175] Jahangard L, Soroush S, Haghighi M, Ghaleiha A, Bajoghli H, Holsboer-Trachsler E, et al. In a double-blind, randomized and placebo-controlled trial, adjuvant allopurinol improved symptoms of mania in in-patients suffering from bipolar disorder. European Neuropsychopharmacology 2014;24:1210–21. https://doi.org/10.1016/j.euroneuro.2014.05.013.
- [176] Akhondzadeh S, Milajerdi MR, Amini H, Tehrani-Doost M. Allopurinol as an adjunct to lithium and haloperidol for treatment of patients with acute mania: A double-blind, randomized, placebo-controlled trial. Bipolar Disord 2006;8:485–9. https://doi.org/10.1111/j.1399-5618.2006.00363.x.
- [177] Fan A, Berg A, Bresee C, Glassman LH, Rapaport MH. Allopurinol augmentation in the outpatient treatment of bipolar mania: A pilot study. Bipolar Disord 2012;14:206–10. https://doi.org/10.1111/j.1399-5618.2012.01001.x.

- [178] Weiser M, Burshtein S, Gershon AA, Marian G, Vlad N, Grecu IG, et al. Allopurinol for mania: A randomized trial of allopurinol versus placebo as add-on treatment to mood stabilizers and/or antipsychotic agents in manic patients with bipolar disorder. Bipolar Disord 2014;16:441–7. https://doi.org/10.1111/bdi.12202.
- [179] Akhondzadeh S, Milajerdi MR, Amini H, Moin M, Bathaei FS, Kamlipour A. Allopurinol as adjunctive treatment for acute mania in hospitalized bipolar patients. Therapy 2005;2:739–44. https://doi.org/10.1586/14750708.2.5.739.
- [180] Machado-Vieira R, Soares JC, Lara DR, Luckenbaugh DA, Busnello J V, Marca G, et al. A double-blind, Randomized, Placebo-Controlled 4-Week Study on the Efficacy and Safety of the Purinergic Agents Allopurinol and Dipyridamole Adjunctive to Lithium in Acute Bipolar Mania NIH Public Access. vol. 69. n.d.
- [181] De Genst E, Silence K, Decanniere K, Conrath K, Loris R, Kinne J, et al. Molecular basis for the preferential cleft recognition by dromedary heavy-chain antibodies. Proceedings of the National Academy of Sciences 2006;103:4586–91. https://doi.org/10.1073/pnas.0505379103.
- [182] Zhang J, Qu L, Wu L, Tang X, Luo F, Xu W, et al. Structural insights into the activation initiation of full-length mGlu1. Protein Cell 2021;12:662—7. https://doi.org/10.1007/s13238-020-00808-5.
- [183] El Salamouni NS, Cater JH, Spenkelink LM, Yu H. Nanobody engineering: computational modelling and design for biomedical and therapeutic applications. FEBS Open Bio 2025;15:236–53. https://doi.org/10.1002/2211-5463.13850.
- [184] Jähnichen S, Blanchetot C, Maussang D, Gonzalez-Pajuelo M, Chow KY, Bosch L, et al. CXCR4 nanobodies (VHH-based single variable domains) potently inhibit chemotaxis and HIV-1 replication and mobilize stem cells. Proceedings of the National Academy of Sciences 2010;107:20565–70. https://doi.org/10.1073/pnas.1012865107.

- [185] Romano C, Yang W-L, O'Malley KL. Metabotropic Glutamate Receptor 5 Is a Disulfide-linked Dimer. Journal of Biological Chemistry 1996;271:28612–6. https://doi.org/10.1074/jbc.271.45.28612.
- [186] Beggiato S, Tomasini MC, Borelli AC, Borroto-Escuela DO, Fuxe K, Antonelli T, et al. Functional role of striatal A2A, D2, and mGlu5 receptor interactions in regulating striatopallidal GABA neuronal transmission. J Neurochem 2016;138:254–64. https://doi.org/10.1111/jnc.13652.
- [187] Taura J, López-Cano M, Fernández-Dueñas V, Ciruela F. Visualizing G Protein-Coupled Receptor-Receptor Interactions in Brain Using Proximity Ligation In Situ Assay. Curr Protoc 2023;3. https://doi.org/10.1002/cpz1.794.
- [188] Ferré S, Karcz-Kubicha M, Hope BT, Popoli P, Burgueño J, Gutiérrez MA, et al. Synergistic interaction between adenosine A2A and glutamate mGlu5 receptors: Implications for striatal neuronal function. Proceedings of the National Academy of Sciences 2002;99:11940–5. https://doi.org/10.1073/pnas.172393799.
- [189] Huang C, Huang J, Zhu S, Tang T, Chen Y, Qian F. Multivalent nanobodies with rationally optimized linker and valency for intravitreal VEGF neutralization. Chem Eng Sci 2023;270:118521. https://doi.org/10.1016/j.ces.2023.118521.
- [190] Grant PS, Kahlcke N, Govindpani K, Hunter M, MacDonald C, Brimble MA, et al. Divalent cannabinoid-1 receptor ligands: A linker attachment point survey of SR141716A for development of high-affinity CB1R molecular probes. Bioorg Med Chem Lett 2019;29:126644. https://doi.org/10.1016/j.bmcl.2019.126644.
- [191] Atack JR, Shook BC, Rassnick S, Jackson PF, Rhodes K, Drinkenburg WH, et al. JNJ-40255293, a Novel Adenosine A _{2A} /A ₁ Antagonist with Efficacy in Preclinical Models of Parkinson's Disease. ACS Chem Neurosci 2014;5:1005–19. https://doi.org/10.1021/cn5001606.
- [192] Chovan JP, Zane PA, Greenberg GE. Automated-extraction, highperformance liquid chromatographic method and pharmacokinetics in rats of a highly A2-selective adenosine agonist, CGS 21680. J

- Chromatogr B Biomed Sci Appl 1992;578:77–83. https://doi.org/10.1016/0378-4347(92)80227-H.
- [193] Guimaraes IM, Carvalho TG, Ferguson SS, Pereira GS, Ribeiro FM. The metabotropic glutamate receptor 5 role on motor behavior involves specific neural substrates. Mol Brain 2015;8:24. https://doi.org/10.1186/s13041-015-0113-2.
- [194] Gallo M, Moreno E, Defaus S, Ortega-Alvaro A, Gonzalez A, Robledo P, et al. Orally Active Peptide Vector Allows Using Cannabis to Fight Pain While Avoiding Side Effects. J Med Chem 2021;64:6937–48. https://doi.org/10.1021/acs.jmedchem.1c00484.
- [195] Zhao Z, Nelson AR, Betsholtz C, Zlokovic B V. Establishment and Dysfunction of the Blood-Brain Barrier. Cell 2015;163:1064–78. https://doi.org/10.1016/j.cell.2015.10.067.
- [196] Davies DC. Blood-brain barrier breakdown in septic encephalopathy and brain tumours. J Anat 2002;200:639–46. https://doi.org/10.1046/j.1469-7580.2002.00065.x.
- [197] C. Papadopoulos, S. Saadoun, Davies D.C., Bell B.A. Emerging molecular mechanisms of brain tumour oedema. Br J Neurosurg 2001;15:101–8. https://doi.org/10.1080/02688690120036775.
- [198] Bobo RH, Laske DW, Akbasak A, Morrison PF, Dedrick RL, Oldfield EH. Convection-enhanced delivery of macromolecules in the brain. Proceedings of the National Academy of Sciences 1994;91:2076–80. https://doi.org/10.1073/pnas.91.6.2076.
- [199] Shin BJ, Burkhardt J-K, Riina HA, Boockvar JA. Superselective Intra-Arterial Cerebral Infusion of Novel Agents After Blood–Brain Disruption for the Treatment of Recurrent Glioblastoma Multiforme: A Technical Case Series. Neurosurg Clin N Am 2012;23:323–9. https://doi.org/10.1016/j.nec.2012.01.008.
- [200] Rapoport SI. Advances in osmotic opening of the blood-brain barrier to enhance CNS chemotherapy. Expert Opin Investig Drugs 2001;10:1809–18. https://doi.org/10.1517/13543784.10.10.1809.

- [201] Škrlj N, Drevenšek G, Hudoklin S, Romih R, Čurin Šerbec V, Dolinar M. Recombinant Single-Chain Antibody with the Trojan Peptide Penetratin Positioned in the Linker Region Enables Cargo Transfer Across the Blood–Brain Barrier. Appl Biochem Biotechnol 2013;169:159–69. https://doi.org/10.1007/s12010-012-9962-7.
- [202] Spencer B, Williams S, Rockenstein E, Valera E, Xin W, Mante M, et al. α -synuclein conformational antibodies fused to penetratin are effective in models of Lewy body disease. Ann Clin Transl Neurol 2016;3:588–606. https://doi.org/10.1002/acn3.321.
- [203] Gomes JR, Cabrito I, Soares HR, Costelha S, Teixeira A, Wittelsberger A, et al. Delivery of an anti-transthyretin Nanobody to the brain through intranasal administration reveals transthyretin expression and secretion by motor neurons. J Neurochem 2018;145:393–408. https://doi.org/10.1111/jnc.14332.
- [204] Soleimanizadeh A, Dinter H, Schindowski K. Central Nervous System Delivery of Antibodies and Their Single-Domain Antibodies and Variable Fragment Derivatives with Focus on Intranasal Nose to Brain Administration. Antibodies 2021;10:47. https://doi.org/10.3390/antib10040047.
- [205] Huang Q, Chen X, Yu S, Gong G, Shu H. Research progress in braintargeted nasal drug delivery. Front Aging Neurosci 2024;15. https://doi.org/10.3389/fnagi.2023.1341295.
- [206] Correa D, Scheuber MI, Shan H, Weinmann OW, Baumgartner YA, Harten A, et al. Intranasal delivery of full-length anti-Nogo-A antibody: A potential alternative route for therapeutic antibodies to central nervous system targets. Proceedings of the National Academy of Sciences 2023;120. https://doi.org/10.1073/pnas.2200057120.
- [207] Veronesi MC, Alhamami M, Miedema SB, Yun Y, Ruiz-Cardozo M, Vannier MW. Imaging of intranasal drug delivery to the brain. Am J Nucl Med Mol Imaging 2020;10:1–31.
- [208] Gomes JR, Cabrito I, Soares HR, Costelha S, Teixeira A, Wittelsberger A, et al. Delivery of an anti-transthyretin Nanobody to the brain through intranasal administration reveals transthyretin expression and secretion

- by motor neurons. J Neurochem 2018;145:393–408. https://doi.org/10.1111/jnc.14332.
- [209] Day RO, Graham GG, Hicks M, McLachlan AJ, Stocker SL, Williams KM. Clinical Pharmacokinetics and Pharmacodynamics of Allopurinol and Oxypurinol. Clin Pharmacokinet 2007;46:623–44. https://doi.org/10.2165/00003088-200746080-00001.
- [210] Kim H-H, Liao JK. Translational Therapeutics of Dipyridamole. Arterioscler Thromb Vasc Biol 2008;28. https://doi.org/10.1161/ATVBAHA.107.160226.
- [211] Bell DSH. Are the Protean Effects of Pentoxifylline in the Therapy of Diabetes and Its Complications Still Relevant? Diabetes Therapy 2021;12:3025–35. https://doi.org/10.1007/s13300-021-01168-x.
- [212] Sweitzer S, De Leo J. Propentofylline: Glial Modulation, Neuroprotection, and Alleviation of Chronic Pain, 2011, p. 235–50. https://doi.org/10.1007/978-3-642-13443-2 8.
- [213] Ossowska K, Kosmowska B, Wardas J. Potential antipsychotic action of the selective agonist of adenosine A1 receptors, 5'-Cl-5'-deoxy-ENBA, in amphetamine and MK-801 rat models. Pharmacological Reports 2020;72:580–8. https://doi.org/10.1007/s43440-020-00093-3.
- [214] Rother M, Erkinjuntti T, Roessner M, Kittner B, Marcusson J, Karlsson I. Propentofylline in the Treatment of Alzheimer's Disease and Vascular Dementia: A Review of Phase III Trials. Dement Geriatr Cogn Disord 1998;9:36–43. https://doi.org/10.1159/000051188.
- [215] Lintunen J, Lähteenvuo M, Tiihonen J, Tanskanen A, Taipale H. Adenosine modulators and calcium channel blockers as add-on treatment for schizophrenia. NPJ Schizophr 2021;7:1. https://doi.org/10.1038/s41537-020-00135-y.
- [216] Liang C-S, Yang F-W, Chiang K-T, Ho P-S. Allopurinol for Treatment-Resistant Schizophrenia and Epilepsy: A Case Report. Pharmacopsychiatry 2010;43:233–4. https://doi.org/10.1055/s-0030-1254092.

- [217] Lara DR, Brunstein MG, Ghisolfi ES, Lobato MI, Belmonte-de-Abreu P, Souza DO. Allopurinol augmentation for poorly responsive schizophrenia. Int Clin Psychopharmacol 2001;16:235–7. https://doi.org/10.1097/00004850-200107000-00008.
- [218] Suhas S, Sreeraj VS, Amrutha C, Desai G, Venkatasubramanian G. Is allopurinol a marvel in the endgame of ultra-resistant schizophrenia? Schizophr Res 2022;241:12–3. https://doi.org/10.1016/j.schres.2022.01.009.
- [219] Rial D, Lara DR, Cunha RA. The Adenosine Neuromodulation System in Schizophrenia, 2014, p. 395–449. https://doi.org/10.1016/B978-0-12-801022-8.00016-7.
- [220] Khaled Y, Abdelhamid AA, Al-Mazroey H, Almannai AK, Fetais S, Al-Srami AS, et al. Higher serum uric acid is associated with poorer cognitive performance in healthy middle-aged people: a cross-sectional study. Intern Emerg Med 2023;18:1701–9. https://doi.org/10.1007/s11739-023-03337-1.
- [221] Borovcanin MM, Janicijevic SM, Mijailovic NR, Jovanovic IP, Arsenijevic NN, Vesic K. Uric Acid Potential Role in Systemic Inflammation and Negative Symptoms After Acute Antipsychotic Treatment in Schizophrenia. Front Psychiatry 2022;12. https://doi.org/10.3389/fpsyt.2021.822579.
- [222] Marangos PJ, Houston M, Montgomery P. [3H]dipyridamole: A new ligand probe for brain adenosine uptake sites. Eur J Pharmacol 1985;117:393–4. https://doi.org/10.1016/0014-2999(85)90017-2.
- [223] O'Connor JJ, O'Neill C. A Role for Adenosine A1 Receptors in GABA and NMDA-Receptor Mediated Modulation of Dopamine Release: Studies Using Fast Cyclic Voltammetry. Sensors 2008;8:5516–34. https://doi.org/10.3390/s8095516.

ACKNOWLEDGEMENTS

Es difícil describir el sentimiento al final de una tesis. Para mí la ha sido una etapa agridulce, pero que siempre recordaré con mucha estima. Y en gran parte eso se debe a las personas que me han acompañado y que me han ayudado durante todo este tiempo.

Por supuesto a la primera persona que debo agradecer es a Paco. Gracias por darme la oportunidad de ser parte de tu grupo, de confiar en mí, incluso cuando las cosas no salían como se esperaba. Espero que puedas seguir contando chistes a futuras generaciones de doctorandos, un gran mecanismo para los días de experimentos fallidos.

En segundo lugar, a Victor; gracias por compartir tantas discusiones científicas conmigo y hacer frente juntos a los artefactos de los péptidos transmembrana. Gracias a todos los PIs del laboratorio. A Esther, una mujer referente a nivel tanto profesional como personal. A Africa, con tanto potencial y tantas ganas de cambiar el mundo; gracias por insistir, por cambiar, por mejorar e intentar que el laboratorio sea cada vez un poco más agradable. A Jordi, una persona plena d'inquietuts (i molt de *hate*); gràcies per ensenyar-nos tant, a ser crítics, a millorar e innovar. A Laura Cuffy, gràcies a tu el laboratori se sentía una mica més com a casa. A Salut, gracias por cuidarnos, y por preocuparte tanto por nosotros, no solo en el laboratorio, pero también en lo personal.

El 4102 se podría decir que es un laboratorio con gran afluencia. Por algo nos hemos ganado la fama de laboratorio más grande de Bellvitge (los de immuno no podrán con nosotros). En el momento en el que yo entre en el laboratorio tuve la suerte de tener de mentores a Marta, Xavi, Hector i Marc. Gracias por haber sido un referente de grupo y no solo compañeros, pero también amigos

en el laboratorio. Marta, gracias por enseñarnos que en la vida son todo posibilidades, que no todo es trabajo y que hay que disfrutar de lo que hacemos. A Xavi, un apasionado de la ciencia y de la montaña; gracias por invitarme a correr, por ser un amigo en el laboratorio incluso cuando no me conocías de nada. A Hector, amante de la lectura, de videojuegos y series; gracias por aportar un punto de locura al laboratorio, se te echa de menos. Y a Marc, un pozo sin fondo de sabiduría y datos científicos poco relevantes, pero muy interesantes; gracias por enseñarme tanto.

Y cuando llegué al laboratorio, debo agradecer a la primera persona que me acogió a su lado, Josep Caraculo; y con este nombre ya se podría entender toda nuestra relación, ya que se caracteriza por el típico amor-odio de hermanos (de verdad, solo mi hermano me ha sacado tanto de quicio). Pero la verdad es que el cariño que te tengo lo supera todo. Gracias por acogerme no solo en el laboratorio pero también fuera, por invitarme a correr carreras por la montaña y forzarme a mejorar. Espero que podamos seguir viendonos aunque te vayas a laboratorios perdidos en el desierto (P.D. Puedes considerar que estas en mi top 5 de mejores amigos). Y después de mí, llegó LauG, la persona más impulsiva y aleatoria que he conocido nunca, puede explotar unas galletas o tirarte una naranja a la cara (mirad su video de tesis, esta basando 100% en hechos reales); pero, también eres la persona más inteligente y trabajadora que he conocido nunca. Ya se que somos muy diferentes, pero siento que podemos compartir cualquier cosa. Gracias por cuidarme tanto estos años Lau. Y finalmente, nuestra generación se cerró con la incorporación de Nuri (ya sé que no te gusta este nombre pero ya no puedo evitarlo). Se que crees que me puedo saturar contigo y que agotas mi batería social, pero no es así. En cambio espero que nuestra amistad se preserve estemos donde estemos, porque me aportas tanto que no quiero perderte. Me has enseñado a cuidar a la gente, a los amigos y me has hecho ver lo importantes que son las amistades. Pero

también me has hecho ver que yo también soy importante, que no debo guardarme mis cosas adentro y que siempre hay alguien que me querrá escuchar. Se que conseguirás grandes cosas, sea en Bélgica, en Suiza, en Roma o en Petrer. Puede que no seáis conscientes pero estos años habéis hecho de mi una persona totalmente diferente, la Laura tímida y callada que entro el laboratorio, ahora es LauS, con mucha más confianza y personalidad, y esto es gracias a vosotros. Os quiero mucho *infelices*.

Y poco a poco empezó a llegar la nueva generación. Una generación que esta revolucionando el laboratorio y que ha conseguido despuntar en lo científico. Ari, gracias por ser como eres, tan alegre, tan positiva y tan agradable; gracias por tu amistad y por tu generosidad, por contagiar tu alegría a los demás. Montse, con un carácter muy diferente al mio, pero que aprecio mucho; gracias por llevar la voz cantante en tantas cosas, y enseñarnos que en la vida hay que tener personalidad y caracter. Zelai, tan dolça i tan humill; gràcies per transmetre tanta pau al laboratori i fer que hi hagi una mica més de good yogui vibes (P.D. mai oblidaré el viatge de cotxe a la cerdanya anant a 150 per les carreteres de Ripoll). Gracias a la siguiente generación, que coge nuestro relevo y hace posible que el laboratorio continue funcionando y mejorando: gracias a Amelie, a Paula Subi, a Nadjia, y a Marina.

Y finalmente quiero agradecer a los "Angeles de Paco". El laboratorio nos ha unido (concretamente Paco), pero los ángeles iran mucho más allá. Quiero quedarme con las horas interminables de cafés, las cervezas post-trabajo, los entrenos en la piscina y los viajes a pirineos, mallorca y europa. A Paula, tan locamente tarada y obsesa por los gatos. No cambies nunca zorra, sé que en la vida pasan muchas desgracias, pero eres una persona fuerte e inteligente y puedes con esto y más (P.D. más te vale salir en mi video de tesis y venir a mi defensa). A Marc, simplement, gràcies per ser-hi; mai he conegut a una persona que doni tant de si per ajudar als altres, i de veritat crec que et mereixes el

millor del mon i que la resta et cuidi igualment (P.D. també t'haig de donar les gràcies per insistir tant en que em mires Futurama, ara es la meva obsessió també).

I a Glò, crec que no tinc paraules suficients per expressar tot el que t'agraeixo. M'has ensenyat tant (de la vida) i m'has acompanyat tant bé aquests últims anys que crec que no ets conscient. La part de ser co-directora de la tesi queda insignificant, ja que aquesta tesi podria ser i es també teva. T'agraeixo molt que m'hagis transmès els teus valors, de una feina ben feta, de ser organitzada i ser critica; però també de saber disfrutar de la vida, de desconnectar de la feina i cultivar els projectes personals. Espero que puguis construir un gran projecte i siguis molt feliç a la teva finca de Mallorca (P.D. no m'he oblidat del joc de taula, te l'imprimeixo a la propera que vagi al lab).

Aunque en Farmaco hayamos sido un poco sectarios, también hemos coincidido con gente increible en Bellvitge. Gracias a Alexa, a Maria, a Lidia, a Isma, a Arturo, a Laura y todos los predocs que alguna vez nos han acompañado en las famosas mojitadas, en Carnaval o cenas de Navidad. Esta etapa ha sido un poco más llevadera gracias a vosotros, gente con ganas de pasarselo bien, de disfrutar fuera del laboratorio y con ganas de conocer nuevos amigos.

I dins de Bellvitge haig de fer una menció especial al departament de Ciències Fisiològiques; per que es un grup que sempre que necessites et donen un cop de mà (a canvi de reactius o reserves de lector). Gràcies a Laura Ferigle, per compartir la frustració de purificar i caracteritzar nanobodies. A Hector, per serhi sempre per resoldre dubtes i trobar a Ekaitz quan el necessitava. I evidentment gràcies a Ekaitz, el meu company euskaldun/català. Aquesta tesi no hagués pogut ser sense la teva ajuda; gràcies per ajudar-me a entendre la ciència i fer-me tornar a creure en que es pot fer ciència sense morir pel camí. Tinc moltes ganes de discutir resultats a la defensa. Eskerrik asko!! Finalment,

gràcies a Adri. Gràcies per compartir amb mi els teus cafès i cerveses, per ensenyar-me a ser una mica més hedonista, però també a exterioritzar tot l'odi cap a les coses que no estan bé. Espero que ens puguem trobar més sovint pujant cims al Pirineu.

He tingut la sort de poder marxar a fora i fer una estada a Brussel·les. Això m'ha donat l'oportunitat d'aprendre molt, però també de conèixer a molta gent, i molt diferent, que m'ha aportat molt. A big thank you to all the MITH lab membres, and specially to Sophie, Sam, Lukasz and Kevin. Kevin, thank you very much for helping me with my experiments (or actually doing them).

Pero desde luego, mi gran experiència en Bruselas fue gracias a los *Bluebooks* (o como se llaman ellos, los *BBT*). Ha sido una suerte coincidir con vosotros, nunca me habria imaginado que gente tan diferente pudiera congeniar tan bien. En primer lloc, vull donar les gràcies a la Mireia, per acompanyar-me des del primer dia e introduir-me al meravellós mon dels Bluebook. I gràcies a tots el de Gansoescalada, a Marta, a Kata i a Pablo per motivar-me a escalar més i inclús acabant fent la mitja marató de Brussel·les. Gràcies per ser tant intensos, aquests quatre mesos haguessin sigut molt avorrits sense vosaltres.

Després de gairebé sis anys fent la tesi, he passat moltes hores tancada al laboratori. No obstant, he pogut conèixer gent fora del laboratori que m'han acompanyat molt durant aquests anys i han fet que surti de la bogeria de la tesi. Gràcies al grup d'expedició de muntanya, a Ana, Pau, Sergi, Miquel i Adri. Gràcies per acollir-me al vostre grup i confiar tant en mi com a guia. Espero que puguem fer moltes més nits en refugis i assolir més cims. Gràcies a la colla de KP, Can Rata i els (+1), gràcies per convidar-me a tots els vostres plans i cases rurals per fer-me sentir una més en el vostre grup.

Però qui més ha fet que em senti com a casa a sigut la família Sala-Gastón. Gràcies a Josep i Lurdes per acollir-me a casa vostra i per cuidar-me tant. Sempre estaré agraïda per tot el que heu fet per mi. Gràcies a Mireia i Mel per estimar-me tant i compartir tants moments amb mi. Gràcies a Pere per convidar-me a Colldelrat i fer-me sentir com a casa. Sou una família increïblement generosa i mai us podré retornar tot el que meu donat aquests anys.

Bartzelonara etortzeko, jende asko atzean utzi egin behar izan nuen, eta azken urte hauetan tesiaren esperientzia nirekin partekatu dute Fenixek. Eskerrik asko, Aizpea, Maria, Paloma eta Amaiari. Bakoitzak tesia Europako punta desberdin batetik egin arren, beti elkar izango dugu momentu latzetan. Espero det gure hurrengo topaketan danek tesia defendatu izana!

Eskerrik asko Ibairi; gure harremana distantzian izan da beti, eta ordea lagun oso mina zaitut. Eskerrik asko nitaz kezkatzeagatik, nigan konfiantza izategatik eta beti hobeto sentiarazteagatik. Badakizu itzultzen naizen bakoitzean mendik igotzeko prest egongo naizela (edo Bilboko jaitara juteko).

Eskerrik asko Maiderri; urte asko izan dira distantzian (10 urte jada!), baina horrek ez du gure adiskidetasuna hautsi. Badakit urte guzti hauetan biok asko aldatu garela, eta hala ere, gure bideak elkar topatu dira berriz ere. Eskerrik asko gure adiskidetasuna zaintzeagatik!

Azkenik eskerrak nire familiari. Eskerrik asko Lourdes, Nekane, Joxantonio, Eli, Izaro eta Haritzi. Badakit gutxitan itzultzen naizela, baina badakit zuek beti niretzat hor egongo zeatela. Bihotzez eskertzen dizuet nigatik egin dezuten guztia. Espero det tesia amaituta maizago elkar ikustea. Eskerrik asko amona eta aitonari, txiki txikitatik zaintzeagatik eta hezitzeagatik.

Eskerrik asko Eneko, niretzat beti hor izateagatik. Azken sei urte hauetan gure harremana inoiz baino gehiago sendotu da. Anaia baino laguna zaitut, gehiegizko konfiantzarekin agian, baina lagun min. Eta espero det inoiz ez

aldatzea. Eskerrik asko Ama, astero milaka dei egiteagatik, eta nire zelulak eta animaliak nola dauden galdetzeagatik. Baita gauza gaixki atetaretzen zitzaikidanean ni lasaitzeagatik, garratzia kendu eta hobeto sentiarazteagatik. Behin tesia gainetik kenduta, etxera gehiago itzultzea espero det. Eskerrikasko Aita; karreran sartu aurretik aurreratu zenidan, ez zela errexa izango. Ez da errexa izan, ez, baina zu beti prest egon zara laguntzeko eta nirekin batera momentu latzei aurre egiteko. Badakit batzutan gehigi kezkatzen zarela, baina jakinarazi nahi dizut ondo nagoela; zuei esker proposatzen dudan edozer lortuko det eta bizitzan aurrera egin. Asko maite zaituztet!

I finalment haig d'agrair a la meva parella, amic i company de vida. Gràcies Joan, gràcies per parar-me pel laboratori per parlar, per mantenir contacte durant la pandèmia, per convidar-me a escalar, a anar a la muntanya, per donar-me mirades furtives per la finestra del lab, per compartir la teva vida amb mi, per acompanyar-me en els moments dolents, però també en els feliços i per crearne de nous cada dia. Se que no et vaig fer cas quan em vas dir que no fes la tesi, que era molt dur; i tot i així, m'has acompanyat i has cregut sempre en mi. Gràcies per estimar-me i per fer-m'ho saber cada dia, per fer-me costat i valorar-me tal com soc. T'estimo molt.